INVESTIGATING ROLES OF THE METABOLIC ENZYME FUMARASE AND THE METABOLITE FUMARATE IN DNA DAMAGE RESPONSE

by

Faeze Saatchi

A Dissertation

Submitted to the Faculty of Purdue University

In Partial Fulfillment of the Requirements for the degree of

Doctor of Philosophy

Department of Biochemistry

West Lafayette, Indiana

May 2019

THE PURDUE UNIVERSITY GRADUATE SCHOOL
STATEMENT OF COMMITTEE APPROVAL

Dr. Ann L. Kirchmaier, Chair
Department of Biochemistry

Dr. Scott D. Briggs
Department of Biochemistry

Dr. Emily Dykhuizen
Department of Medicinal Chemistry and Molecular Pharmacology

Dr. Elizabeth J. Tran
Department of Biochemistry

Approved by:

Dr. Andrew Mesecar
Head of the Graduate Program

I dedicate this to my parents who have always loved and supported me and showed me that so much can be done with so little.

ACKNOWLEDGMENTS

I would like to first acknowledge my advisor, Dr. Ann Kirchmaier, for her continuous support and guidance during my Ph.D. She has been an amazing mentor and has helped me with my research and writing of this thesis. I am grateful to all members of my thesis committee, Dr. Scott Briggs, Dr. Emily Dykhuizen and Dr. Elizabeth Tran for their insightful comments and constructive criticism. Their feedbacks have been invaluable to my research and training. I would also like to thank all faculties and trainees who attended our joint chromatin meetings. I have greatly enjoyed the stimulating discussions we had during the presentations, and the feedback and questions I got during my presentations has helped me better my research and presentation skills. I am also thankful to all past members of the lab who have provided technical and moral support during my time in the lab. It has been a pleasure and a privilege to interact with every individual I have worked with over the years. Lastly, I would like to thank my parents, my brother and my sister who have supported and encouraged me throughout the years. I am also grateful to other family members and friends who have supported me along the way.

TABLE OF CONTENTS

LIST OF TABLES

LIST OF FIGURES

LIST OF ABBREVIATIONS

2-HG	2-hydroxyglutarate
α-KG	α-ketoglutarate
Acetyl-CoA	Acetyl coenzyme A
AML	Acute myeloid leukemia
AMP	Adenosine monophosphate
BIR	Break induced replication
ChIP	Chromatin immunoprecipitation
DDC	DNA damage checkpoint
dHJ	double Holliday Junction
DNA2	DNA synthesis defective
DNMT	DNA methyltransferase
DOT1	Disruptor of telomeric silencing
DRC	DNA replication checkpoint
DSB	Double stranded break
DSBR	Double stranded break repair
EXO1	Exonuclease
FAD	Flavin adenine dinucleotide
FH	Fumarate hydratase
FUM1	Fumarase
HAT	Histone acetyltransferase
HDAC	Histone deacetylase
HIF-1	Hypoxia inducible factor
HLRCC	Hereditary leiomyomatosis and renal cell cancer
HR	Homologous recombination
HTZ1	Histone variant
HMT	Histone methyltransferase
HU	Hydroxyurea
IDH	Isocitrate dehydrogenase
IMP	inosine monophosphate, chromatin remodeller
INO80	Inositol requiring
iPOND	Identification of proteins on nascent DNA
IR	Ionizing radiation
JHD2	JmjC domain-containing histone demethylase 2
JHDM	JmjC domain containing histone demethylase
MEC1	Mitosis entry checkpoint
MMS	Methyl methanesulfonate
MRC1	Mediator of replication checkpoint 1
MRE11	Mitotic recombination
NAD^+	Nicotinamide adenine dinucleotide
NHEJ	Non-homologous end joining
PCR	Polymerase chain reaction
PP1	Protein phosphatase 1
PP2A	Protein phosphatase 2A

PTM	Post-translational modification
RAD53	RADiation sensitive, effector kinase in DNA damage checkpoint
RFA	Replication factor A
RPA	Replication protein A
SAE2	Sporulation in the absence of spo eleven
SAH	S-adenosylhomocysteine
SAM	S-adenosylmethionine
SDH	Succinate dehydrogenase
SDSA	Synthesis dependent strand annealing
SET1	SET domain containing, histone H3 Lysine4 methyltransferase
SGS1	Slow growth suppressor, helicase involved in DNA replication and DNA end resection
SPRINP	Single primer reaction in parallel
SSA	Single stranded annealing
SWR1	Swi2/Snf2-related, chromatin remodeller
TET	Ten-eleven translocation
UV	Ultraviolet
XRS2	X-ray sensitive, component of the MRX complex
YKU70	Yeast KU protein, subunit of telomeric Ku complex, also binds to sites of DNA damage to promote repair

ABSTRACT

Author: Saatchi, Faeze. PhD
Institution: Purdue University
Degree Received: May 2019
Title: Investigating Roles of the Metabolic Enzyme Fumarase and the Metabolite Fumarate in DNA Damage Response
Committee Chair: Ann Kirchmaier

In eukaryotic cells, DNA is packaged into a structure named chromatin which contains DNA and proteins. Nucleosomes are building blocks of chromatin and contain DNA wrapped around a histone octamer. Chromatin modifications (histone post-translational modifications and histone variants) play central roles in various cellular processes including gene expression and DNA damage response. Chromatin modifying enzymes use metabolites as co-substrates and co-factors, and changes in metabolic pathways and metabolite availability affects chromatin modifications and chromatin-associated functions. Moreover, recent studies have uncovered direct roles of metabolic enzymes in chromatin-associated functions. Fumarase, a TCA cycle enzyme that catalyzes the reversible conversion of fumarate to malate in mitochondria (a hydration reaction), is an example of an enzyme with dual functions in metabolism and genome integrity. Cytoplasmic fraction of yeast fumarase, Fum1p, localizes to the nucleus and promotes growth upon DNA damage. Fum1p promotes homologous recombination by enhancing DNA end resection. Human fumarase is involved in DNA repair by non-homologous end joining. Here, we provide evidence that yeast Fum1p and the histone variant Htz1p are also involved in DNA replication stress response and DNA repair by non-homologous end joining (NHEJ). Using mutants lacking the histone variant *HTZ1*, we show that high cellular levels of fumarate, by deletion of *FUM1* or addition of exogenous fumarate, suppressed the sensitivity to DNA replication stress by modulation of activity of Jhd2p. This suppression required sensors and mediators of the intra-S phase checkpoint, but not factors involved in the processing of replication intermediates. These results imply that high cellular levels of fumarate can confer resistance to DNA replication stress by bypassing or complementing the defects caused by loss of *HTZ1* and replication fork processing factors. We also show that upon induction of DSBs, exogenous fumarate conferred resistance to

mutants with defects in NHEJ, early steps of homologous recombination (DNA end resection pathway) or late steps of homologous recombination (strand invasion and exchange). Taken together, these results link the metabolic enzyme fumarase and the metabolite fumarate to DNA damage response and show that modulation of DNA damage response by regulating activity of chromatin modifying enzymes is a plausible pathway linking metabolism and nutrient availability to chromatin-associated functions like genome integrity.

CHAPTER 1. INTRODUCTION

1.1 The importance of genome stability

Cells in eukaryotic organisms contain DNA that encodes the information required for cellular functions. Genetic material is continuously exposed to internal and external damaging agents. If DNA is not repaired or repaired inaccurately, DNA-dependent processes including DNA replication and transcription are negatively affected. Defects in DNA repair have been implicated in a variety of human diseases including increased susceptibility to cancer, neurodegenerative disorders and immunodeficiencies (Jackson and Bartek 2009; Rulten and Caldecott 2013; Aparicio *et al.* 2014; Prochazkova and Loizou 2016). Genetic aberration can arise during DNA replication due to errors in base pairing by DNA polymerases as well as during certain normal cellular processes including rearrangement of immunoglobin and T cell receptor loci, which uses programmed DNA break and repair during lymphoid cell development to generate diversity in the immune cell repertoire (Prochazkova and Loizou 2016). In addition, during mating-type switching in yeast, a double strand break (DSB) created by the endonuclease HO to initiate homologous recombination (HR) between the *MAT* locus and the *HML* or *HMR* donor loci to mediate switching of the cell mating type (Haber 2012). Reactive oxygen species generated during oxidative respiration can attack DNA causing adducts that block DNA replication and transcription (Cadet *et al.* 2003; Rodriguez-Rocha *et al.* 2011; Nita and Grzybowski 2016). Moreover, environmental factors including exposure to ultraviolet light (UV), ionizing radiation (IR) and genotoxic chemicals can induce various types of DNA damage (Emerson and Bertuch 2016). To maintain integrity of the genome, all organisms from bacteria to human have developed multiple mechanisms to repair damaged DNA.

Damaged DNA that is not repaired properly can lead to genomic instability, apoptosis or senescence, and results in functional consequences including rapid aging, impaired growth and predisposition to immunodeficiencies, neurological disorders and cancer (Subba Rao 2007). In addition, induction of DSBs is a fundamental mechanism underlying anti-cancer therapeutic approaches including radiation therapy or chemotherapeutic agents like topoisomerase inhibitors and crosslinking agents (O'Connor 2015). Understanding how DNA lesions are repaired can facilitate design of more effective treatments.

Below, I will discuss two major DNA repair pathways, non-homologous end joining (NHEJ) and homologous recombination (HR) (Figure 1.1), with a focus on the current knowledge of the field in the model organism *Saccharomyces cerevisiae* with mammalian orthologs mentioned as appropriate.

1.2 DNA damage repair

1.2.1 Repair of DSBs

Double stranded breaks are the most cytotoxic form of DNA damage and can occur due to DNA replication fork collapse, activity of endonucleases, and exposure to radiation or certain chemicals including zeocin. Two major pathways for repair of DSBs will be discussed below.

1.2.1.1 Non-homologous end joining (NHEJ)

The NHEJ pathway repairs DNA DSBs by direct joining of the two ends of DNA DSB. The NHEJ process can be error-free (with high fidelity) or error prone (resulting in diverse DNA sequences at the repair junction) (Daley *et al.* 2005; Emerson and Bertuch 2016). The DSB is first recognized by Yku70-Yku80 heterodimer (KU70-KU80 heterodimer in higher eukaryotes) which acts as a scaffold for recruitment of other NHEJ factors including the Dnl4p, Lif1p and Nej1p (Zhang *et al.* 2007; Wu *et al.* 2008). Dnl4p (LIG4 in humans) is an ATP-dependent DNA ligase required for NHEJ (Wilson *et al.* 1997). Dnl4p interacts with Lif1p (ortholog of human XRCC4) in a 1:2 stoichiometric ratio, and this interaction stabilizes Dnl4p protein levels (Herrmann *et al.* 1998). Binding of Dnl4p-Lif1p to DSBs stabilizes binding of Ku heterodimer to DNA ends, and this stabilization suppresses DNA repair by HR (Zhang *et al.* 2007). Nej1p (ortholog of XLF in mammalian cells) binds to other core NHEJ factors including Lif1p and Yku70p, and stabilizes association of Yku70p at DSBs (Chen and Tomkinson 2011). Moreover, Nej1p promotes reactivation of Dnl4p by enhancing its deadenylation (Chen and Tomkinson 2011).

Binding of the Yku heterodimer to DNA ends protects the ends from exonucleases and retains Dnl4p-Lif1p and Nej1p at the sites of break. In mammalian cells, LIGASE IV-XRCC4 and XLF (orthologs of Dnl4p-Lif1p and Nej1p) form filaments that bridge the DNA ends (Hammel *et al.* 2010, 2011; Ropars *et al.* 2011). Whether this process is conserved in yeast is not known (Emerson and Bertuch 2016). Next, DNA ends are processed by end processing factors, including Pol4p and

Rad27p, to create ends compatible for joining by ligation (Daley *et al.* 2005; Emerson and Bertuch 2016). Pol4p is a DNA polymerase associated with gap filling in NHEJ (Chan *et al.* 2008; Galli *et al.* 2015). Rad27p is a 5' nuclease that interacts with Pol4p and Dnl4p-Lif1p and promotes NHEJ in plasmid repair assays in which substrates form 5' flaps (Wu *et al.* 1999; Tseng and Tomkinson 2004). However, other studies have shown that Rad27p is dispensable for NHEJ events that require removal of flaps or overhangs (Daley *et al.* 2005), indicating that other nuclease(s) might also be involved in DNA end processing during NHEJ. After DSB ends are processed, Dnl4p repairs the DNA by ligating the nick (Wilson *et al.* 1997; Emerson and Bertuch 2016).

1.2.1.2 Homologous recombination (HR)

HR is a process in which a homologous region or a sister chromatid is used as a template to re-synthesize the site of damage. HR is typically error-free and is initiated by DNA end resection. During DNA end resection, DNA ends are processed by helicases and nucleases to create 3' ssDNA overhangs (described in more detail below).

Upon DSB, HR is initiated by the MRX complex in *S. cerevisiae* (referred to as the MRN complex in higher eukaryotes). This complex contains three subunits: Mre11p, Rad50p and Xrs2p (Mre11, RAD50 and NBS1 in higher eukaryotes) in a 2:2:1 stoichiometric ratio (Chen *et al.* 2001). This complex has two main functions: 1) recruitment of the Tel1p kinase (ATM kinase in mammalian cells) and activation of the DNA damage checkpoint (Nakada *et al.* 2003) (See Section 1.3 for details), and 2) initiation of the DNA end resection process (described below and Figure 1.2).

To initiate DNA end resection, MRX complex functions with the Sae2p (CtIP in mammals). Mre11p subunit has 3' to 5' exonuclease activity as well as a weak endonuclease activity. *in vitro,* addition of Sae2p stimulates the endonuclease activity of Mre11p (Cannavo and Cejka 2014). Mre11p initiates the DNA ends resection process by creating a nick near DNA ends, up to 300 nucleotides away from the break site (Garcia *et al.* 2011). This creates an entry point for 3' to 5' exonuclease activity of Mre11p to degrade DNA back towards the DSB end as well as a substrate for 5' to 3' activity of exonucleases like Exo1p and Dna2p (Garcia *et al.* 2011; Cejka 2015; Gnügge and Symington 2017) (See Figure 1.2). Dna2p functions in conjunction with the DNA helicase Sgs1p (Zhu *et al.* 2008). Exo1p and Dna2p/Sgs1p comprise two parallel pathways for long range DNA end resection (Niu *et al.* 2010; Nicolette *et al.* 2010; Cannavo *et al.* 2013) (See Figure 1.2).

The ssDNA generated by Exo1p or Dna2p/Sgs1p is then coated by the ssDNA binding heterotrimer RPA, which contains subunits named Rfa1p, Rfa2p. Rfa3p (Alani *et al.* 1992). Next, RPA is replaced by the filament forming protein Rad51p in *S. cerevisiae* (Sugiyama *et al.* 1997; Sugiyama and Kowalczykowski 2002). RPA binding promotes binding of Rad51p to DNA by inhibition of formation of DNA secondary structures (Alani *et al.* 1992; Sugiyama *et al.* 1997, 1998). RPA-coated ssDNA also functions in activation of the DNA damage checkpoint which will be discussed in more detail in Section 1.2.1.4. Displacement of RPA by Rad51p is accelerated by Rad52p (functionally analogous to human BRCA2) which binds to both RPA and Rad51p (Shinohara *et al.* 1992; New *et al.* 1998; Hays *et al.* 1998). Rad52p facilitates formation of Rad51p (RAD51 in mammalian cells) nucleoprotein filaments (New *et al.* 1998; Sugiyama and Kowalczykowski 2002). Rad51p filaments, also termed pre-synaptic filaments, mediate strand invasion and exchange and binding of Rad52p to Rad51p and RPA promotes this strand exchange (Sung 1997; New *et al.* 1998; Shinohara and Ogawa 1998).

In addition to Rad52p, Rad54p also binds to and stabilizes Rad51p filaments and promotes strand exchange *in vitro* (Petukhova *et al.* 1998; Mazin *et al.* 2003; Wolner and Peterson 2005). Strand invasion by Rad51p-coated ssDNA creates a D-loop intermediate, a heteroduplex DNA formed from the invading ssDNA tail and the chromosomal homolog (Li and Heyer 2008). This step in HR is called synapsis (Li and Heyer 2008). Rad54p is also involved in HR after synapsis, where Rad51p-coated ssDNA are disassembled by Rad54p (Petukhova *et al.* 1998; Solinger *et al.* 2002; Li and Heyer 2009). This allows access to the 3'-OH end by DNA polymerases and extension of the invading ssDNA (Solinger *et al.* 2002; Li and Heyer 2008, 2009).

Following synapsis and D-loop formation, the 3' end of the invading strand primes DNA synthesis. Following extension of the invading strand, the D-loop intermediate can be resolved in multiple ways including synthesis-dependent strand annealing (SDSA), DSB repair (DSBR) or break induced repair (BIR) (see Figure 1.3 (Krogh and Symington 2004; Li and Heyer 2008; San Filippo *et al.* 2008) for detailed review).

In SDSA, the invading strand is disengaged after DNA synthesis. Next, the newly synthesized strand is annealed to the ssDNA on the other end of the break site followed by gap filling and ligation. This results in a non-crossover product (West 2003; Heyer *et al.* 2010; Verma and

Greenberg 2016) (Figure 1.3). Alternatively, after strand invasion, the second end of the DSB can be captured to form a structure called a double Holliday Junction (dHJ) (Li and Heyer 2008; Heyer *et al.* 2010). After gap filling and ligation, the dHJ structure can be resolved in a cross-over or non-crossover manner (Li and Heyer 2008) (Figure 1.3). This process is named DSB repair (DSBR). In BIR, the invading strand is used to establish a replication fork that can synthesize the remaining entire chromosome arm (Malkova *et al.* 1996; Lydeard *et al.* 2007). In contrast to DSBR and SDSA, the second end of the break is never engaged in BIR (Figure 1.3) (Malkova *et al.* 1996).

1.2.1.2.1 Role of Rad52p in HR

In addition to facilitating Rad51p filament formation and strand exchange discussed in Section 1.2.1.2, Rad52p is also involved in annealing homologous ssDNA coated with RPA (Sugiyama *et al.* 1998) during SDSA and single strand annealing (SSA). SSA is a process in which DSBs generated between direct repeat sequences are repaired by reannealing the complementary strands (Pâques and Haber 1999). The role of Rad52p in SSA is annealing of complementary ssDNA regions exposed by DNA end resection and bound by RPA (Shinohara *et al.* 1998; Pâques and Haber 1999; Davis and Symington 2001). In SDSA, following extension of the invading strand and its disengagement from the D-loop, annealing of the second end is mediated by Rad52p (Figure 1.3) (Sugiyama *et al.* 2006).

1.2.1.3 DNA repair pathway choice for DSBs

The choice of DNA repair pathway is primarily dependent on the cell cycle. In vertebrates, HR is predominant during S/G_2 when the sister template is available for recombination whereas NHEJ process can occur throughout the cell cycle but is prevalent outside of S/G_2 (Karanam *et al.* 2012). In yeast, NHEJ mainly happens in G_1 whereas HR occurs in S/G_2. In yeast cells arrested in G_1, DNA end resection fails to initiate after induction of a DSB at the *MAT* locus by expression of the HO endonuclease implying that HR is inactive in G_1 (Ira *et al.* 2004). Cyclin-dependent protein kinases are important for controlling the DNA repair pathway choice. Cdc28p/Cdk1p is a cyclin dependent kinase which in its active form inhibits transition from anaphase to G_1 and is activated at “Start”, a point when the cells commits to progress to S phase (Toone *et al.* 1997). Cdc28p can phosphorylate Sae2p and Dna2p, and this phosphorylation promotes DNA end resection (Huertas *et al.* 2008; Chen *et al.* 2011).

In addition to the regulation of DNA repair pathway choice by cell-cycle, regulation of DNA end resection is a major determinant of DSB repair pathway choice. Factors that inhibit or promote DNA end resection can promote NHEJ or HR, respectively. For example, binding of the Ku heterodimer to inhibit DNA repair by HR whereas binding of Mre11p and Sae2p to DSBs promote recruitment of Dna2p, Exo1p and facilitates DNA end resection as well as repair by HR (Mimitou and Symington 2008; Shim *et al.* 2010). In fact, the Ku dimer competes with the MRX complex and Exo1p nuclease for binding to intact DNA ends (Mimitou and Symington 2008; Shim *et al.* 2010). Deletion of *YKU70* and *YKU80* cause an increase of Mre11p binding and DNA end resection in G_1 whereas overexpression of Yku70p and Yku80p causes depletion of Mre11p at DSBs and decreased DNA end resection in G_2 (Clerici *et al.* 2008). Moreover, deletion of *YKU70* partially suppresses the sensitivity of *mre11*Δ mutants to IR (Bressan *et al.* 1999). Although the above evidence implies a competition for binding to DSBs, detailed mechanistic studies are required to determine how different DSB DNA repair factors function in DNA repair pathway choice.

1.2.1.4 Checkpoint activation

A single unrepaired DSB can trigger a signaling cascade through activation of a kinase cascade that causes G_2/M cell cycle arrest (Sandell and Zakian 1993; Lee *et al.* 1998; Pellicioli *et al.* 2001). Tel1p (ortholog of ATM in mammalian cells) and Mec1p (ortholog of mammalian ATR) are two checkpoint kinases that preferentially phosphorylate Ser or Thr residues followed by Gln (Kim *et al.* 1999) and have partially overlapping functions in response to DSBs. For example, both can phosphorylate H2A on Ser129 (termed γ-H2A), a modification associated with sites of DNA damage (Downs *et al.* 2000; Shroff *et al.* 2004) (see Section 1.5.1.1). Tel1p is recruited to DSBs through interaction with the C-terminus of the Xrs2p subunit of the MRX complex (Nakada *et al.* 2003). Mec1p interacts with Ddc2p (ortholog of mammalian ATRIP) even in the absence of an exogenous source of DNA damage (Paciotti *et al.* 1998; Rouse and Jackson 2000). Mec1p-Ddc2p is recruited to the sites of damage through interaction with RPA-coated ssDNA (Zou and Elledge 2003).

In addition to Ddc2p, checkpoint activation by Mec1p requires another complex that localizes to sites of DSB and acts as a sensor: the PCNA-like heterotrimeric complex containing Rad17p, Ddc1p and Mec3p (Melo *et al.* 2001; Majka and Burgers 2003). The Rad17p-Ddc1p-Mec3p

complex in budding yeast is the ortholog of the 9-1-1 complex in higher eukaryotes, which contains RAD9, HUS1 and RAD1 (Ellison and Stillman 2003). The yeast Rad17p-Ddc1p-Mec3p complex is loaded onto ssDNA-dsDNA junctions by RFC-like complex containing Rad24p (ortholog of mammalian RAD17) (Majka and Burgers 2003). The Ddc1p subunit of the yeast Rad17p-Ddc1p-Mec3p complex mediates activation of Mec1p (Majka *et al.* 2006; Navadgi-Patil and Burgers 2009).

1.2.2 Repair of DNA replication errors

In all eukaryotes, multiple DNA replication machineries (replisomes) initiate DNA replication, each from a different origin of replication across the genome, to ensure timely replication of the entire genome during S phase.

Sequences difficult to replicate including AT-rich regions and repeat DNA sequences that form three dimensional structures like telomeres and centromeres, collisions between the replication and the transcription machinery, and DNA-protein crosslinks as well as DNA lesions and environmental genotoxins can all challenge the replisome and cause DNA replication stress (Zeman and Cimprich 2014; Mazouzi *et al.* 2014; Gadaleta *et al.* 2017). In most cases, DNA replication stress causes a transient pausing of the replisome. However, certain types of DNA damage or events that are challenging for DNA replication, like formation of inter-strand crosslinks, the presence of bulky DNA adducts and depletion of dNTP by hydroxyurea (HU) cause longer lasting challenges, and can create stalled replication forks, thereby activating the intra-S phase checkpoint in a Mec1p- and Sgs1p-dependent manner (Lopes *et al.* 2001; Cobb *et al.* 2003) (discussed in more detail in Section 1.3 and 3.2.8). The DNA replication checkpoint stabilizes the stalled forks, and promotes DNA synthesis restart in addition to inhibiting origin firing and blocking cell cycle progression (Jossen and Bermejo 2013; Hustedt *et al.* 2013; Pardo *et al.* 2016). Stalled replication forks that are not stabilized can collapse, leading to incomplete DNA synthesis, formation of DSBs, increased genetic instability, and chromosomal rearrangements (Hustedt *et al.* 2013; Alexander and Orr-Weaver 2016). I will discuss the intra-S phase checkpoint in more detail in Section 1.3.

1.3 Intra-S phase checkpoint activation

The signaling pathways activated during intra-S phase checkpoint can be divided into two pathways: the DNA damage checkpoint (DDC) and the DNA replication checkpoint (DRC). These two pathways use different mediators, but converge at the effector kinase Rad53p, which regulates multiple cellular processes including cell cycle arrest, increased expression of DNA repair factors, an increase in dNTP pools and inhibition of late origin firing (Pardo *et al.* 2016) (See Figure 1.4). Phosphorylation of Rad53p is a hallmark of DDC and DRC in budding yeast (Pardo *et al.* 2016). Below, each signaling pathway will be discussed in more detail.

1.3.1 DNA replication checkpoint (DRC)

The DRC branch of the intra-S phase checkpoint is activated in response to stalled replication forks. DRC is initiated by the sensor kinase Mec1p which is recruited to RPA-coated ssDNA at stalled replication forks (Pardo *et al.* 2016). In response to DNA replication stress, Rad9p is dispensable for Mec1p-dependent Rad53p activation. Instead, Mec1p transduces the DRC signal to Rad53p by phosphorylation of the mediator Mrc1p (see Figure 1.4) (Alcasabas *et al.* 2001). Phosphorylated Mrc1p can then recruit and activate Rad53p (Alcasabas *et al.* 2001; Osborn and Elledge 2003; Chen and Zhou 2009). Another factor that plays an important role in DRC is the helicase Sgs1p. Sgs1p interacts with RPA and Dna2p at DNA replication forks and can also be phosphorylated by Mec1p (Cobb *et al.* 2003; Cejka *et al.* 2010; Hegnauer *et al.* 2012). Phosphorylation of Sgs1p promotes its interaction with Rad53p (Hegnauer *et al.* 2012). The helicase activity of Sgs1p at DNA replication fork is important for maintaining stability of the forks (Cobb *et al.* 2003, 2005; Bjergbaek *et al.* 2005).

Activation of Rad53p leads to inhibition of late origin firing by phosphorylation and inactivation of origin activating factors Sld3p and Dbf4p (Santocanale and Diffley 1998; Zegerman and Diffley 2010; Lopez-Mosqueda *et al.* 2010). Inhibition of late origin firing during replication stress is thought to prevent generation of additional replication stress in unreplicated parts of the genome by preventing exhaustion of RPA (Toledo *et al.* 2013). In addition, Mec1p and Rad53p phosphorylate and activate Dun1p, a serine/threonine kinase that increases dNTP synthesis following checkpoint activation in S phase. Dun1p in turn phosphorylates Sml1p (Zhao and Rothstein 2002; Smolka *et al.* 2006). Sml1p is an inhibitor of ribonucleotide reductases (Desany

et al. 1998; Zhao *et al.* 2001). Phosphorylation of Sml1p by Dun1p targets Sml1p for degradation (Zhao *et al.* 2001; Zhao and Rothstein 2002). Thus degradation of phosphorylated Sml1p increases the activity of ribonucleotide reductases, leading to increased dNTP pools available for replication (Zhao and Rothstein 2002).

1.3.2 DNA damage checkpoint (DDC)

DDC is activated in response to DNA lesions in S phase. In the DDC branch of the intra-S phase checkpoint, Mec1p activation leads to phosphorylation of a mediator protein named Rad9p in budding yeast (ortholog of 53BP1 in mammals) (Vialard *et al.* 1998). The mechanism of recruitment of Rad9p will be discussed in more detail in Section 1.4.2. Phosphorylated Rad9p promotes recruitment of the effector kinase Rad53p (CHK2 in mammals) to the sites of damage (Schwartz *et al.* 2002). Rad53p is mainly phosphorylated and activated by Mec1p (Sun *et al.* 1998; Gilbert *et al.* 2001; Sweeney *et al.* 2005). However, Tel1p can also play a minor role in phosphorylation and activation of Rad53p in a Mec1p-independent manner when multiple DSBs are generated (Mantiero *et al.* 2007).

Following repair of damaged DNA, cells resume cell cycle progression by inactivation of DNA damage checkpoint through a process termed checkpoint recovery (Clémenson and Marsolier-Kergoat 2009). In budding yeast, the Srs2p helicase can remove the Rad51p from ssDNA *in vitro* and *srs2*Δ mutants have defects in checkpoint recovery that can be suppressed by loss of Rad51p (Krejci *et al.* 2003; Veaute *et al.* 2003; Yeung and Durocher 2011).

Alternatively, in the presence of persistent DNA damage, cells can turn off the DNA damage checkpoint and resume cell cycle progression by a process called checkpoint adaptation (Clémenson and Marsolier-Kergoat 2009). In yeast cells containing an unrepairable DSB, Ddc2p foci disappear upon checkpoint adaptation, whereas Ddc1p foci do not dissociate from DSBs (Melo *et al.* 2001). This implies that regulation of Mec1-Ddc2p rather than Rad17p-Ddc1p-Mec3p is responsible for checkpoint adaptation. During checkpoint adaptation, Rad53p becomes dephosphorylated and inactivated by phosphatases Ptc2p and Ptc3p(Leroy *et al.* 2003).

1.4 Chromatin modifications

In eukaryotic cells, DNA is packaged into chromatin using histones. The nucleosome is the fundamental unit of chromatin that consists of ~147 base pairs of DNA wrapped around a histone octamer (Luger *et al.* 1997). The canonical histone octamer contains two copies of each histone H2A, H2B, H3 and H4. Histones can be post-translationally modified. The post-translational modifications (PTMs) of histones include a variety of chemical modifications such as acetylation, methylation, phosphorylation, ubiquitination and sumoylation. In addition to histones, DNA can also be modified. Yeast species (budding yeast and fission yeast) lack DNA modifications (Capuano *et al.* 2014), but commonly described in other organisms. These include 5-methylcytosine (5mC), 5-hydroxymethylcytosine (5hmC), 5-formylcytosine (5fC) and 5-carboxymethylcytosine (5caC) (Breiling and Lyko 2015).

DNA and histone modifications are collectively referred to as chromatin modifications. In addition to histone modifications, histone variants can replace canonical histones and have specialized functions. Histone variants are paralogs of canonical histones containing variations in the amino acid sequence. Below, I will review the deposition and removal of histone acetylation, methylation and the histone variant H2A.Z as well as DNA methylation.

1.4.1 DNA methylation

DNA methyltransferases (DNMTs) transfer a methyl group from S-adenosylmethionine (SAM) to 5-carbon of cytosine residues in DNA. Methylation on the 5-carbon of the cytosine residue is named 5mC. 5mC can be oxidized to 5hmC, and further oxidized to 5fC and eventually to 5caC. Oxidation of 5mC to 5hmC, 5fC and 5caC is mediated by TET dioxygenases (see (Fan *et al.* 2015) for a review and Figure 1.5 A). The reaction mediated by TET dioxygenases is α-ketoglutarate (α-KG)-dependent -dependent and requires Fe^{2+} to catalyze demethylation and release CO_2 and succinate (see (Li *et al.* 2015) for a review and Figure 1.5 A). α-KG is a TCA cycle intermediate produced from isocitrate by isocitrate dehydrogenase (IDH) (see Figure 1.6).

1.4.2 Histone methylation

Histone methylation is catalyzed by histone methyltransferases. Histone methyltransferases use S-adenosyl-methionine (SAM) as a methyl group donor and produce a methylated amino acid residue and S-adenosyl-homocycsteine (SAH) as products (See Figure 1.5 B and Figure 1.7). Histone

methylation can be removed by two classes of histone demethylases: the LSD family of FAD-dependent histone demethylases, and the JmjC class of α-KG-dependent histone demethylases (JHDM). Histone demethylation is a redox reaction. The LSD family of histone demethylases convert FAD to $FADH_2$ during the reaction. The α-KG-dependent histone demethylases remove methyl groups by a dioxygenase reaction that requires Fe^{2+}, O_2 and the metabolite α-KG (see Figure 1.5 B and Figure 1.7). JmjC domain-containing histone demethylases remove the methyl group by a decarboxylation reaction in which α-KG is converted to succinate (see (Fan *et al.* 2015) for a review and Figure 1.5 B).

1.4.3 Histone acetylation

Histone acetylation is a well characterized PTM associated with transcription. The negative charge of the acetyl group neutralizes the positively charged side chain of lysine residues, which can decrease the ionic interaction between the DNA backbone and histones, creating an open chromatin structure (Gorisch *et al.* 2005; Bannister and Kouzarides 2011). Histone acetylation is regulated by the activity of histone acetyltransferases and histone deacetylases. Histone acetyltransferases use acetyl-CoA as an acetyl group donor (see Figure 1.5 C) while histone deacetylases (HDACs) oppose the action of histone acetyltransferases by removing the acetyl group and restoring the positive charge of the lysine residue. There are four classes of HDACs: Class I-IV. Class I HDACs are most closely related to yeast Rpd3p while Class II HDACs, are related to yeast Hda1p. Class III, also named sirtuins, are homologous to yeast Sir2p while Class IV only has a single member in humans: HDAC11. Among these classes of HDACs, sirtuins use NAD^+ as a co-factor (see Figure 1.5 C and Figure 1.7) while other classes of histone deacetylases share a catalytic mechanism that requires a zinc ion (see (Bannister and Kouzarides 2011; Seto and Yoshida 2014) for a detailed review)

1.5 The role of chromatin modifications in DNA damage response

Chromatin modifications play various roles in regulation of chromatin structure and function. For example, the DNA-histone interaction between negatively charged DNA backbone and positively charged lysine and arginine residues of histones can be affected by modifications like lysine acetylation and phosphorylation that modify the charge of the side chain of the amino acid. Moreover, histone modifications can act as a platform for recruitment of proteins with specific

binding domains. For example, bromodomain-containing proteins can bind acetylated histones while chromodomain containing protein bind methylated histones (Bottomley 2004).

PTMs of histone as well as ATP-dependent chromatin remodeling complexes alter the chromatin structure to allow access to DNA replication machinery, transcription machinery and DNA repair factors (for a review see (Papamichos-Chronakis and Peterson 2013; Price and D'Andrea 2013; Hauer and Gasser 2017)). Below, I will review some of the known roles of histone variants and histone PTMs involved in DNA damage response.

1.5.1.1 H2A.X and γ-H2A.X

In mammals, H2A.X is a member of the histone H2A family. H2A.X constitutes about 10% of the total H2A in human fibroblasts (Rogakou *et al.* 1998; Bonner *et al.* 2008; Yuan *et al.* 2010). Upon, DSB, H2A.X is rapidly phosphorylated at Ser139, and its phosphorylated form, γ-H2A.X, is commonly used as a marker for DDR (Rogakou *et al.* 1998; Bonner *et al.* 2008). γH2A.X spreads bi-directionally over a large region at DSBs (up to one megabase in human cells) (Rogakou *et al.* 1999). Although *S. cerevisiae* lacks the histone variant H2A.X, the canonical histone H2A can be phosphorylated by Tel1p and Mec1p at Ser129 (Shroff *et al.* 2004). This modification is referred to as γ-H2A in budding yeast and functions equivalently to γ-H2A.X in higher eukaryotes (Shroff *et al.* 2004). γ-H2A spreads up to 50 kb on each side of DSB in yeast (Shroff *et al.* 2004). γ-H2A is required for recruitment of various DNA damage response factors including Rad9p, Rad53p, the NuA4 acetyltransferase and the INO80C chromatin remodeling complex (INO80C) to sites of damage (van Attikum *et al.* 2004; Morrison *et al.* 2004; Downs *et al.* 2004; Javaheri *et al.* 2006). γ-H2A promotes association of Rad9p and activation of Rad53p upon DNA damage and is required for delaying in cell cycle progression (Javaheri *et al.* 2006). Recruitment of INO80C to DSBs by γ-H2A promotes ssDNA formation following DSB induction (van Attikum *et al.* 2004; Morrison *et al.* 2004), and recruitment of NuA4 to DSBs by γ-H2A promotes histone H4 acetylation around DSBs (Downs *et al.* 2004). These data support a model in which γ-H2A plays an important role for multiple events following DNA damage, including histone acetylation, chromatin remodeling, DNA end resection and DNA damage checkpoint activation.

γH2A.X is detected around DSBs in mammalian cells as nuclear foci only a few minutes after irradiation (Paull *et al.* 2000). In yeast, γH2A is detectable 15 min after induction of a DSB at the

MAT locus by expression of the HO endonuclease (Lee *et al.* 2014). Elimination of γH2A at the *MAT* locus in yeast (following HO induction) is concurrent with appearance of DNA repair products (Keogh *et al.* 2006). The rate of γH2A.X disappearing is slower than the rate of foci formation as γH2A.X is detectable five hours after IR in mammalian cells (Siino *et al.* 2002), and four hours after HO induction in yeast (Keogh *et al.* 2006).

In vitro data indicate that protein phosphatase 1 (PP1) and protein phosphatase 2A (PP2A) can dephosphorylate γH2A.X (Siino *et al.* 2002; Chowdhury *et al.* 2005). Moreover, PP2A and γH2A.X can be co-immunoprecipitated after DNA damage induction in mammalian cells (Chowdhury *et al.* 2005). When protein phosphatases inhibitors are used in immunoblotting assays, γH2A.X levels induced upon DNA damage are higher and did not disappear as rapidly as compared to in the absence of inhibitors (Chowdhury *et al.* 2005), however, phosphatase inhibitors do not affect the rate of disappearance of γH2A foci formed after HO induction (Keogh *et al.* 2006). Similarly, in mammalian cells, inhibition of protein phosphatases does not affect loss of γH2A.X foci (Svetlova *et al.* 2007). These data support a model in which that γH2A.X or γH2A is dephosphorylated after being exchanged out of chromatin.

1.5.1.2 Histone variant H2A.Z

H2A.Z, termed Htz1p in yeast, is an evolutionarily conserved histone variant that shows ~60% sequence similarity with the canonical histone H2A. H2A.Z occupancy has been associated with various cellular functions including gene expression (Santisteban *et al.* 2000), gene silencing (Dhillon and Kamakaka 2000), establishment of heterochromatin boundaries (Meneghini *et al.* 2003), centromere structure (Greaves *et al.* 2007) and chromosome segregation (Rangasamy *et al.* 2004), and DNA repair (Xu *et al.* 2012; Jiang *et al.* 2015).

In yeast, Htz1p is primarily associated with promoters of both actively transcribed genes and repressed genes, and is enriched in nucleosomes flanking transcriptional start sites (Raisner *et al.* 2005) as well as near telomeres where it acts as a boundary to prevent spreading of heterochromatin (Meneghini *et al.* 2003). In mammalian cells, in addition to promoters of active and inactive genes (Bruce *et al.* 2005; Gévry *et al.* 2007), H2A.Z is also found in pericentric heterochromatin (Rangasamy *et al.* 2003), as well as at insulators (Bruce *et al.* 2005). H2A.Z is also incorporated around DSB sites in mammalian cells where it promotes histone acetylation and ubiquitination

(Xu *et al.* 2012). Similarly, Htz1p is also incorporated around DSBs, albeit transiently, and promotes DNA end resection and checkpoint activation in yeast (Kalocsay *et al.* 2009). In fact, loss of *HTZ1* is associated with increased sensitivity to DNA damaging agents and increased genome instability (Morillo-Huesca *et al.* 2010; Papamichos-Chronakis *et al.* 2011).

Deposition and removal of Htz1p is regulated by the activity of SWR-C and INO80C chromatin remodeling complexes, respectively (Krogan *et al.* 2003; Mizuguchi *et al.* 2004; Kobor *et al.* 2004). Htz1p is incorporated into chromatin by exchange of H2A-H2B dimers with Htz1p-H2B dimers by the ATP dependent chromatin remodeling complex SWR-C (Mizuguchi *et al.* 2004; Luk *et al.* 2010). The INO80C promotes exchange of H2A.Z-H2B dimers for H2A-H2B dimers by disrupting nucleosome-DNA interaction at H2A-H2B interface (Brahma *et al.* 2017).

Both SWR-C and INO80C have also been described in regulation of gene expression as well as genome integrity (Morillo-Huesca *et al.* 2010; Papamichos-Chronakis *et al.* 2011; Srivatsan *et al.* 2018). SWR-C is recruited to DSBs early after DSB induction (van Attikum *et al.* 2007). Swr1p promotes DNA end resection and *swr1*Δ mutants shows no synthetic genetic interaction with *exo1*Δ mutants in the presence of zeocin, implying that SWR-C and Exo1p function in the same pathway (Adkins *et al.* 2013). INO80C removes H2A.Z from DSB sites in human cells and promotes DNA repair by HR (Alatwi and Downs 2015). H2A.Z has also been described in DNA end resection. Incorporation of H2A.Z in nucleosomes enhances nuclease activity of Exo1p *in vitro* (Adkins *et al.* 2013). Moreover, deletion of *HTZ1* or *SWR1* decreases the amount of ssDNA generated after induction of DSBs (Kalocsay *et al.* 2009; Adkins *et al.* 2013; Lademann *et al.* 2017). INO80C promotes formation of Rad51p nucleofilaments around DSBs, and mutants lacking *ARP8* (a subunit of INO80C complex that binds to core histones and is required for nucleosome mobilization by INO80C (Shen *et al.* 2003)) show reduced enrichment of Rad51p which can be partially restored by deletion of *HTZ1* or *SWR1* (Lademann *et al.* 2017). Therefore, Htz1p plays an important role in both early and late steps of DNA repair by HR. Moreover, in mammalian cells, H2A.Z promotes KU70 association with regions around DSBs and increases efficiency of DNA repair by NHEJ (Jiang *et al.* 2015).

1.5.1.3 Regulation of histone post-translational modifications

Several histone methyltransferases, demethylases and histone methylation sites have been described in DNA damage response. Here, I will mainly focus on histone methylation modifications found in yeast and their known roles in DNA damage response.

H3 K4 methylation: In budding yeast, H3 K4 mono- di- and tri- methylation is mediated by Set1p, the sole H3 K4 histone methyltransferase in *S. cerevisiae* (Briggs *et al.* 2001). H3 K4 methylation is mostly associated with promoters as well as coding regions of actively transcribed genes (Santos-Rosa *et al.* 2002; Ng *et al.* 2003). However, mutants with defects in H3 K4 methylation show negative synthetic genetic interactions with mutants lacking components of the MRX complex (complex involved in initiation of DNA end resection during HR, see Section 1.2.1.2 and Figure 1.2) consistent with a role for H3 K4 methylation in DNA damage response (Faucher and Wellinger 2010). Histone H3 K4me3 and Set1p are detected at DSBs and promote DNA repair by NHEJ (Faucher and Wellinger 2010). Moreover, in humans, KDM5A and KDM5B, the H3 K4me2 and me3-specific histone demethylases are associated with chromatin following radiation and promote association of KU70 and BRCA1 with DSBs (Seiler *et al.* 2011; Li *et al.* 2014).

H3 K36 methylation: H3 K36 methylation is commonly found in gene bodies but is also involved in various aspects of DNA damage response. Set2p (in yeast) or SETD2 (in mammalian cells) is the sole H3 K36 specific histone methyltransferase (Edmunds *et al.* 2008). Depletion of STED2 results in increased sensitivity to DNA damaging agents like IR, and reduced numbers of RPA and RAD51 foci formed after IR (Pfister *et al.* 2014). In addition, yeast strains lacking *SET2* show sensitivity to phleomycin (a DSB inducing DNA damage agent) (Jha and Strahl 2014). *set2*Δ mutants, are also sensitive to persistent DSB induction at the *MAT* locus by HO endonuclease compared to wild-type and have defects in DNA repair by NHEJ as measured by plasmid re-ligation assay (Jha and Strahl 2014). In *Schizosaccharomyces pombe*, acetylation and methylation of H3 K36 are cell cycle-regulated. H3 K36 acetylation is mediated by the Gcn5 histone acetyltransferase, and predominantly occurs during S/G_2,whereas H3 K36 methylation is catalyzed by Set2 and H3 K36me3 is mainly found in G_1 (Pai *et al.* 2014). H3 K36ac by Gcn5 promotes formation of RPA and Rad51 foci (in the HR pathway) as well as survival after IR exposure while H3 K36me3 promotes repair by NHEJ (Pai *et al.* 2014). These results indicate that histone PTMs

play a role in genome integrity as well as in DNA repair pathway choice during different stages of the cell cycle (see Section 1.2.1.3).

H3 K79 methylation: The best characterized role of H3 K79 methylation is in DNA damage checkpoint activation. The DNA damage checkpoint mediator Rad9p binds to H3 K79 methylation through its tandem tudor domain (Giannattasio *et al.* 2005; Wysocki *et al.* 2005). Binding of Rad9p to H3 K79 methylation promotes phosphorylation of Rad9p by Mec1p kinase (ortholog of human ATR). Phosphorylated Rad9p promotes recruitment of the effector kinase Rad53p and phosphorylation and activation of Rad53p by Mec1p (Giannattasio *et al.* 2005; Wysocki *et al.* 2005) (see Section 1.2.1.4). Mutation of H3 K79, the tudor domain of Rad9p or deletion of *DOT1*, the H3 K79-specific histone methyltransferase in yeast, results in defects in DNA damage checkpoint activation and increased sensitivity to irradiation (Game *et al.* 2005; Giannattasio *et al.* 2005; Wysocki *et al.* 2005).

1.5.1.4 Histone demethylases in DNA damage response

Increasing evidence show that histone demethylases play a role in DNA damage response (in addition to other cellular processes including gene expression and DNA replication) (see (Cloos *et al.* 2008; Black *et al.* 2012, 2013)). Interestingly, several histone demethylases have been described as oncogenic factors and overexpression of histone demethylases is found in different types of human cancer (Yang *et al.* 2010; Pedersen and Helin 2010; Shi *et al.* 2011; Black *et al.* 2012). Here, I will discuss some of the findings on the roles of histone demethylases in DNA damage response.

KDM4D, a human JmjC domain containing histone demethylase (which can remove H3 K9 and H3 K36 methylation), is recruited to sites of DNA damage following irradiation (Khoury-Haddad *et al.* 2014). Depletion of KDM4D sensitizes the cells to IR, causes defects in DNA damage-induced phosphorylation of several ATM substrates including γ-H2A.X and formation of RAD51 and 53BP1 foci (Khoury-Haddad *et al.* 2014).

KDM5B, a JmjC domain-containing histone demethylase in human, has also been described in DNA damage response. A study by Li *et al.* demonstrated KDM5B accumulates at DSBs and depletion of KDM5B sensitizes the cells to IR, impairs recruitment of Ku70 to site of DNA damage

and decreases efficiency of both HR and NHEJ (Li *et al.* 2014). Catalytic activity of KDM5B was shown to be required for its role in DNA damage response (Li *et al.* 2014).

The results of our studies also point to a role for yeast Jhd2p in DNA replication stress (see Section 3.2.4). This is the first report for the role of a yeast histone demethylase in DNA damage response indicating that this function is conserved between organisms.

1.6 The link between chromatin modifications and metabolism

Histone and DNA methylation are interconnected with metabolites as histone and DNA methyltransferases utilize SAM as a methyl donor. SAM is synthesized in the cytosol using methionine and ATP. Dietary supplementation, or deficiencies in methyl donors or deficiencies precursors have been linked to changes in DNA and histone methylation in animal models (Zhang 2015). High dietary intake of methyl donors can modulate global DNA methylation levels in a tissue-specific manner (Pogribny *et al.* 2006a; Zhang 2015). A methyl deficient diets in rats caused global hypermethylation DNA in the brain and global hypomethylation of DNA in the liver (Pogribny *et al.* 2006a). In another study, a methyl deficient diet caused a loss of CpG methylation in repetitive DNA elements, decreased H4 K20 trimethylation levels as well as decreased expression of the H4 K20-specific histone methyltransferase (Suv4-20h2) in rats (Pogribny *et al.* 2006b).

Histone acetyltransferases use acetyl-CoA as an acetyl group donor, while sirtuins use NAD^+ as a co-factor. Acetyl-CoA feeds into the TCA cycle during conversion of oxaloacetate to citrate (see Figure 1.6), and is also used as a building block for production of macromolecules. The level of acetyl-CoA is dynamic and can be affected by nutrient availability. For example, using yeast metabolic cycle that synchronizes the cell population in quiescent-like phase or growth cycle, nutrient rich medium promotes production of acetyl-CoA, histone acetylation and expression of genes related to growth and entry into growth from a quiescent-like phase (Cai *et al.* 2011). These studies highlight the link between histone modifications and DNA methylation

and nutrition, and illustrate how chromatin modification states can be modulated by changes in metabolite availability.

1.7 Role of metabolic enzymes and metabolites in regulation of chromatin modifications

Metabolism can respond to internal or external signals to meet the metabolic needs of the cell and promote adaptation to environmental changes. Metabolism can also directly or indirectly influence chromatin modifications and regulate chromatin functions as discussed above in Section 1.6. R-2-HG is an oncometabolite that accumulates in cancer cells containing neomorphic mutations in genes encoding isocitrate dehydrogenase (*IDH1* and *IDH2*). Isocitrate dehydrogenase converts isocitrate to α-KG (see Figure 1.6), and mutations in *IDH* are commonly found in gliomas and acute myeloid leukemia (AML) (Dang *et al.* 2009; Gross *et al.* 2010; Ward *et al.* 2010). Succinate and fumarate also accumulate to millimolar levels in tumors containing loss of function mutations in genes encoding succinate dehydrogenase (*SDH*) or fumarate hydratase (*FH*). SDH converts succinate to fumarate (see Figure 1.6) Fumarate hydratase (*FH*) converts fumarate to malate in the TCA cycle (see Figure 1.6) (Pollard *et al.* 2005; Xiao *et al.* 2012).

2-HG, fumarate and succinate are structurally related to α-KG, and act as competitive inhibitors of α-KG-dependent dioxygenases (Xu *et al.* 2011; Xiao *et al.* 2012). Inactivation of SDH and accumulation of succinate results in an increase in steady-state levels of histone methylation, that can be reversed by treatment with α-KG (Smith *et al.* 2007; Cervera *et al.* 2009; Xiao *et al.* 2012). Similarly, inactivation of FH and accumulation of fumarate increases the level of methylated histone H3 (Jiang *et al.* 2015). As illustrated here, and in Section 1.6, dietary and cancer-associated changes in cellular levels of metabolites, or production of oncometabolites, link nutrition and metabolism to chromatin modifying enzymes and chromatin-associated functions.

1.8 Role of fumarase in DNA damage response

Fumarate hydratase (also named fumarase, FH) is an enzyme in the TCA cycle that catalyzes the reversible hydration/dehydration of fumarate to malate (see Figure 1.6). Fumarase is also found in the cytosol in yeast and human (Yogev *et al.* 2011). In yeast, both cytosolic and mitochondrial fumarase are encoded by the same gene, *FUM1*, located on chromosome 16 (Knox *et al.* 1998; Sass *et al.* 2001). The premature Fum1p contains a mitochondrial targeting sequence that is

processed in the mitochondrial matrix. A fraction of the mature fumarase is translocated back to the cytosol by retrograde movement (Knox *et al.* 1998; Sass *et al.* 2001).

In addition to its role in the TCA cycle, fumarase has also been described in DNA damage response in both yeast and human cells (Yogev *et al.* 2010; Jiang *et al.* 2015; Leshets *et al.* 2018). In yeast, cytoplasmic form of Fum1p localizes to the nucleus upon DNA damage, and expression of fumarase exclusively in mitochondria causes sensitivity to various DNA damage agents (Yogev *et al.* 2010). In addition, Fum1p interacts with the Sae2p (Sae2p interacts with the MRX complex and enhances the endonuclease activity of Mre11p (see Figure 1.2)) and stabilizes Sae2p protein levels, promotes DNA end resection, and DNA repair by HR (Leshets *et al.* 2018). Our studies point to a role for yeast fumarase in response to DNA replication stress (see Section 3.2) as well as induction of DSBs (see Section 4.2).

In mammalian cells, fumarase binds to chromatin around DSB sites through interaction with the histone variant H2A.Z. Production of fumarate by chromatin-associated fumarase promotes binding of KU70, and DNA repair by NHEJ by inhibition of the H3 K36-specific histone demethylase KDM2B (Jiang *et al.* 2015) (see Figure 1.8).

1.9 Objective

The objective of this thesis was to understand the link between metabolism and metabolite availability, regulation of chromatin modifying enzymes and how this relationship impacts genome integrity. Here, using *S. cerevisiae*, we studied the role of the TCA cycle enzyme fumarase and availability of the metabolite fumarate in modulation of the DNA damage response. We have used mutants with defects in different pathways and steps of the DNA damage response and evaluated how loss of the TCA cycle enzyme fumarase or addition of exogenous fumarate affects DNA damage sensitivity upon DNA replication stress and DSBs.

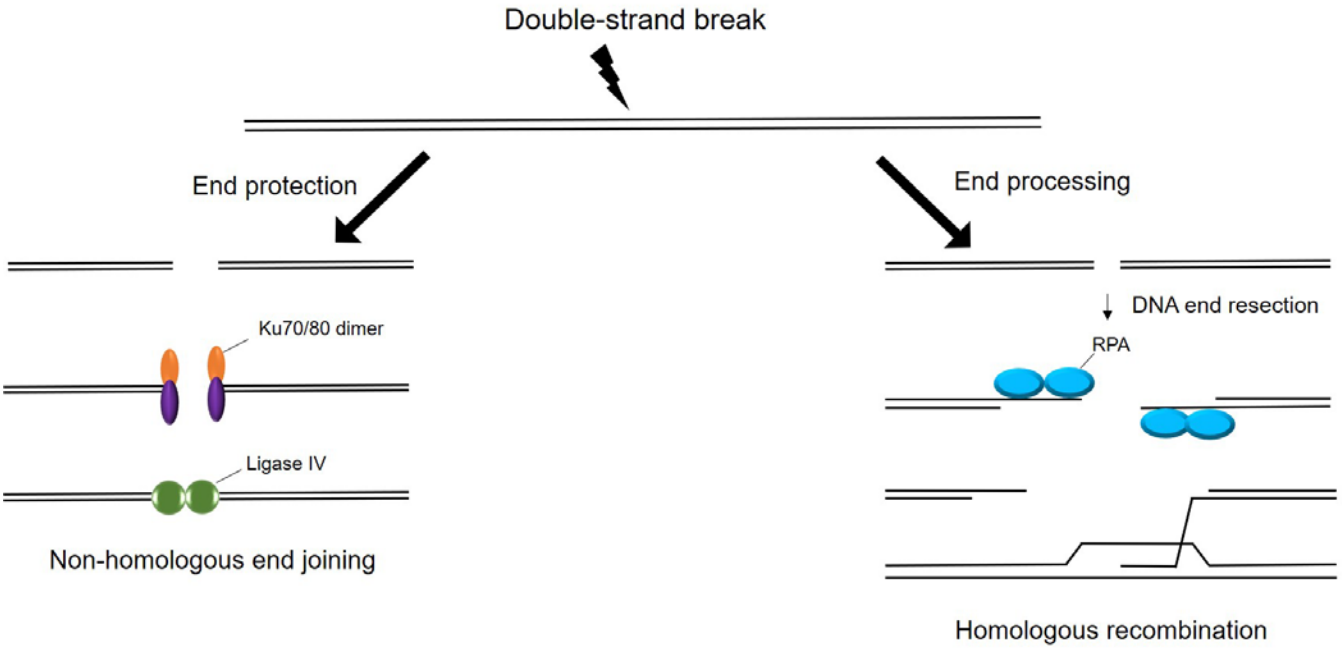

Figure 1.1 Two major pathways for repair of DSBs.

Following DSBs, DNA can be repaired by non-homologous end joining (NHEJ) or homologous recombination (HR). During NHEJ, the DNA ends are protected from exonucleases by binding of Ku70/80 dimer. DNA ends are joined by the activity of DNA ligase IV. During HR, DNA ends are processed by exonucleases creating ssDNA which is bound by the ssDNA binding heterotrimeric protein complex RPA. RPA is next displaced allowing formation of nucleoprotein filaments, strand invasion, DNA synthesis and repair.

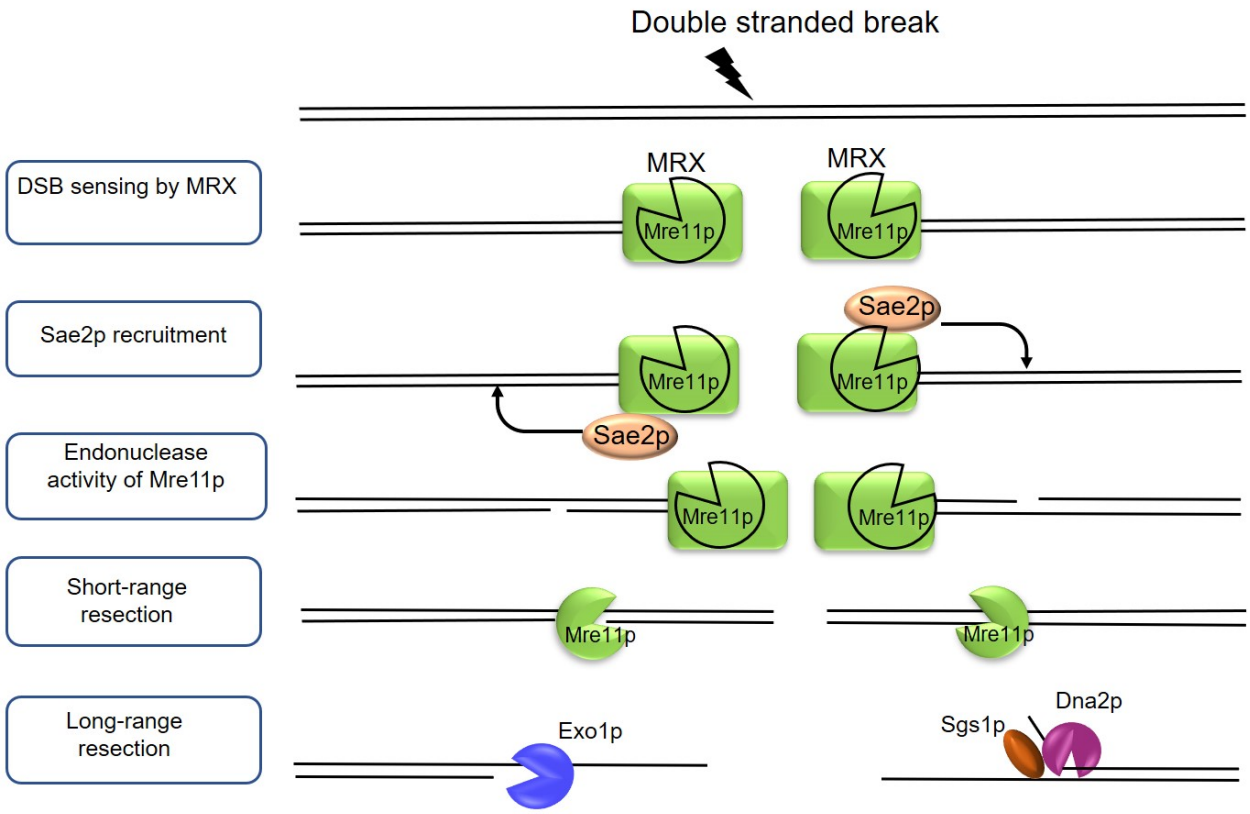

Figure 1.2 Choreography of events during DNA end resection following DSB.

MRX is first recruited to sites of DSB. The endonuclease activity of Mre11p is stimulated by Sae2p creating a nick near DSBs. Next, the 3' to 5' exonuclease activity of Mre11p removes DNA towards the break creating short stretches of ssDNA. Two parallel pathways mediate long range DNA end resection: Exo1p, and Dna2p (which works in conjunction with the Sgs1p helicase). Exo1p and Dna2p have 5' to 3' exonuclease activity and mediate the long-range DNA end resection.

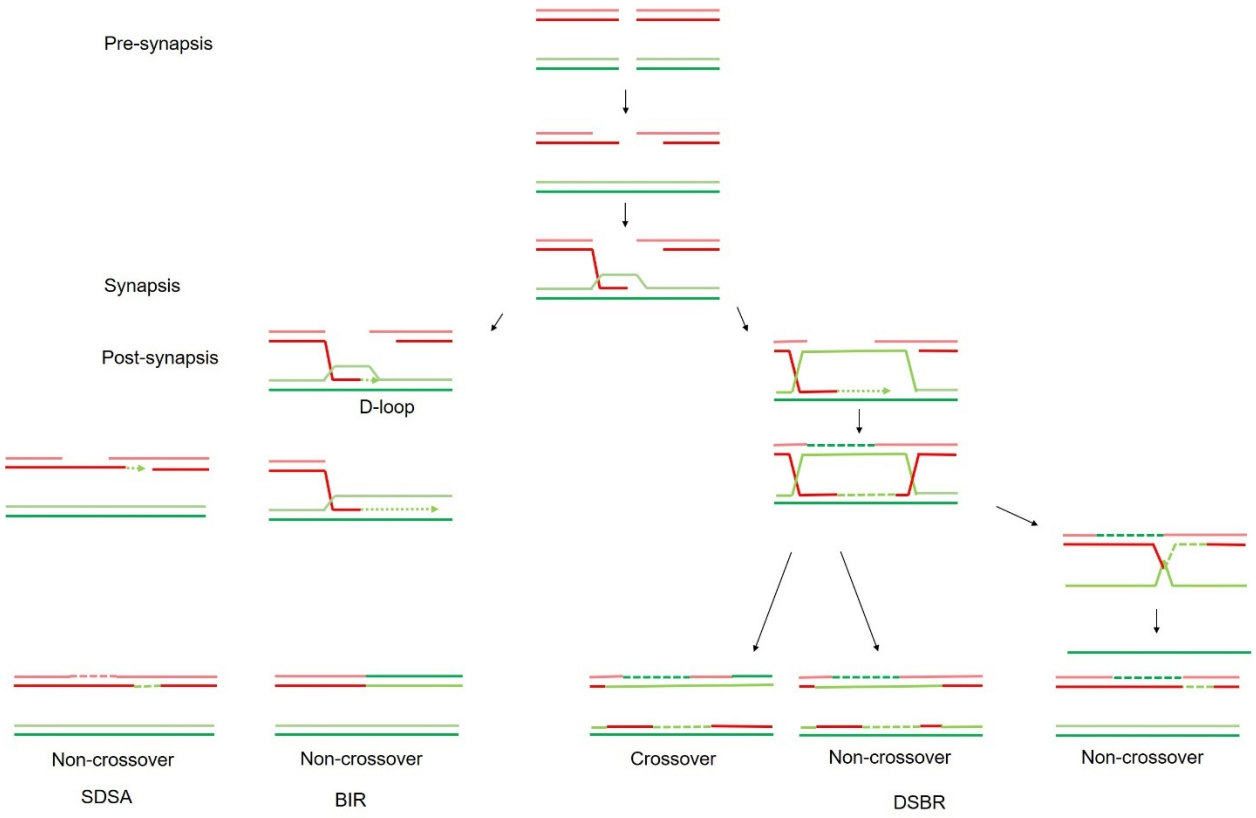

Figure 1.3 Mechanisms for repair of DSBs by HR.

HR can be divided into three steps: pre-synapsis, synapsis and post-synapsis. In pre-synapsis, DSBs are processed by DNA end resection factors which creates 3' ssDNA overhang. In synapsis, strand invasion by Rad51p-coated ssDNA creates a D-loop structure. In post-synapsis, the D-loop can be repaired by at least three different pathways: 1) Synthesis-Dependent Strand Annealing (SDSA) in which the invading strand is removed from the D-loop and annealed to the second end of the break. This annealing is facilitated by Rad52p. The product of SDSA is non-crossover. 2) Break Induced Repair (BIR) in which the D-loop is used to form a replication fork, and the entire chromosome arm is synthesized using the homologous chromosome. BIR leads to a non-crossover product and can cause loss-of-heterozygosity. 3) DSB Repair (DSBR) in which both ends of DSB are engaged and a double Holliday junction is formed. Next, the double Holliday junction can be resolved into a cross-over or a non-crossover product.

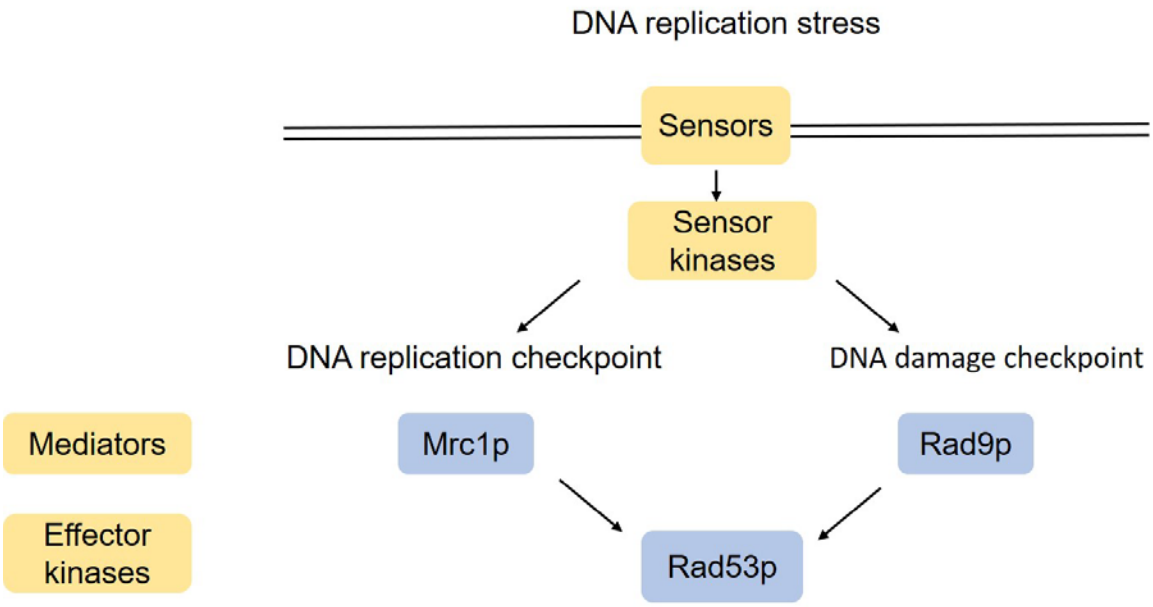

Figure 1.4 Two branches to intra-S phase checkpoint.

DNA replications stress can activate signaling pathways leading to phosphorylation and activation of the effector kinase Rad53p. Although the two pathways respond to different signals but elicit the same cellular response (see Section 1.3 for a more detailed discussion.

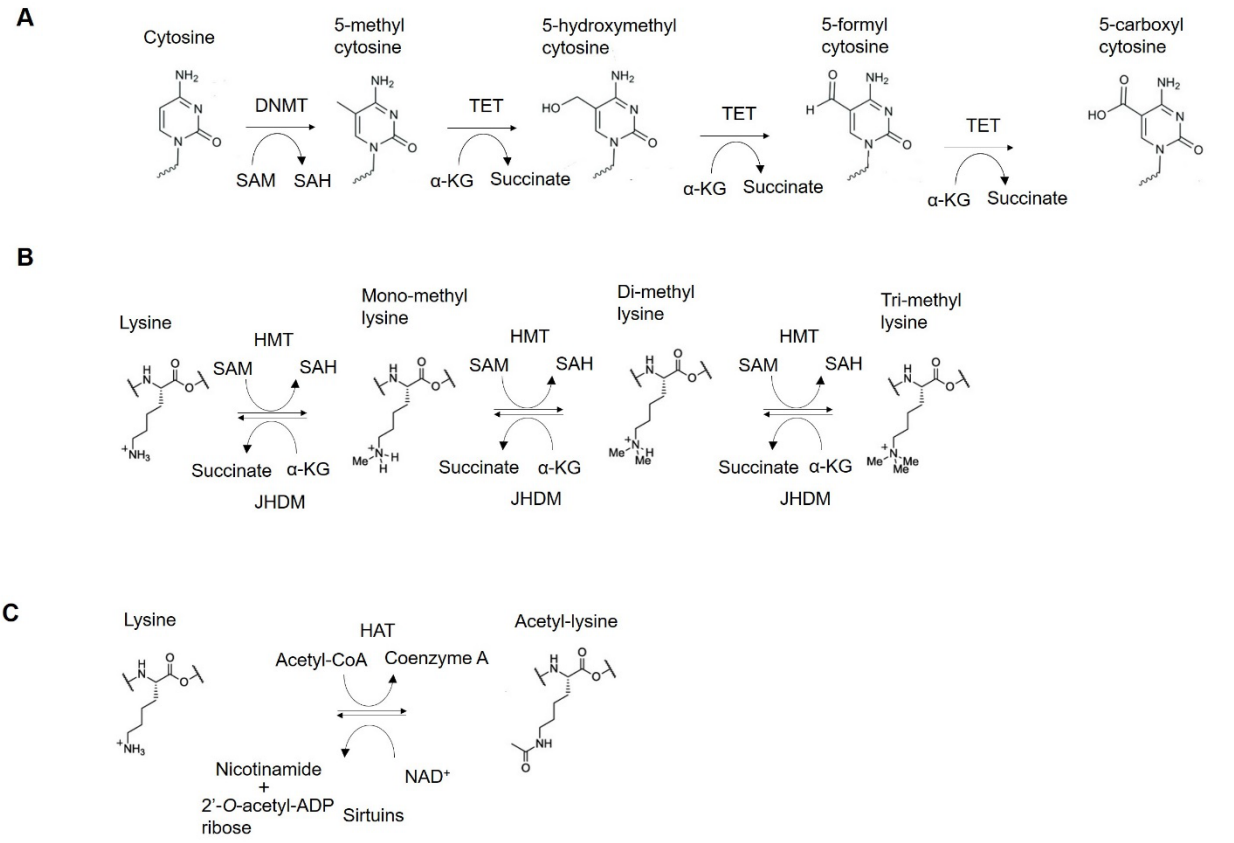

Figure 1.5 Reactions catalyzed by chromatin modifying enzymes

A) DNMTs transfer methyl group from SAM to the 5-carbon of the cytsone to create 5-methyl cytosine. This reaction produces SAH as a product. TET dioxygenases use α-KG as a co-substrate to remove the methyl group from 5-methyl cytosine creating 5- hydroxymethyl cytosine, 5-formylcytosine and 5-carboxycytosine. B) HMTs transfer methyl group from SAM to the lusine residue of histones producting SAH as a product while JHDMs convert α-KG to succinate when removing a methyl group from methylated lysine residues. HATs transfer acetyl group from Acetyl-CoA to lysine residues. C) Sirtuins use NAD+ as a co-factor to remove acetyl groups D) LSD family of histone deacetylases reduce FAD to $FADH_2$.

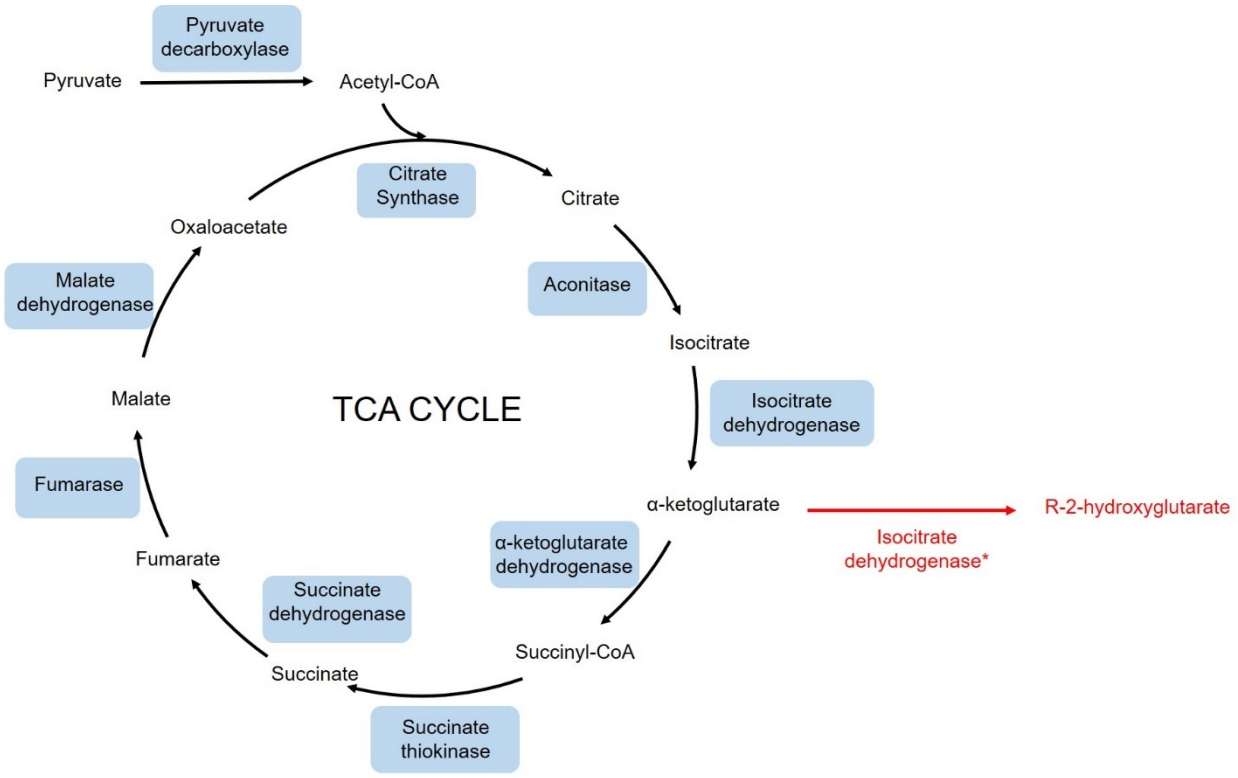

Figure 1.6 TCA cycle, pyruvate dehydrogenase and mutant isocitrate dehydrogenase reactions

Enzymes discussed in the text: isocitrate dehydrogenase, converts isocitrate to α-ketoglutarate. Succinate dehydrogenase: converts succinate to fumarate. Fumarate: converts fumarate to malate. The black arrows show reactions that occur in a normal cell. The red arrow shows a reaction that can occur in tumor cells containing a neomorphic mutation in isocitrate dehydrogenase. Neomorphic isocitrate dehydrogenase converts α-ketoglutarate to 2-hydroxyglutarate.

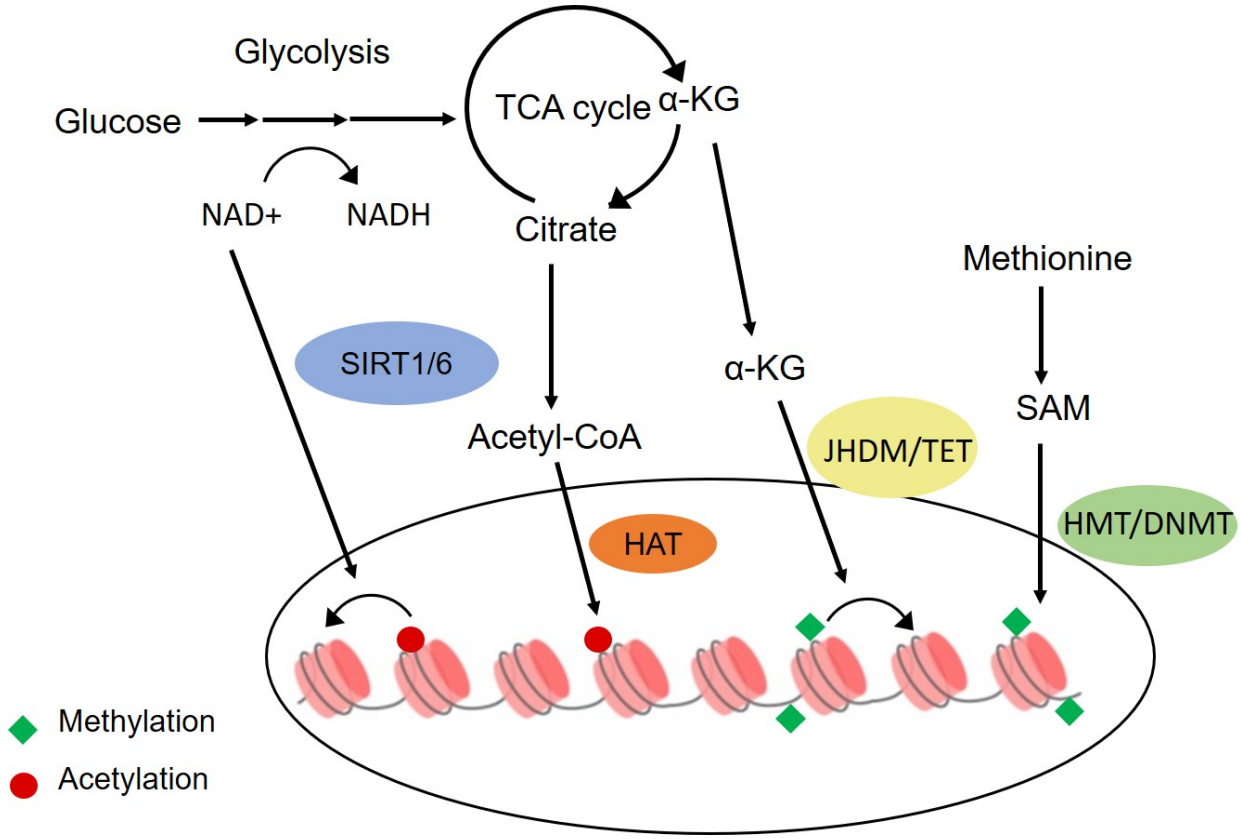

Figure 1.7 Chromatin-modifying enzymes use metabolites as co-factors or co-substrtates.

Sirtuins (a class of histone deacetylases) like SIRT1 and SIRT6 use NAD+ as a cofactor. Histone acetyltransferases use Acetyl-CoA as acetyl group donor. JmjC domain histone demthylases and TET dioxygenases use α-ketoglutarate as a co-substrate. Histone and DNA methyltransferases use SAM as a methyl group donor.

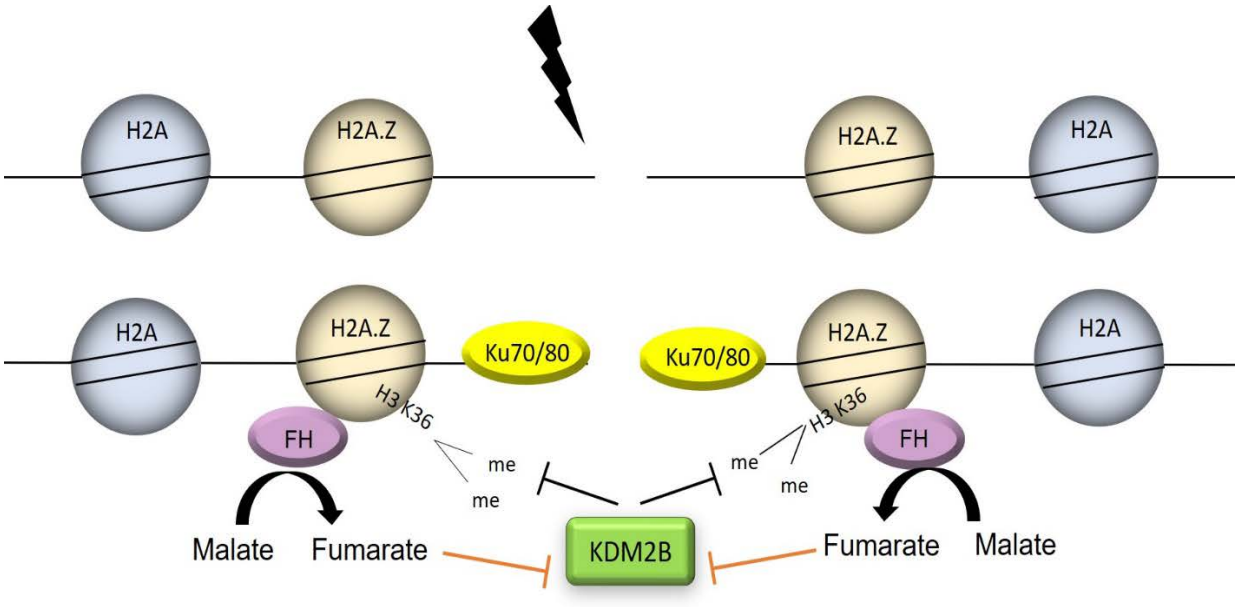

Figure 1.8 Role of mammalian fumarate hydratase (FH) in DNA repair by NHEJ.

FH is recruited to sites of DSB through interaction with the histone variant H2A.Z. Activity of chromatin-associated FH and production of fumarate promotes association of NHEJ factors including KU70 and increases efficiency of DNA repair by NHEJ. FH and fumarate promote NHEJ by inhibition of the JmjC domain-containing histone demethylase KDM2B, a histone demethylase responsible for removal of H3 K36 methylation.

CHAPTER 2. MATERIALS AND METHODS

2.1 Yeast strains and plasmid construction

Yeast strains and plasmids used in this study are listed in Table 2.1 and Table 2.2, respectively. Oligonucleotides used to generate yeast strains or plasmids are listed in Table 2.3. Yeast strains containing deletions of open reading frames were generated by standard PCR-based gene disruption strategies (Guthrie and Fink 1991). Plasmids containing histone mutants were generated by site-directed mutagenesis (described below) and confirmed by sequencing. pAK1330 was generated using pAK875 as template, and oligonucleotides oALK1628 and oALK1629. pAK1331 was generated using pAK278, and oligonucleotides oALK1628 and oALK1629. pAK1338 was generated using pAK875, and oligonucleotides oALK1648 and oALK1649. pAK1339 was generated using pAK875, and oligonucleotides oALK1650 and oALK1651. pAK1341 was generated using pAK872, and oligonucleotides oALK1650 and oALK1651. Strains expressing histone mutants were made by plasmid shuffling (Adams *et al.* 1998).

2.2 Site-directed mutagenesis

Plasmids containing histone mutants were generated using the Single-Primer Reactions IN Parallel (SPRINP) (Edelheit *et al.* 2009). Briefly, parental plasmids were amplified by PCR in two separate reactions using either the forward or reverse primer and Phusion DNA polymerase (NEB Cat. no. M0530S). Two single-primer PCR products were combined and denatured at 95°C to separate the newly synthesized DNA from the template strand. Next, the reactions were gradually cooled to allow re-annealing. Mixed reactions were amplified for 10 additional cycles using Phusion DNA polymerase. DNA was treated with DpnI (NEB Cat. no. R0176S) to digest the parental plasmid, and then was transformed into competent DH5α cells by electroporation.

2.3 Growth assay of sensitivity to DNA damaging agents

Cells were grown overnight in rich (YPD) medium, diluted to 10^4 cells/µL and three µL of 10-fold serial dilutions were spotted onto YPD containing 2×PBS (274 mM NaCl, 16 mM Na_2HPO_4, 4 mM KH_2PO_4, 5.4 mM KCl) with or without noted amounts of HU or monoethyl fumarate (Sigma, Cat. no. 128422). Images were taken after two to three days of growth at 30°C.

2.4 Preparation of yeast nuclear extracts

Nuclear extracts were prepared from 200 mL cultures grown in YPD to an OD_{600} of 0.6 and treated with or without 200 mM HU for three hours as described by Miller *et al*. (Miller *et al.* 2008). Briefly, cells were harvested, washed with ice-cold water and resuspended in three mL of spheroplasting buffer (1 mM sorbitol, 50 mM potassium phosphate pH=6.5 (containing 34 mM K_2HPO_4 and 65 mM KH_2PO_4, 14 mM β-mercaptoethanol). Next, cells were pelleted, resuspended in three mL of spheroplasting buffer containing 5 mg/mL of lyticase (Sigma, Cat. no. L4025), and then incubated at 30°C until spheroplasted. Sepheroplasted cells were pelleted at 5000×g for five min at 4°C, and then washed in three mL of spheroplasting buffer. Cells were pelleted, resuspended in five mL of lysis buffer (18% Ficoll 400, 20 mM potassium phosphate pH=6.8 (containing 49 mM K_2HPO_4 and 51 mM KH_2PO_4), 1 mM $MgCl_2$, 0.5 mM EDTA, 1 mM PMSF, 1 µg/mL Leupeptin/Pepstatin mix), lysed with 20 strokes using a Dounce homogenizer, and spun at 3000×g for 10 min. to remove cell debris. The nuclei were pelleted at 50,000×g for 30 min at 4°C using a SW-41 rotor. Nuclei were resuspended in 200 µL of NP buffer (0.34 mM Sucrose, 20 mM KCl, 5 mM $MgCl_2$, 1 mM PMSF, 1.0 µg/mL Leupeptin/Pepstatin mix) for storage at 4°C.

2.5 Preparation of whole cell extracts

Three mL of yeast cultures grown overnight in YPD to an OD_{600} of 0.8 were harvested, flash frozen on dry ice and stored at -80°C. Cell pellets were resuspended in 250 µL of 2.0 M NaOH containing 8% β-mercaptoethanol, incubated in ice for five min. and pelleted by centrifugation at 14,500×g at 4°C for two min. Cell pellets were resuspended in 250 µL of high salt extraction buffer (40 mM HEPES NaOH pH=7.5, 350 mM NaCl, 0.1% Tween 20, 10% glycerol), and re-pelleted by centrifugation at 14,500×g at 4°C for two min. Pellets were resuspended in 2×SDS loading dye (200 mM Tris-HCl pH=6.8, 20% SDS, 20% glycerol, 0.08% bromophenol blue, 10% β-mercaptoethanol), prior to loading onto 7% and 12% SDS-PAGE gels for immunoblotting (see below).

2.6 Immunoblotting

2.6.1 Analyses of Fum1-GFP Localization.

Whole cell extracts or nuclear fractions were prepared from logarithmically growing cultures (as described above) from indicated genotypes and treated with or without 200 mM HU for three hours, and separated by electrophoresis on 12% SDS-PAGE gel. Following electrophoresis, proteins were transferred to PVDF membrane that had been pre-soaked in methanol for five min. followed by soaking in transfer buffer (25 mM Tris and 1.44% glycine pH=8.3, 20% methanol, 0.02% SDS). Next, membranes were incubated with 5% milk in PBS-T (137 mM NaCl, 8 mM Na_2HPO_4, 2 mM KH_2PO_4, 2.7 mM KCl, 0.1%Tween 20) for one hour at room temperature followed by incubation with anti-GFP antibody (Abcam ab290, 1:5000 in 2% milk in PBS-T) overnight at 4°C. Membranes were washed three times in PBS-T for 10 min each. ECL anti-rabbit Horseradish-peroxidase-linked IgG (Cat. no. NA934; Amersham) was used as secondary antibody at 1:10,000 dilution in 2% milk in PBS-T. Membranes were washed again as above and visualized by adding one mL Luminata Crescendo Western HRP Substrate (Millipore Cat. no. WBLUR0500) on the membrane for one min followed by imaging using the ChemiDoc XRS+. Blots were then quantified using Image Lab™ software. Membranes were stripped by 0.2 M NaOH at room temperature and re-probed with anti-proliferating cell nuclear antigen (1:10,000 in 2% milk in PBS-T) antibody (Daganzo *et al.* 2003; Franco *et al.* 2005) and ECL anti-rabbit Horseradish-peroxidase-linked IgG (Cat. no. NA934; Amersham) as secondary antibody at 1:10,000 dilution in 2% milk in PBS-T. Fold enrichment of Fum1p was calculated relative to PCNA as shown in Figure 3.1 legend.

2.6.2 Analyses of Rad53p phosphorylation.

Logarithmically growing cells were treated with noted amounts of hydroxyurea (HU) or zeocin with or without 5 mM monoethyl fumarate in YPD containing 2×PBS. In the case of HU, aliquots of 3×10^7 cells were collected before, and every two hours after treatment for eight hours. For zeocin, 4×10^7 cells were collected before, and every two hours after treatment for 16 hours. Whole cells extracts were prepared as described above, then loaded onto 7 % SDS-PAGE gels. Proteins were transferred to PVDF membranes as described above. Membranes were blocked in 5% milk in PBS-T for one hour at room temperature, then incubated with anti-Rad53p antibodies (Abcam ab104232, 1:2000 in 2% milk in PBS-T) overnight at 4°C. Membranes were washed three times

in PBS-T for 10 min each, followed by incubation with ECL anti-rabbit Horseradish-peroxidase-linked IgG (1:10,000 in 2% milk in PBS-T). Blots were developed and imaged as described above.

2.6.3 Analyses of H3 K4 methylation levels

1×10^7 cells from logarithmically growing cultures were harvested before and after a one-hour treatment with 5 mM monoethyl fumarate. Whole cell extracts were prepared as described above, and separated on 12% SDS-PAGE gels. Transfer and blocking steps were performed as described above and membranes were incubated with anti-H3K4me3 antibodies (Active motif 39159 1:5000 in 2% milk in PBS-T) for one hour at room temperature. Membranes were washed, incubated with ECL anti-Rabbit secondary antibodies, developed and imaged as described above. Membranes were stripped and re-probed using anti-H3 (Abcam ab1791, 1:5000 in 2% milk in PBS-T) antibodies and ECL anti-Rabbit secondary antibodies as described above. Blots were developed and imaged as above.

2.6.4 Statistical analysis.

H3 K4 me3 levels were normalized to H3 levels and statistical analyses were conducted using the Wilcoxon rank sum test with MSTAT v6.3 as outlined in Figure 3.9

2.7 Analysis of cell cycle by flow cytometry

Logarithmically growing cells with the indicated genotypes were grown at 30°C in rich medium (YPD) to OD_{600} ~0.4. Cells were arrested in G_1 by addition of α-factor at final concentration of 10 µg/mL for three hours. cells were washed three times with YPD, resuspended in YPD containing 2×PBS and 100 µg/mL protease, and treated with 100 or 200 mM HU, with or without 5 mM monoethyl fumarate. One mL of cells was collected prior to HU treatment, and again every 20 min after release from G_1 for four hours. Cells were pelleted by centrifugation, resuspended in 70% ethanol, and incubated at room temperature for one hour before storing overnight at 4°C. Cells were then washed twice in FACS buffer (200 mM Tris-HCl pH 7.5, 20 mM EDTA), and resuspended in 100 µL of FACS buffer containing 0.1% RNase, then incubated for two hours at 37°C. Cells were washed with 1×PBS, and incubated in 100 µL of propidium iodide solution (0.05 mg/mL propidium iodide in 1×PBS) overnight in the dark at 4°C. Prior to analysis, 400 µL of

1×PBS was added to each sample. Samples were briefly sonicated (Branson Sonifier 450, VWR Scientific) and analyzed by Beckman Coulter Cytoflex S, and FlowJo software (version 7.6.5).

2.8 Measuring efficiency of NHEJ by plasmid re-joining Assay

The yeast centromeric plasmid pAK54 was digested with the restriction enzymes SmaI or XbaI. Linearized DNA was purified by electrophoresis and isolated by extraction using QIAquick Gel Extraction kit (Qiagen). 120 ng of the linearized plasmid was transformed into indicated strains using lithium acetate. Briefly, 5×10^6 cells from each strain were resuspended in 30 µL of 0.1 M lithium acetate. 120 ng of linearized plasmid and 270 µL of PEG/TEL (40% PEG3000, 0.1 M lithium acetate, 10 mM Tris-HCl pH=8.0 and 1 mM EDTA) was added. After incubation at 30°C for 1 hour, cells were heat shocked at 42°C for 10 minutes and plated onto complete synthetic media lacking histidine. Colonies were counted after incubation at 30°C for three days. To determine the transformation efficiency, transformation with undigested plasmid was done in parallel and the re-joining efficiency was determined as the ratio of number of colonies obtained by using the linearized plasmid divided by the number of colonies obtained using circularized plasmids and normalized to wild-type. The average and standard deviation of re-joining efficiency for three independent measurements were reported.

2.9 Analysis of RPA foci formation

To analyze the number of cells containing RPA foci, yeast strains expressing a subunit of RPA C-terminally tagged with GFP (Rfa1p-GFP) were grown in complete synthetic media. Logarithmically growing cultures were exposed to 20µg/mL zeocin in the presence or absence of 5 mM fumarate. Aliquots were collected before and 30 min, one hour, two hours and four hours after treatment. Cells were harvested by centrifugation, washed twice with 1×PBS and fixed by incubation with 4% paraformaldehyde for 15 min. Next, cells were washed once in phosphate/sorbitol buffer (84 mM K_2HOP_4, 16 mM KH_2PO_4, 1.2M sorbitol, pH=7.5) and resuspended in 100µL of phosphate/sorbitol buffer. Cells were then sonicated for three seconds and visualized by Olympus BX51 fluorescence microscope. For each timepoint and condition, RPA foci formation was analyzed for at least 100 cells and the average and standard deviation of two independent experiments were reported.

Table 2.1 List of yeast strains used in this study

Strain	Genotype	Source
AKY42	*MAT*a *his3*Δ1 *leu2*Δ0 *met15*Δ0 *ura3*Δ0 (BY4741)	(Baker Brachmann *et al.* 1998)
AKY5078	AKY42 *htz1*Δ::*KanMX*	(Winzeler *et al.* 1999)
AKY6320	AKY42 *fum1*Δ::*KanMX*	(Winzeler *et al.* 1999)
AKY6384	*MAT***a** *his3*Δ1 *leu2*Δ0 *met15*Δ0 *ura3*Δ0 *FUM1-GFP(S65T)-HIS3MX*	(Huh *et al.* 2003)
AKY6405/ AKY6406	AKY6320 *htz1*Δ::*URA3*	This study
AKY6427	AKY42 *rad52*Δ::*KanMX*	(Winzeler *et al.* 1999)
AKY6428	AKY42 *yku70*Δ::*KanMX*	(Winzeler *et al.* 1999)
AKY6576/ AKY6577	AKY5078 *yku70*Δ::*NatMX*	This study
AKY6584	AKY42 *mre11*Δ::*KanMX*	(Winzeler *et al.* 1999)
AKY6585	AKY42 *rad50*Δ::*KanMX*	(Winzeler *et al.* 1999)
AKY6309	AKY42 *jhd1*Δ::*KanMX*	(Winzeler *et al.* 1999)
AKY6310	AKY42 *jhd2*Δ::*KanMX*	(Winzeler *et al.* 1999)
AKY6311	AKY42 *rph1*Δ::*KanMX*	(Winzeler *et al.* 1999)
AKY6701/ AKY6702	AKY6309 *htz1*Δ::*URA3*	This study
AKY6697/ AKY6698	AKY6310 *htz1*Δ::*URA3*	This study

Table 2.1 continued

AKY8712/ AKY8713	AKY6311 *htz1*Δ::*URA3*	This study
AKY6973	AKY42 *exo1*Δ::*KanMX*	(Winzeler *et al.* 1999)
AKY6974	AKY42 *sae2*Δ::*KanMX*	(Winzeler *et al.* 1999)
AKY6975	AKY42 *sgs1*Δ::*KanMX*	(Winzeler *et al.* 1999)
AKY7067/ AKY7068	AKY6973 *htz1*Δ::*URA3*	This study
AKY7069/ AKY7070	AKY6974 *htz1*Δ::*URA3*	This study
AKY6586	AKY42 *xrs2*Δ*::KanMX*	(Winzeler *et al.* 1999)
AKY8027/ AKY8028	AKY5078 *mre11*Δ*::HphMX*	This study
AKY8029/ AKY8030	AKY5078 *rad50*Δ*::HphMX*	This study
AKY8031/ AKY8032	AKY5078 *xrs2*Δ*::HphMX*	This study
AKY944	*MAT**a** ade2-1 leu2-3,112 his3-11,15 trp1-1 ura3-1 can1-100 hht1-hhf1::LEU2 hht2-hhf2::HIS3* plus pAK388	(Yang and Kirchmaier 2006)
AKY6663/ AKY6664	AKY944 *htz1*Δ*::HphMX*	This study
AKY2007/ AKY2008	AKY944 plus pAK278	(Yang and Kirchmaier 2006)
AKY2330/ AKY2331	AKY944 plus pAK872	(Yang *et al.* 2008)
AKY2025/ AKY2026	AKY944 plus pAK874	This study
AKY2027/ AKY2028	AKY944 plus pAK875	This study
AKY7053/ AKY7054	AKY6663 plus pAK872	This study

Table 2.1 continued

AKY7049/ AKY7050	AKY6663 plus pAK874	This study
AKY7051/ AKY7052	AKY6663 plus pAK875	This study
AKY6667/ AKY6668	AKY2007 *htz1*Δ*::HphMX*	This study
AKY8388/ AKY8389	AKY42 *bar1*Δ*::HphMX*	This study
AKY8390/ AKY8391	AKY5078 *bar1*Δ*::HphMX*	This study
AKY8404	AKY42 *ddc1*Δ*::KanMX*	(Winzeler *et al.* 1999)
AKY8406	AKY42 *rad17*Δ::*KanMX*	(Winzeler *et al.* 1999)
AKY8407	AKY42 *rad24*Δ::*KanMX*	(Winzeler *et al.* 1999)
AKY8408/ AKY8409	AKY42 *rad9*Δ**::***HphMX*	This study
AKY8442/ AKY8443	AKY5078 *rad9*Δ**::***HphMX*	This study
AKY6797	AKY42 *ecm5*Δ**::***HphMX*	(Winzeler *et al.* 1999)
AKY8410/ AKY8411	AKY6797 *htz1*Δ::*URA3*	This study
AKY6798	AKY42 *gis1*Δ**::***HphMX*	(Winzeler *et al.* 1999)
AKY8412/ AKY8413	AKY6798 *htz1*Δ::*URA3*	This study
AKY2458	AKY42 *rad9*Δ:*KanMX*	(Winzeler *et al.* 1999)
AKY8438/ AKY8439	AKY2458 *htz1*Δ::*URA3*	This study
AKY8440/ AKY8441	AKY8225 *htz1*Δ::*URA3*	This study

Table 2.1 continued

AKY8442/ AKY8443	AKY8404 *htz1*Δ::*URA3*	This study
AKY8446/ AKY8447	AKY8406 *htz1*Δ::*URA3*	This study
AKY8448/ AKY8449	AKY8407 *htz1*Δ::*URA3*	This study
AKY8816/ AKY8817	AKY944 *jhd1*Δ::*KanMX*	This study
AKY8480/ AKY8481	AKY944 *jhd2*Δ::*KanMX*	This study
AKY8482/ AKY8483	AKY944 *rph1*Δ::*KanMX*	This study
AKY8484/ AKY8485	AKY944 *ecm5*Δ::*KanMX*	This study
AKY8486/ AKY8487	AKY944 *gis1*Δ::*KanMX*	This study
AKY8818/ AKY8819	AKY6663 *jhd1*Δ::*KanMX*	This study
AKY8488/ AKY8489	AKY6663 *jhd2*Δ::*KanMX*	This study
AKY8490/ AKY8491	AKY6663 *rph1*Δ::*KanMX*	This study
AKY8492/ AKY8493	AKY6663 *ecm5*Δ*::KanMX*	This study
AKY8494/ AKY8495	AKY6663 *gis1*Δ*::KanMX*	This study
AKY8035	*MAT***a** *his3*Δ1 *leu2*Δ0 *met15*Δ0 *ura3*Δ0 *RFA1-GFP(S65T)-HIS3MX*	(Huh *et al.* 2003)
AKY8691/ AKY8692	AKY8035 *htz1*Δ::*URA3*	This study
AKY8563/ AKY8564	AKY8480 plus pAK278	This study
AKY8565/ AKY8566	AKY8480 plus pAK872	This study

Table 2.1 continued

AKY8567/ AKY8568	AKY8480 plus pAK874	This study
AKY8569/ AKY8570	AKY8480 plus pAK875	This study
AKY8579/ AKY8580	AKY8482 plus pAK278	This study
AKY8595/ AKY8596	AKY8484 plus pAK278	This study
AKY8611/ AKY8612	AKY8486 plus pAK278	This study
AKY8627/ AKY8628	AKY8488 plus pAK278	This study
AKY8629/ AKY8630	AKY8488 plus pAK872	This study
AKY8631/ AKY8632	AKY8488 plus pAK874	This study
AKY8633/ AKY8634	AKY8488 plus pAK875	This study
AKY8643/ AKY8644	AKY8490 plus pAK278	This study
AKY8659/ AKY8660	AKY8492 plus pAK278	This study
AKY8693/ AKY8694	AKY8494 plus pAK278	This study
AKY8877/ AKY8878	AKY8816 plus pAK278	This study
AKY8903/ AKY8904	AKY8818 plus pAK278	This study
AKY8710	AKY42 *ade12*Δ*::KanMX*	(Winzeler *et al.* 1999)
AKY8869/ AKY8870	AKY8710 *htz1*Δ*::HphMX*	This study
AKY977	*MAT**a** ade2-1 leu2-3,112 his3-11,15 trp1-1 can1-100 sml1::HIS3*	(Zhao *et al.* 1998)

Table 2.1 continued

AKY8687/ AKY8688	AKY977 *htz1*Δ*::URA3*	This study
AKY8937/ AKY8938	AKY42 plus pAK48	This study
AKY8939/ AKY8940	AKY42 plus pAK1356	This study
AKY8941/ AKY8942	AKY5078 plus pAK48	This study
AKY8943/ AKY8944	AKY5078 plus pAK1356	This study
AKY8947/ AKY8948	AKY42 *mrc1*Δ::*HphMX*	This study
AKY8947/ AKY8948	AKY5078 *mrc1*Δ::*HphMX*	This study
AKY8408/ AKY8409	AKY42 *rad9*Δ::*HphMX*	This study
AKY8442/ AKY8443	AKY5078 *rad9*Δ::*HphMX*	This study
AKY5075	AKY42 *swr1*Δ::*KanMX*	(Winzeler *et al.* 1999)

Table 2.2 List of plasmids used in this study

Plasmid	Description	Source
pAK278	*HHT2-HHF2 ARS4/CEN6/TRP1*	(Kelly *et al.* 2000)
pAK388	*HHT2-HHF2 ARS4/CEN6/URA3*	P.Kaufman
pAK872	H3K4R/H4 *ARS4/CEN6/TRP1*	(Fingerman *et al.* 2007)
pAK874	H3K36R/H4 *AR4S/CEN6/TRP1*	(Fingerman *et al.* 2007)
pAK875	H3K79R/H4 *ARS4/CEN6/TRP1*	(Fingerman *et al.* 2007)
pAK15	*pFA6-KanMX4*	(Wach *et al.* 1994)
pAK808	*pFA6-NatMX4*	(Goldstein and McCusker 1999)
pAK804	*pFA6-HphMX4*	(Goldstein and McCusker 1999)
pAK48	*pRS415 (ARS4/CEN6/LEU2)*	(Christianson *et al.* 1992)
pAK1356	*PYK1p-FLAG-JHD2*	(Mersman *et al.* 2009)
pAK54	*pRS313 (ARS4/CEN6/HIS3)*	(Sikorski and Hieter 1989)

Table 2.3 List of oligonucleotides used in this study

Region	Oligonucleotide	Application	Source
KanMX	oALK72 5' CTGCAGCGAGGAGCCGTAAT	Reverse Screening Primer	(Miller *et al.* 2008)
NatMX	oALK217 5' TTCGTCGTCGGGGAACACCTT	Reverse Screening Primer	(Yang and Kirchmaier 2006)
HphMX	oALK612 5'GTAGAAACCATCGGCGCAGC	Reverse Screening Primer	(Chen *et al.* 2012)
URA3	oALK908 5'CGTTCACCCTCTACCTTAGC	Reverse Screening Primer	This study
JHD1	oALK1685 5'ACATCTAATAGAAGTGGGTGATTATAATGAGTAAGAAGAC GTAATGATCATAAAACAAAA oALK1686 5'TCAATTGCTAAAGTAGATCTCATTCATCGAGAGCATAGGAT GAAATAAAAGATACAAGAA	Gene Disruption	This study
JHD1	oALK1525 5'GTAATGATCATAAAACAAAATACTAATAAGCTATGGTGCA CGTACGCTGCAGGTCGAC oALK1526 5'GAAATAAAAGATACAAGAACGTGGCGGACAAGAAGAAAT TATCGATGAATTCGAGCTCG	Gene Disruption	This study
JHD1	oALK1683 5'GCGTTCTCCCCATTTCAATA	Forward Screening Primer	This study
JHD2	oALK1640 5'ATTAACTAATCTCATCTTGCACAAAAAACGTATCACTATCC GTACGCTGCAGGTCGAC oALK1641 5'TATTCTAAAAAATCATTACGCCATACACAAATATTGAAGA ATCGATGAATTCGAGCTCG	Gene Disruption	This study
JHD2	oALK1652 5'GCCAAGTGCCATCAAGAACT	Forward Screening Primer	This study

Table 2.3 continued

RPH1	oALK1642 5’ATAAGACTGTCTTGGTGAGGATATTCAGTTGCGTGAAATCC GTACGCTGCAGGTCGAC oALK1643 5’TCAAAATGAGAGATCTCGGTAAACTGGCAATCGTGAGATC GATGAATTCGAGCTCG	Gene Disruption	This study
RPH1	oALK1653 5’GGGTTTGGTGAATCGAGAAA	Forward Screening Primer	This study
ECM5	oALK1644 5’CGTGTATGTTCTTGTTCGTACGTCCATCTCCATAGTTATACG TACGCTGCAGGTCGAC oALK1645 5’AAGTAAATAGTGATTTTAATCAATAAGATAGTATTACGTTA TCGATGAATTCGAGCTCG	Gene Disruption	This study
ECM5	oALK1654 5’GGCGCAATTAACCAAGTCCT	Forward Screening Primer	This study
GIS1	oALK1646 5’TTTTTTTTAATTTGAAGAATAGCTACAAAAACAGACTACAC GTACGCTGCAGGTCGAC oALK1647 5’AAATTTTTTTTGAACCCATTTTGTATATCATTTTCTTGACAT CGATGAATTCGAGCTCG	Gene Disruption	This study
GIS1	oALK1655 5’AACGCGTGTGTGAGTTGTGT	Forward Screening Primer	This study
MRE11	oALK1595 5’GACGCAAGTTGTACCTGCTCAGATCCGATAAAACTCGACT GCTACGCTGCAGGTCGAC oALK1596 5’TGTACTTGATCCCTATATTATATTATATCCTATTTATAACAT CGATGAATTCGAGCTCG	Gene Disruption	This study
MRE11	oALK1597 5’GAAATGGAAGTCGATCCATCA	Forward Screening Primer	This study

Table 2.3 continued

RAD50	oALK1598 5’CCATTGAGAGGCAAAAACAAGGGAACGGAAAGCAGGGCT ACGCTGCAGGTCGAC oALK1599 5’AAAGACCCCATAATATCTACGAAGGGATAGACTTTGATTG ATCGATGAATTCGAGCTCG	Gene Disruption	This study
RAD50	oALK1600 5’TCTAACAAGCCATCAAAAGCA	Forward Screening Primer	This study
XRS2	oALK1542 5’AGATGAGCAACAATACTGAGAAGGTGATAACTATAAATTT CGTACGCTGCAGGTCGAC oALK1543 5’TATAATTTAATGAAATTGGAAATACTCGGAAAATTTATCAA TCGATGAATTCGAGCTCG	Gene Disruption	This study
XRS2	oALK1544 5’AGGGACAGTCATAGCGGTCA	Forward Screening Primer	This study
MRC1	oALK1690 5’TCGTTATTCGCTTTTGAACTTATCACCAAATATTTTAGTGCG TACGCTGCAGGTCGAC oALK1691 5’CTGGAGTTCAATCAACTTCTTCGGAAAAGATAAAAAACCA ATCGATGATGAATTCGAGCTCG	Gene Disruption	This study
MRC1	oALK1694 5’GTTGGAAAAAAACCAAGAACAGACAAACAACTAAGGAAG TTCGTTATTCGCTTTTGAACT oALK1695 5’GGGTGCCATCTTTTTTAATGCGACTACTTCAAGACAGCTTC TGGAGTTCAATCAACTTCT	Gene Disruption	This study
MRC1	oALK1692 5’GCCAGAAAGAAACCCAAGAA	Forward Screening Primer	This study

Table 2.3 continued

HTZ1	oALK761 5’AATTTCGCACTATAGCCGCACGTAAAAATAACTTAACATATTAACTATGCGGCATCAGAG oALK762 5’AGGGAGAATTACGGGAAATGGGAAAGAAAAACTATTCTTCACGCATCTGTGCGGTATTTC	Gene Disruption	This study
HTZ1	oALK821 5’AAAACTCCGCACGTTGCTTG	Forward Screening Primer	This study
BAR1	oALK268 5’ATCATACCAAAATAAAAAGAGTGTCTAGAAGGGTCATATACGTACGCTGCAGGTCGAC	Gene Disruption	(Kirchmaier and Rine 2006)
BAR1	oALK269 5’TGATATTTATATGCTATAAAGAAATTGTACTCCAGATTTCATCGATGAATTTCGAGCTCG	Gene Disruption	(Kirchmaier and Rine 2006)
BAR1	oALK398 5’GATCTTCGCGTGATTTAATTCTAGTGGTTCGTATCGCCTAAAATCATACCAAAATAAAAAGAGTG	Gene Disruption	(Kirchmaier and Rine 2006)
BAR1	oALK399 5’TTATTAATGCTTTCCATGTATTAAAAATGACTATATATTTGATATTTAATATGCTATAAAGAAATTG	Gene Disruption	(Kirchmaier and Rine 2006)

Table 2.3 continued

BAR1	oALK105 5’ATGAGTCCTTAAGAAGGCCG	Forward Screening Primer	(Kirchmaier and Rine 2006)
FUM1	oALK1473 5’AGAAATTCCATAAAGTCTAACTATTAAACGGATAAGAGATACACGTACGCTGCAGGTCGAC oALK1474 5’ATAAGACATAAAAAACTTGTATATTATTAGGTATTTAGCTCGTATCGATGAATTCGAGCTCG	Gene Disruption	This study
FUM1	oALK1464 5’GAACTAATGCTGCCAGAGAA	Forward Screening Primer	This study
YKU70	oALK1489 5’ATGATTTGTTAAGTGACTCTAAGCCTGATTTTAAAACGGGAATCGTACGCTGCAGGTCGAC oALK1490 5’ATATTGTATGTAACGTTATAGATATGAAGGATTTCAATCGTCTATCGATGAATTCGAGCTCG	Gene Disruption	This study
YKU70	oALK1482 5’ATCAACAATGCAATCCCAAC	Forward Screening Primer	This study
RAD9	oALK1615 5’TAGAAAAGAGCATAGTGAGAAAATCTTCAACATCAGGGCTCGTACGCTGCAGGTCGAC oALK1616 5’TCCCTTTCTATCAATTATGAGTTTATATATTTTTATAATTATCGATGAATTCGAGCTCG	Gene Disruption	This study

Table 2.3 continued

RAD9	oALK1617 5’GGGGAAGTGTCAGCAATGTT	Forward Screening Primer	This study
HHT2	oALK1628 5’CCTTGAATGTTATCTCTTAGAATCCTTCTGTGACGCTTGGC oALK1629 5’GCCAAGCGTCACAGAAGGATTCTAAGAGATAACATTCAAG G	Site-Directed Mutagenesis (K4R)	This study
HHT2	oALK1648 5’GATTTTCTAGCTGTTTGTCTAGTTCTGGCCATTGTGGAGTG oALK1649 5’CACTCCACAATGGCCAGAACTAGACAAACAGCTAGAAAAT C	Site-Directed Mutagenesis (K36R)	This study
HHT2	oALK1650 5’GTGTGAGGCTTCCTAACACCACCGGTAGATGGGG oALK1651 5’CCCCATCTACCGGTGGTGTTAGGAAGCCTCACAC	Site-Directed Mutagenesis (K79R)	This study
HHF2	oALK705 5’TTATTCTTTTCTCTATCTTTTTTCC	Sequencing	(Yang 2008)
HHT2	oALK706 5’GTTTTGTGACTTCCACTTTGGCCCT	Sequencing	(Yang 2008)

CHAPTER 3. ROLE OF THE METABOLIC ENZYME FUMARASE AND THE METABOLITE FUMARATE IN DNA REPLICATION STRESS

3.1 Introduction

All organisms have developed mechanisms to detect, signal and repair damaged DNA to ensure accurate and complete duplication, and inheritance of their genome. Genomic instability is a major driver of tumorigenesis, and multiple factors contribute to genome instability, including failure to properly repair damaged DNA caused by endogenous sources like errors during DNA replication or exogenous agents including ultraviolet (UV) light or chemicals. Perturbed replication contributes to early genomic instability in cancers (Bartkova *et al.* 2005; Gorgoulis *et al.* 2005), and replication stress can promote tumorigenesis in mice (Bilousova *et al.* 2005). In the past few years, metabolic enzymes and metabolites including fumarate hydratase (also called fumarase) and fumarate, succinate dehydrogenase (SDH) and succinate, as well as isocitrate dehydrogenase (IDH) and R-2-hydroxyglutarate (R-2-HG) have emerged as modulators of DNA damage responses in bacteria, yeast, and mammals (Yogev *et al.* 2010; Jiang *et al.* 2015; Singer *et al.* 2017; Sulkowski *et al.* 2017, 2018; Leshets *et al.* 2018).

Fumarase is a well-characterized TCA cycle enzyme found in the mitochondria that catalyzes the reversible reaction of converting fumarate to malate (Woods *et al.* 1988). Fumarase is also present in the cytosol in organisms ranging from yeast to humans (Tolley and Craig 1975; Akiba *et al.* 1984; Yogev *et al.* 2011). In yeast, both cytosolic and mitochondrial fumarase are encoded by a single gene, *FUM1* (Wu and Tzagoloff 1987). Yeast Fum1p contains an N-terminal sequence that is processed in the mitochondrial matrix (Stein *et al.* 1994; Sass *et al.* 2001). Rapid folding of mature Fum1p inhibits its import into mitochondria, and a subset of processed fumarase is released back into the cytosol by retrograde movement (Knox *et al.* 1998; Karniely and Pines 2005).

Fumarase also acts as a tumor suppressor, and defects in the gene encoding fumarase (FH) in humans are commonly found in hereditary leiomyomatosis and renal cell cancer (HLRCC) (Launonen *et al.* 2001; Tomlinson *et al.* 2002; Kiuru *et al.* 2002; Lehtonen *et al.* 2004; Menko *et al.* 2014) as well as in glioblastomas, neuroblastomas and other cancers (Khalil 2007; Fieuw *et al.* 2012). Recent studies have provided a link between fumarase plus the metabolite fumarate and

genome integrity, revealing a previously under-appreciated way in which such metabolic defects have the potential to contribute to tumorigenesis. Amongst the first evidence for the role of fumarase in maintaining genome integrity in eukaryotes emerged from studies in the budding yeast *Saccharomyces cerevisiae* that showed fumarase promotes growth upon exposure to various types of DNA damage (Yogev *et al.* 2010). Recently, yeast fumarase has been shown to promote HR through interaction with and stabilization of Sae2p, the endonuclease associated with the MRX complex at double stranded DNA breaks (DSBs) during DNA end resection (Leshets *et al.* 2018).

Chromatin modifications, including histone methylation, also play a central role in regulation of DNA damage responses for various types of DNA damage in organisms ranging from yeast to humans (House *et al.* 2014; Hauer and Gasser 2017), and recent studies have begun to uncover links between metabolic enzymes plus metabolites, including fumarase plus fumarate, and chromatin during DNA damage responses. Fumarate can modulate histone methylation by acting as a competitive inhibitor of α-ketoglutarate (α-KG)-dependent dioxygenases, including JmjC-domain-containing histone demethylases (Xiao *et al.* 2012; Jiang *et al.* 2015). During DSB repair by non-homologous end joining, NHEJ, in humans, fumarase is recruited to chromatin at the site of DSBs through DNA-PK-dependent phosphorylation as well as interaction with the histone variant H2A.Z (Jiang *et al.* 2015). H2A.Z transiently becomes associates with DSBs (Kalocsay *et al.* 2009; Xu *et al.* 2012) through the actions of the H2A.Z/Htz1p-specific chromatin remodeling complexes SWR1C and INO80C (Krogan *et al.* 2003; Mizuguchi *et al.* 2004; Papamichos-Chronakis *et al.* 2006, 2011; van Attikum *et al.* 2007; Lademann *et al.* 2017). Mammalian H2A.Z, and the budding yeast ortholog Htz1p, can promote DNA repair by NHEJ as well as homologous recombination (Papamichos-Chronakis *et al.* 2011; Xu *et al.* 2012). In human cells, activity of fumarase can be detected in chromatin fractions after exposure to irradiation, IR, and fumarate (but not malate) improves repair by NHEJ through inhibition of the H3 K36-specific lysine demethylase KDM2B (Jiang *et al.* 2015). Moreover, nuclear localization of human fumarase or depletion of KDM2B promotes cell survival after exposure to IR (Jiang *et al.* 2015).

Deletion of *FUM1* in yeast, and loss of the catalytic activity of fumarase in human cells, or loss of function mutations in fumarase in HLRCC tumors, cause accumulation of fumarate to high cellular levels (several hundred-fold increase in yeast, millimolar levels in humans) (Pollard *et al.* 2005; Lin *et al.* 2011; Sulkowski *et al.* 2018). Also, elevated levels of fumarate or succinate (another

competitive inhibitor of α-KG-dependent dioxygenases (Xiao *et al.* 2012; Laukka *et al.* 2016)) correlate with elevated levels of DSBs in patient-derived HLRCC and SDH-related hereditary paraganglioma and pheochromocytoma, SDH PGL/PCC (Sulkowski *et al.* 2018). However, how such changes in metabolite availability affect DNA repair and other cellular functions is poorly understood.

Here, we explored the relationship between yeast Fum1p, the metabolite fumarate, and Htz1p during DNA replication stress. We demonstrate that yeast fumarase was induced, and enriched in the nuclei upon treatment with hydroxyurea (HU), and observed synthetic genetic interaction upon exposure to HU in cells lacking *FUM1* and *HTZ1*. We further demonstrate that exogenous fumarate suppressed the DNA replication stress sensitivity of *htz1*Δ mutants in a manner independent of modulating nucleotide pools, but dependent on components required for activation of the intra-S phase checkpoint, also known as the S Phase checkpoint. In the presence of fumarate, intra-S phase checkpoint activation and adaptation (as measured by phosphorylation status of Rad53p) remained largely intact. Consistent with fumarate promoting histone methylation to confer resistance to DNA replication stress, deletion of the JmjC domain-containing Jhd2p, a H3 K4 demethylase (Liang *et al.* 2007; Seward *et al.* 2007; Tu *et al.* 2007), was sufficient to confer resistance to HU in *htz1*Δ mutants, and this suppression required H3 K4 methylation. Moreover, fumarate inhibited Jhd2p-dependent methylation of H3 K4 *in vivo*. Together, our findings highlight a fumarate-sensitive role for Jhd2p and histone methylation in responses to DNA replication stress as well as link Htz1p to proper processing of replicative intermediates through the DNA replication checkpoint during intra-S phase checkpoint activation.

3.2 Results

3.2.1 Loss of *FUM1* suppresses sensitivity to replication stress in *htz1* mutants.

Fumarase has previously been implicated in DSB repair (Yogev *et al.* 2010; Jiang *et al.* 2015; Sulkowski *et al.* 2018; Leshets *et al.* 2018). To assess the impact of fumarase on responses to DNA replication stress, we first analyzed expression and cellular localization of Fum1p in *S. cerevisiae* upon exposure to HU. Logarithmically growing yeast expressing Fum1p C-terminally tagged with GFP were treated with HU for three hours, and expression and nuclear localization of Fum1p were monitored by quantitative protein blots. As shown in Figure 3.1, after treatment with HU, Fum1p

levels in whole cell extracts increased more than two-fold, and Fum1p became enriched in the nuclear fraction by more than five-fold (Figure 3.1). This further enrichment of Fum1p in the nuclear fraction implied DNA replication stress had triggered localization of Fum1p to the nucleus (see also (Yogev *et al.* 2010)).

In humans, fumarase is recruited to chromatin during NHEJ-mediated repair of DSBs through interaction with the histone variant H2A.Z, and depletion of H2A.Z reduces enrichment of fumarase at sites of DSB (Jiang *et al.* 2015). In yeast, Htz1p promotes genome stability and chromosome segregation (Krogan *et al.* 2004; Kalocsay *et al.* 2009). Similarly, the chromatin remodeling complexes SWR1C and INO80C, which regulate the deposition and eviction of Htz1p, also contribute to genome integrity (Krogan *et al.* 2003; Mizuguchi *et al.* 2004; Papamichos-Chronakis *et al.* 2006, 2011; van Attikum *et al.* 2007; Lademann *et al.* 2017).

To explore the relationship between Htz1p and yeast fumarase during DNA replication stress, we examined genetic interactions in cells lacking *HTZ1* and/or *FUM1* in growth assays of serial dilutions onto rich medium lacking or containing HU. In the presence of HU, *htz1*Δ, but not *fum1*Δ, mutants exhibited growth defects relative to wild-type yeast and relative to in the absence of HU (Figure 3.2A first versus third panel). However, this sensitivity in the presence of HU was suppressed in *fum1*Δ *htz1*Δ mutants, implying that loss of *FUM1* had partially bypassed a requirement for *HTZ1* during replication stress.

3.2.2 Exogenous fumarate suppresses the sensitivity to DNA damage in *htz1*Δ mutants.

As deletion of *FUM1* causes accumulation of fumarate in the cell (Pollard *et al.* 2005; Lin *et al.* 2011), the above observation (Figure 3.2A) raised the possibility that elevated levels of fumarate caused by deletion of *FUM1* had conferred resistance to HU in the *htz1*Δ *fum1*Δ mutants. To test this possibility, we compared growth of *htz1*Δ mutants to wild-type yeast in the presence and absence of HU, and with or without adding exogenous fumarate to the growth medium at concentrations comparable to the levels found in HLRCC tumors (Pollard *et al.* 2005). As shown in Figure 3.2A (third versus fourth panel), the addition of exogenous fumarate largely suppressed the sensitivity of *htz1*Δ mutants to HU as well as further enhanced growth of *htz1*Δ *fum1*Δ mutants in HU. Similar to *htz1*Δ mutants, strains lacking *SWR1* exhibited growth defects relative to wild-type on rich (YPD) medium as well as medium containing HU, and the sensitivity of *swr1*Δ

mutants to HU was also partially suppressed by the addition of exogenous fumarate (Figure 3.3). Exogenous fumarate alone did not adversely affect the number of colonies in the absence of HU in these experiments, however, colony sizes of all strains tested decreased in the presence of exogenous fumarate (e.g. Figure 3.2). The cause of this decrease in colony size is unknown.

Rad52p promotes loading of the nucleoprotein filament recombinase Rad51p onto ssDNA and strand exchange at DSBs, and is essential for homology-dependent DNA repair (Game and Mortimer 1974; New *et al.* 1998; Shinohara and Ogawa 1998; Pâques and Haber 1999; Symington 2002). In *Schizosachromyces pombe*, Rad52 is also required for recombination-independent restart of replication from terminally arrested forks in which nascent DNA is protected by Rad51 from excessive ssDNA formation by the exonucleases Exo1 or Mre11, and for properly merging a converging fork with a terminally arrested fork (Lambert *et al.* 2010; Hashimoto *et al.* 2010; Schlacher *et al.* 2011, 2012; Iraqui *et al.* 2012; Higgs *et al.* 2015; Ait Saada *et al.* 2017). In contrast to what had been observed for *htz1*Δ mutants, addition of exogenous fumarate did not suppress the sensitivity to HU in cells lacking *RAD52* (Figure 3.2A). Genes encoding the MRX complex are also members of the *RAD52* epistasis group. The MRX complex, consisting of Mre11p, Rad50p and Xrs2p, acts as a major DSB sensor, but also functions to stabilize components of the replication machinery at stalled forks (Lisby *et al.* 2004; Tittel-Elmer *et al.* 2009). Like *rad52*Δ mutants, *mre11*Δ, *rad50*Δ and *xrs2*Δ mutants exhibited severe growth defects in the presence of HU, and addition of exogenous fumarate did not suppress these defects (Figure 3.2B and Figure 3.4). These results indicated that fumarate complemented sensitivity to DNA replication stress created by the absence of the histone variant, but not Rad52p or the MRX complex.

3.2.3 Suppression of the DNA replication stress sensitivity of *htz1*Δ mutants by fumarate is not due to modulation of nucleotide pools.

Exposure to HU results in stalled replication forks via inhibition of ribonucleotide reductase, which leads to depletion of nucleotide pools (Krakoff *et al.* 1968). This depletion is thought to result in the creation of stretches of ssDNA at stalled forks that become coated with RPA, which is required to recruit Mec1p-Ddc2p and promote activation of the kinase Mec1p, and activation of the intra-S phase checkpoint (Zou and Elledge 2003). Therefore, we tested the possibility that fumarate had promoted growth of *htz1*Δ mutants upon exposure to HU by modulating the nucleotide pools. We first tested whether increasing the dNTP pool by deletion of *SML1*, which encodes an inhibitor of

ribonucleotide reductase (Zhao *et al.* 1998; Chabes *et al.* 1999), could promote growth of *htz1*Δ mutants in the presence of HU by comparing wild-type, *sml1*Δ, *htz1*Δ and *sml1*Δ *htz1*Δ mutants in growth assays. Instead, we observed a negative synthetic genetic interaction in the absence of *SML1* and *HTZ1* as the *sml1*Δ *htz1*Δ mutants exhibited a severe growth defect in rich medium (YPD) compared to the *sml1*Δ or *htz1*Δ single mutants, whereas the growth of *sml1*Δ *htz1*Δ mutants in the presence of HU was comparable to that of *htz1*Δ mutants (Figure 3.5). Addition of exogenous fumarate suppressed the sensitivity to DNA replication stress of both *htz1*Δ and *sml1*Δ *htz1*Δ mutants, implying fumarate suppressed the sensitivity to HU through a mechanism independent of elevating nucleotide pools.

Fumarate is also a product in the purine nucleotide cycle, and can function as a weak inhibitor of adenylosuccinate lyase, which converts adenylosuccinate into adenosine monophosphate (AMP) plus fumarate in the purine nucleotide cycle (Barnes and Bishop 1975) (Figure 3.5B). This raised the possibility that regulation of AMP production by inhibition of adenylosuccinate lyase activity and/or accumulation of adenylosuccinate upon addition of exogenous fumarate had suppressed the sensitivity of *htz1*Δ mutants to HU. Therefore, we tested whether decreased production of adenylosuccinate and disruption of the purine nucleotide cycle by deletion of the gene encoding adenylosuccinate synthase (*ADE12*) could block fumarate-dependent suppression of the sensitivity of *htz1*Δ mutants to HU. As shown in Figure 3.5C, *ade12*Δ mutants did not exhibit growth defects compared to wild-type in presence of HU, whereas *ade12*Δ *htz1*Δ mutants were hypersensitive to HU relative to wild-type yeast or *htz1*Δ mutants, indicating a negative synthetic genetic interaction during DNA replication stress. However, addition of exogenous fumarate to the medium partially suppressed the sensitivity of *ade12*Δ *htz1*Δ mutants to HU, indicating that adenylosuccinate and the integrity of the purine nucleotide cycle were dispensable for fumarate-mediated suppression in *htz1*Δ mutants. Taken together, these results implied that fumarate suppressed the sensitivity to DNA replication stress of *htz1*Δ mutants independently of modulating nucleotide levels.

3.2.4 Loss of *JHD2* phenocopies fumarate-dependent suppression of DNA replication stress sensitivity in *htz1*Δ mutants.

Fumarate is a competitive inhibitor of α-KG dependent dioxygenases, including JmjC domain-containing histone demethylases (Xiao *et al.* 2012; Yang *et al.* 2013; Jiang *et al.* 2015). Histone H3 K4, H3 K36 and H3 K79 methylation play important roles in maintaining genome stability

including during DNA replication, DNA damage responses and repair as well as in activation of DNA damage checkpoints (Wysocki *et al.* 2005; Lazzaro *et al.* 2008; Faucher and Wellinger 2010; Rizzardi *et al.* 2012; Pai *et al.* 2014; Jha and Strahl 2014). Therefore, we hypothesized that fumarate had suppressed the sensitivity to DNA replication stress in *htz1*Δ mutants in the above experiments by modulating the levels of histone lysine methylation through inhibition of one or more JmjC domain-containing histone demethylases. We reasoned that if inhibition of a JmjC histone demethylase by fumarate promoted growth upon DNA replication stress in the *htz1*Δ mutants, then deletion of that histone demethylase might act similarly. Therefore, we tested the sensitivity of mutants lacking individual JmjC histone demethylases to HU in the presence or absence of *HTZ1*, including cells lacking *JHD1* (removes H3 K36me2 and me1 (Tsukada *et al.* 2006; Tu *et al.* 2007; Fang *et al.* 2007)), *JHD2* (removes H3 K4me3 and me2 (Liang *et al.* 2007; Tu *et al.* 2007; Ingvarsdottir *et al.* 2007)), *RPH1* (removes H3 K36me3 and me2 (Tu *et al.* 2007; Kim and Buratowski 2007)), *ECM5* (unknown target) or *GIS1* (predicted to remove H3 K36 methylation (Tu *et al.* 2007; Kwon and Ahn 2011; Sein *et al.* 2015)) (Figure 3.6A).

When grown on rich medium (YPD), smaller colonies were observed in *htz1*Δ, *jhd1*Δ *htz1*Δ, *rph1*Δ *htz1*Δ, *ecm5*Δ *htz1*Δ and *gis1*Δ *htz1*Δ mutants compared to wild-type, whereas the colony sizes of *jhd2Δ htz1*Δ mutants were similar to wild-type, implying that deletion of *JHD2* complemented growth defects caused by loss of *HTZ1* (Figure 3.6B left panels). In contrast to *htz1*Δ mutants, deletion of single histone demethylases did not result in sensitivity to HU compared to wild-type (Figure 3.6B first versus third panels). *jhd1*Δ *htz1*Δ mutants were as sensitive to HU as *htz1*Δ mutants, whereas *rph1*Δ *htz1*Δ, *ecm5*Δ *htz1*Δ and *gis1*Δ *htz1*Δ mutants were slightly more sensitive to HU compared to *htz1*Δ mutants. In contrast, *jhd2*Δ *htz1*Δ mutants showed no sensitivity to HU compared to wild-type or *htz1*Δ mutants, indicating that deletion of *JHD2* relieved the sensitivity of *htz1*Δ mutants to DNA replication stress (Figure 3.6B first versus third panels). Addition of exogenous fumarate had no further effect on sensitivity of *jhd2*Δ *htz1*Δ mutants to DNA replication stress. In contrast, deletion of *RPH1*, *ECM5* or *GIS1* in strains lacking *HTZ1* resulted in sensitivity to exogenous fumarate alone (Figure 3.6B first versus second panels). This sensitivity precluded our ability to determine the impact of loss of *RPH1*, *ECM5* or *GIS1* on fumarate-dependent suppression of sensitivity to HU in the *htz1*Δ mutants under the conditions tested. Overall, the results of our analyses indicate that deletion of *JHD2* was sufficient to alleviate

the sensitivity to replication stress of *htz1*Δ mutants, and implied that inhibition of the histone demethylase Jhd2p by fumarate may have conferred resistance to DNA replication stress in the *htz1*Δ mutants by promoting histone H3 K4 methylation.

To explore this possibility, we compared sensitivity to HU in wild-type or *htz1*Δ mutants lacking chromosomal copies of genes encoding histones H3/H4 and expressing wild-type H3/H4 or H3 mutants in which lysine methylation sites had been mutated to arginine plus wild-type H4 from a plasmid. Yeast lacking H3 K4 methylation showed growth defects in the presence of HU, consistent with previously reported sensitivity of *set1*Δ or H3 K4R mutants to HU (Faucher and Wellinger 2010). In contrast, yeast lacking H3 K36 or H3 K79 methylation did not (Figure 3.7, first versus third panel), consistent with previously reported lack of sensitivity of *set2*Δ mutants (Biswas *et al.* 2008; Jha and Strahl 2014), and *dot1*Δ or H3 K79R mutants to HU (Rossodivita *et al.* 2014; Stulemeijer *et al.* 2015). Moreover, we observed synthetic growth defects between *htz1*Δ and H3 K4R or H3 K36R mutants when grown on rich medium (YPD) relative to single mutants or wild-type (Figure 3.7, first panel), consistent with previous reports of synthetic growth defects between *set1*Δ and *htz1*Δ mutants (Venkatasubrahmanyam *et al.* 2007), or *set2*Δ and *swr1*Δ mutants (Fuchs *et al.* 2012). These growth defects were exacerbated in the presence of HU (Figure 3.7, first versus third panel). In contrast, no growth defects were observed in *htz1*Δ H3 K79R relative to *htz1*Δ mutants in rich medium, but *htz1*Δ K79R mutants were hypersensitive to DNA replication stress relative to either single mutant (Figure 3.7, first versus third panel). Addition of fumarate suppressed the sensitivity to DNA replication stress of wild-type strains expressing H3 K4R as well as *htz1*Δ strains expressing H3 K4R, H3 K36R or H3 K79R mutants, but to varying degrees (Figure 3.7). Together, these results implied that fumarate could suppress sensitivity to replication stress caused by defects in multiple methylation events, and that methylation of an individual residue was not solely required for this suppression. We have been unable to generate and test triple mutants lacking *HTZ1* with histone H3 K4R,K36R or H3 K4R,K79R as these mutant combinations appear to be lethal. Together, these data were consistent with fumarate-dependent suppression functioning through multiple pathways involving different histone methylation sites, or non-histone protein methylation (see Discussion).

3.2.5 Suppression of DNA replication stress sensitivity of *htz1*Δ mutants by deletion of *JHD2* requires H3 K4 methylation

In addition to methylated H3 K4 being enriched in transcriptionally active regions, both methylated H3 K4 and Set1p, the sole H3 K4-specific methyltransferase in yeast, become enriched at DSB sites, and mutants lacking *SET1* show growth defects in the presence of HU as well as genotoxic agents that induce DSBs (Faucher and Wellinger 2010). To test whether suppression of sensitivity to HU in *jhd2*Δ *htz1*Δ mutants observed in Figure 3.6 required methylated H3 K4, synthetic interaction analyses were conducted using wild-type yeast, plus *htz1*Δ, *jhd2*Δ, and *jhd2*Δ *htz1*Δ mutants expressing wild-type H3/H4 or H3 mutants in which individual lysine methylation sites had been mutated to arginine plus H4 from a plasmid. These analyses, shown in Figure 3.8, indicated that the observed increase in colony size in *jhd2*Δ *htz1*Δ mutants compared to *htz1*Δ mutants when grown on rich medium (YPD) did not require H3 K4 (Figure 3.8, top row, first panel), H3 K36 (Figure 3.8, middle row, first panel) or H3 K79 methylation (Figure 3.8, bottom row, first panel), implying a histone methylation-independent role for Jhd2p in promoting growth exists. However, unlike *jhd2*Δ *htz1*Δ mutants expressing wild-type histones, *jhd2*Δ *htz1*Δ mutants expressing H3 K4R were as sensitive to HU as *htz1*Δ mutants expressing H3 K4R (Figure 3.8, top row, third panel compared to first). In contrast, *jhd2*Δ *htz1*Δ mutants expressing H3 K36R (Figure 3.8, middle row, third panel compared to first) or H3 K79R mutants (Figure 3.8, bottom row, third panel compared to first) were not sensitive to HU, similar to *jhd2*Δ *htz1*Δ mutants expressing wild-type H3/H4. Together, these findings were consistent with *jhd2*Δ-dependent suppression of growth sensitivity in *htz1*Δ mutants upon DNA replication stress requiring H3 K4, but not H3 K36 or H3 K79 methylation. Consistent with our results in Figure 3.6 and Figure 3.7, addition of exogenous fumarate partially suppressed the sensitivity of *jhd2*Δ *htz1*Δ H3 K4R mutants to HU (Figure 3.8), implying that fumarate could confer resistance to DNA replication stress by multiple mechanisms, one of which was H3 K4 methylation-independent.

3.2.6 Fumarate is a modulator of Jhd2p activity and H3 K4me3 levels

Collectively, the above findings led us to predict that elevated H3 K4 methylation levels, via either deletion of *JHD2* or exposure to exogenous fumarate, could suppress replication stress sensitivity in *htz1*Δ mutants. To test whether exogenous fumarate could inhibit Jhd2p activity, we analyzed the effect of exogenous fumarate on H3 K4 methylation in wild-type or *htz1*Δ strains

overexpressing Jhd2p as this background facilitates detection of changes in methylation states of H3 K4 (Mersman *et al.* 2009). Logarithmically growing cultures from strains harboring an empty vector or a plasmid for overexpression of Jhd2p were harvested before and after exposure to fumarate for one hour, and whole cell extracts were used to analyze global levels of H3 K4me3 relative to H3 in immunoblots. As shown in Figure 3.9, overexpression of Jhd2p results in reduced levels of H3 K4me3 in both wild-type (see also (Mersman *et al.* 2009)) and *htz1*Δ mutants. However, after treatment with fumarate, the levels of H3 K4me3 in wild-type yeast or *htz1*Δ mutants overexpressing Jhd2p were significantly increased relative to cells containing vector alone ($P < 0.05$), implying that fumarate had inhibited Jhd2p *in vivo*. These results were consistent with previous reports of elevation of H3 K4 methylation levels in mammalian cells upon treatment with fumarate or siRNA targeting fumarase (Xiao *et al.* 2012).

3.2.7 The impact of fumarate on cell cycle progression and checkpoint activation upon DNA replication stress

Like wild-type yeast, *htz1*Δ and *swr1*Δ mutants do not accumulate spontaneous DSBs as measured by Pulsed-Field Gel Electrophoreses (Morillo-Huesca *et al.* 2010), and, upon release into HU, *htz1*Δ and *swr1*Δ mutants exhibit wild-type replication bubbles and forks, with no evidence of accumulation of stalled, broken or recessed forks at or near early origins by 2D gel analyses, indicating initiation and fork progression *per se* in these mutants is relatively normal (Dhillon *et al.* 2006; Srivatsan *et al.* 2018). Also, like in wild-type, late origins fail to fire in HU in *htz1*Δ mutants, consistent with late origin firing being negatively regulated by Rad53p via proper intra-S phase checkpoint activation in HU in the absence of Htz1p (Dhillon *et al.* 2006). However, although the early and late origin replication program is conserved (Dhillon *et al.* 2006), the timing of origin firing is delayed in *htz1*Δ mutants (Dhillon *et al.* 2006), and loss of *HTZ1* or *SWR1* delays completion of replication relative to wild-type (Dhillon *et al.* 2006; Srivatsan *et al.* 2018). In addition, although *htz1*Δ mutants exhibit a decreased rate of progression through S phase, the efficiency of checkpoint-dependent cell cycle arrest in early S phase in HU (Dhillon *et al.* 2006), and recovery from exposure to HU in *htz1*Δ mutants remains similar to wild-type (Srivatsan *et al.* 2018). To test whether fumarate affected cell cycle kinetics in *htz1*Δ mutants, we analyzed cell cycle progression of wild-type yeast and *htz1*Δ mutants in the presence or absence of HU and/or fumarate. To do so, we first synchronized the cells in G_1 with α-factor before releasing into rich

medium with or without HU or fumarate. Cells were harvested before, and at 20-min intervals after release, and their DNA content was analyzed by flow cytometry. As shown in Figure 3.10, addition of HU slowed progression of both wild-type yeast and *htz1*Δ mutants through S phase, as expected. In the absence of HU, fumarate did not dramatically affect the cell cycle profile of wild-type yeast or the *htz1*Δ mutants during the first S phase. These results implied fumarate did not function by promoting entry into Start in the *htz1*Δ mutants via eliminating a delay in the induction of G_1 cyclins (Dhillon *et al.* 2006). In the presence of HU, addition of fumarate did not dramatically affect the cell cycle profile in wild-type yeast or *htz1*Δ mutants during the first cell cycle. However, we observed a fumarate-dependent delay in progression through the second cell cycle during DNA replication stress in both wild-type yeast and *htz1*Δ mutants.

The observed changes in the cell cycle progression by fumarate in the presence of DNA replication stress, and reports of defects in phosphorylation of Rad53p in *htz1*Δ mutants in response to DNA damage (Dhillon *et al.* 2006; Kalocsay *et al.* 2009) prompted us to assess the impact of fumarate on the DNA damage checkpoint activation and deactivation. We analyzed checkpoint responses by monitoring the phosphorylation status of Rad53p in wild-type yeast and *htz1*Δ mutants grown in rich medium following exposure to HU in the presence or absence of exogenous fumarate (Figure 3.11). Cultures were first synchronized in G_1 by addition of α-factor, then released into HU-containing growth media containing or lacking fumarate. Cells were then collected before and every 30 min to two hours after addition of HU for a total of eight hours. The phosphorylation status of Rad53p was then analyzed from each timepoint by immunoblotting using Rad53p-specific antibodies and whole cell extracts. As shown in Figure 3.11, phosphorylated Rad53p was detected within one hour of treatment with HU in wild-type yeast and *htz1*Δ mutants in the presence or absence of fumarate, indicating that exogenous fumarate had little or no impact on activation of Rad53p. In *htz1*Δ mutants, phosphorylated Rad53p diminished after six hours of treatment with HU, whereas phosphorylated Rad53p was still detectable in wild-type yeast, indicating that *htz1*Δ mutants had defects in maintaining checkpoint activation and had adapted to DNA replication stress earlier than had wild-type. Addition of fumarate did not dramatically affect this early checkpoint deactivation. Taken together, checkpoint activation and deactivation in wild-type yeast or *htz1*Δ mutants were largely unaffected upon addition of exogenous fumarate under these conditions.

3.2.8 Suppression of sensitivity to DNA replication stress of *htz1*Δ mutants by fumarate requires intra-S phase checkpoint sensors and mediators

The intra-S phase checkpoint consists of two branches: the DNA damage checkpoint, DDC, and the DNA replication checkpoint, DRC. In both DDC and DRC, induced phosphorylation of Rad53p is dependent on signaling events that act upstream of the sensor Mec1p kinase, which is recruited to ssDNA coated with RPA via Mec1p's interacting partner Ddc2p (Rouse and Jackson 2002; Zou and Elledge 2003), although DDC tends to be a slower, sustained response whereas DRC is rapid, but transient (Pardo *et al.* 2016). In DDC, Mec1p uses the adaptor Rad9p to transduce the signal to Rad53p in response to DNA damage (Weinert and Hartwell 1988; Gilbert *et al.* 2001; Sweeney *et al.* 2005) (see (Pardo *et al.* 2016) for review). In contrast, Mrc1p, travels with the DNA replication fork (Katou *et al.* 2003; Lou *et al.* 2008; Komata *et al.* 2009), and acts as a "threshold-driven" sensor during DRC. Upon phosphorylation by Mec1p, Mrc1p mediates a signal to Rad53p that is strong enough to activate the intra-S phase checkpoint only when numerous forks are impeded (Alcasabas *et al.* 2001; Tanaka and Russell 2001, 2004; Duncker *et al.* 2002; Shimada *et al.* 2002; Tercero *et al.* 2003; Osborn and Elledge 2003; Xu *et al.* 2006; Smolka *et al.* 2006; Chen and Zhou 2009) (see (Pardo *et al.* 2016) for review). DDC and DRC appear to regulate downstream targets somewhat differently during intra-S phase checkpoint activation. For example, *MRC1* is required to inhibit late origin firing in HU and MMS (Methyl methanesulfonate), whereas *RAD9* is not (Alcasabas *et al.* 2001; Bacal *et al.* 2018).

Multiple factors act as DNA damage sensors for both the DDC and DRC branches of the intra-S phase checkpoint signaling pathway to activate Mec1p, including the Ddc1p–Mec3p–Rad17p complex, and Rad24p. Ddc1p–Mec3p–Rad17p is analogous to the 9-1-1 complex in mammals. Rad24 is the large subunit of an alternative RF-C complex that loads Ddc1p–Mec3p–Rad17p onto DNA at the 5' junction between RPA-bound ssDNA and dsDNA (Majka and Burgers 2003; Zou *et al.* 2003; Furuya *et al.* 2004), such as those present at Okazaki fragments. Loss of these factors results in defects in or loss of phosphorylation of Rad53p upon DNA replication stress (Paciotti *et al.* 1998; Shimomura *et al.* 1998; Kondo *et al.* 1999; Gilbert *et al.* 2001; Alcasabas *et al.* 2001).

To test whether the fumarate-dependent resistance to HU in *htz1*Δ mutants required sensors of the checkpoint signaling pathway, we examined sensitivity to replication stress in strains in which components of the intra-S phase checkpoint had been deleted. We found that deletion of *RAD17*,

RAD24, or *DDC1* from wild-type did not result in sensitivity to HU under the conditions tested, and their deletion in *htz1*Δ mutants did not increase the sensitivity of *htz1*Δ mutants to HU (Figure 3.12A, first versus third panel). However, deletion of *RAD17*, *RAD24*, or *DDC1* prevented fumarate-dependent resistance to HU in the *htz1*Δ mutants (Figure 3.12A), indicating the 9-1-1 complex was required for fumarate to confer resistance to DNA replication stress. Similarly, cells lacking the DDC mediator Rad9p did not exhibit sensitivity to HU under the conditions tested, and inactivation of DDC by loss of *RAD9* instead partially restored growth of *htz1*Δ mutants in HU. Addition of exogenous fumarate did not enhance this effect (Figure 3.13 and data not shown).

We also assessed the impact of loss of *HTZ1* and/or exposure to fumarate on DRC. Deletion of the DRC mediator *MRC1* (Figure 3.12A, bottom row, first versus third panel) caused a growth defect in medium containing HU (see also (Alcasabas *et al.* 2001; Tanaka and Russell 2001; Osborn and Elledge 2003)), and *mrc1*Δ *htz1*Δ mutants showed enhanced sensitivity to HU as compared to wild-type yeast or *htz1*Δ mutants (see also (Srivatsan *et al.* 2018) for *mrc1*Δ *swr1*Δ mutants), implying that the presence of Hz1p was critical to limit abnormal replication intermediates when Mrc1p was not present to stabilize the fork. We therefore repeated these growth assays using a lower concertation of HU to assess the effect of fumarate on this sensitivity (Figure 3.12B), but addition of fumarate to the growth medium could not suppress the sensitivity of *mrc1*Δ *htz1*Δ mutants to HU. Together, these results implied that the resistance to replication stress conferred to *htz1*Δ mutants by exposure to fumarate required several intact intra-S phase checkpoint sensors and mediators and were consistent with fumarate having promoted a different step in the intra-S phase checkpoint signaling pathway that had been compromised by loss of *HTZ1*.

We next examined the relationship between *SGS1* and *HTZ1* plus fumarate (Figure 3.14A). Sgs1p, a 3’-5’ RecQ helicase and yeast ortholog of the Bloom Syndrome protein BLM, is a stable component of the replication fork where it interacts with RPA and Dna2p (Cejka *et al.* 2010; Hegnauer *et al.* 2012). Upon intra-S phase checkpoint activation with HU, Sgs1p binds Rad53p, stabilizes DNA pol α and DNA pol ε association with stalled forks, and may contribute to fork stability by reversing recessed forks and preventing inappropriate recombination by resolving strand exchange (Versini *et al.* 2003; Cobb *et al.* 2003; Bjergbaek *et al.* 2005; Bernstein *et al.* 2009, 2010; Hegnauer *et al.* 2012). When phosphorylated by Mec1p, Sgs1p functions in the DRC pathway with Mrc1p to activate Rad53p, although Sgs1p’s helicase activity *per se* is not required

for this phosphorylation event (Bjergbaek *et al.* 2005; Hegnauer *et al.* 2012). In the absence of replication stress, *sgs1*Δ mutants grew with similar efficiency as wild-type, whereas *sgs1*Δ *htz1*Δ mutants exhibited a growth defect relative to either single mutant in the absence of replication stress (Figure 3.14A, first panel). Growth defects of *sgs1*Δ and *sgs1*Δ *htz1*Δ mutants in HU could not be suppressed by the addition of fumarate (Figure 3.14A, third versus fourth panel), implying Htz1p was critical for ensuring survival during replication stress in the absence of Sgs1p, like the other DRC component Mrc1p (Figure 3.12). However, fumarate could not bypass this role of Htz1p.

While Sgs1p is epistatic to Mrc1p in activation of Rad53p, Sgs1p also binds Rad51p (Wu *et al.* 2001) and functions in a pathway parallel to Mrc1p during replication fork recovery to stabilize association of DNA polymerase ε at forks (Bjergbaek *et al.* 2005). As Sgs1p-dependent stabilization of DNA polymerase ε at forks requires the helicase activity of Sgs1p as well as Rad51p, this pathway has been proposed to be involved in resolving reversed forks and promoting recombination-dependent restart of forks, prompting us to examine the relationship between Htz1p and factors involved in processing forks for replication restart.

3.2.9 Suppression of sensitivity to DNA replication stress of *htz1*Δ mutants by fumarate and end resection.

During replication stress, MRN-Ctp1, the *S. pombe* ortholog of MRX-Sae2p, facilitates replication restart in a DSB-independent pathway by limiting uncontrolled resection by the exonuclease Exo1 at terminally arrested forks (Teixeira-Silva *et al.* 2017). In the absence of DSBs at stalled forks, short-range resection by MRN-Ctp1 creates ssDNA gaps that enable loading of RPA, Rad52 and Rad51, as well as replication restart (Lambert *et al.* 2010; Tsang *et al.* 2014; Nguyen *et al.* 2015; Teixeira-Silva *et al.* 2017). To test whether the fumarate-dependent resistance to HU in the *htz1*Δ mutants could be related to fork resection and restart, we revisited sensitivity to replication stress in strains in which components of the MRX complex had been deleted (Figure 3.14B). In the absence of replication stress, *rad50*Δ, *xrs2*Δ, and *mre11*Δ mutants grew with similar efficiency as wild-type, and *rad50*Δ *htz1*Δ, *xrs2*Δ *htz1*Δ, and *mre11*Δ *htz1*Δ mutants grew with similar efficiency as *htz1*Δ mutants (Figure 3.14B, first panel), consistent with previous reports that loss of *HTZ1* does not inherently result in accumulation of broken forks (Dhillon *et al.* 2006; Srivatsan *et al.* 2018). Consistent with a critical role of the MRX complex in processing replicative

intermediates arising during replication stress, cells lacking *RAD50, XRS2* or *MRE11* were hypersensitive to HU relative to wild-type or *htz1*Δ mutants. In contrast, deletion of *HTZ1* in *rad50*Δ or *xrs2*Δ, but not *mre11*Δ mutants partially suppressed their sensitivity to HU (Figure 3.14B, first versus third panel), and addition of exogenous fumarate further suppressed this sensitivity, but only in the absence of *HTZ1* (Figure 3.14B). The significance of this difference in phenotypes between the subunits of the MRX complex is not understood. However, upon γ-irradiation, Mre11p can form weak nuclear foci in the absence of *XRS2*, and is nuclear in cells lacking *RAD50* (Lisby *et al.* 2004), plus a Rad50-independent function of Mre11 in repair of DSBs has previously been documented in *Archaea* (Kish and DiRuggiero 2008). Regardless, these results implied chromatin composition impacted the fate of arrested forks in the absence of a functional MRX complex, and, therefore, viability.

The endonuclease Sae2p and the exonuclease Exo1p promote survival during replication stress by counteracting the formation of aberrant branched structures at stalled forks associated with DSB formation and fork collapse (Colosio *et al.* 2016). Sae2p and Mre11p stimulate each other's nuclease activity (Lengsfeld *et al.* 2007; Cannavo and Cejka 2014), Sae2p promotes end resection with the MRX complex during DSB repair (Lengsfeld *et al.* 2007; Mimitou and Symington 2008), and facilitates release of the MRX complex from DNA ends to promote repair (Puddu *et al.* 2015). Sae2p can also process structures mimicking replicative intermediates *in vitro*, and appears to have functions distinct from Mre11p in counteracting reversed fork cleavage (Ghodke and Muniyappa 2016; Colosio *et al.* 2016). Exo1p can resect nascent strands in reversed forks, thereby limiting their formation into structures that could lead to DSBs (Colosio *et al.* 2016). In *S. pombe*, long-range resection at terminally arrested forks requires Exo1 (but not Rqh1 (Sgs1p)) and is Ctp1 (Sae2p)-dependent (Teixeira-Silva *et al.* 2017). When examining the relationship between *SAE2*, *EXO1*, and *HTZ1* plus fumarate, we found *sae2*Δ and *exo1*Δ mutants grew with similar efficiency as wild-type, and *sae2*Δ *htz1*Δ plus *exo1*Δ *htz1*Δ mutants grew with similar efficiency as *htz1*Δ mutants on rich medium (Figure 3.14A, first panel). *sae2*Δ mutants were mildly sensitive to HU, and *sae2*Δ *htz1*Δ mutants were more sensitive than either single mutant to replication stress (Figure 3.14A, first versus third panel). However, like in *htz1*Δ mutants, fumarate fully suppressed the hypersensitivity of *sae2*Δ mutants to replication stress, and partially suppressed the hypersensitivity of *sae2*Δ *htz1*Δ mutants (Figure 3.14A, third versus fourth panel), consistent with

exposure to fumarate leading to bypass of a defect caused by the absence of either Sae2p or Htz1p. Unlike *sae2*Δ mutants, cells lacking *EXO1* (in which resection of a regressed, terminally arrested fork would be expected to be limited as in *Schizosaccharomyces pombe* (Teixeira-Silva *et al.* 2017)) grew similar to wild-type on HU, indicating Exo1p was not required to process/restart stalled forks under the conditions tested (Figure 3.14A, see also (Doerfler and Schmidt 2014)). *exo1*Δ *htz1*Δ and *htz1*Δ mutants were similarly sensitive to replication stress, implying that limiting resection by Exo1p and Htz1p function may fall in the same pathway at replication forks (see (Adkins *et al.* 2013) for *exo1*Δ *swr1*Δ interactions with UV and zeocin). This defect in *exo1*Δ *htz1*Δ mutants was partially suppressed by exogenous fumarate (Figure 3.14A third versus fourth panel). Together, these results were consistent with exposure to fumarate having enabled bypass of defects related to processing stalled forks.

3.2.10 Suppression of sensitivity to DNA replication stress of *htz1*Δ mutants by fumarate is independent of displacement of Ku from replicative intermediates.

YKU70 encodes a component of the Ku complex, which is best known for its ability to bind DSB ends and promote NHEJ (Boulton and Jackson 1996). Ku70p also has a NHEJ-independent function during replication stress in which Ku70p binds reversed forks to regulate end resection, by limiting homology-directed repair (Foster *et al.* 2011; Teixeira-Silva *et al.* 2017). At terminally arrested forks in *S. pombe*, MRN-Ctp1, is proposed to displace Ku via short-range resection. This short-range resection is Ctp1-dependent and Exo1-independent, and Exo1 is not required for replication restart at stalled forks lacking DSBs (Teixeira-Silva *et al.* 2017). However, in the absence of Ku70, Rad50 and Ctp1 are no longer required to promote initial resection of a stalled fork lacking a DSB. Instead, stalled forks now can be resected by Exo1, but HR-mediated fork restart becomes delayed. Consistent with conservation of this process, loss of *YKU70* in budding yeast suppresses MMS sensitivity and mildly suppresses HU sensitivity of *mre11* nuclease dead and *sae2*Δ mutants (Foster *et al.* 2011).

To test the relationship between *YKU70, HTZ1* and fumarate during replication stress, we conducted analogous growth assays in *htz1*Δ strains containing or lacking *YKU70*. However, the sensitivity to replication stress of *htz1*Δ mutants did not require *YKU70*, and fumarate could suppress the sensitivity to HU of *htz1*Δ mutants similarly in the presence and absence of *YKU70* (Figure 3.14C). These results implied fumarate did not suppress sensitivity to replication stress in

the *htz1*Δ mutants by promoting removal of Ku from ends of reversed forks, but rather suppressed a Ku70p-independent defect in the *htz1*Δ mutants.

3.3 Discussion

Collectively, our findings are consistent with a role for metabolism in maintaining genome integrity. Here, we demonstrated that yeast fumarase, and fumarate, the product of catalysis by fumarase, act as intra-S phase checkpoint response factors (summarized in Table 1). Consistent with fumarate promoting replication fork integrity, we found that an increase in cellular levels of fumarate by deletion of *FUM1,* or addition of exogenous fumarate relieved the sensitivity to replication stress of yeast lacking *HTZ1* (Figure 3.2), or *SWR1* (Figure 3.4). Evidence from our genetic studies are consistent with fumarate conferring resistance to HU by modulation of histone methylation levels primarily through inhibition of the JmjC domain-containing histone demethylase Jhd2p (Figure 3.6) rather than via modulation of nucleotide pools (Figure 3.5), cell cycle progression (Figure 3.10), or checkpoint activation (Figure 3.11). We have shown that deletion of *JHD2* suppressed the sensitivity of *htz1*Δ mutants to replication stress (Figure 3.6 and Figure 3.8), and physiologically relevant amounts of fumarate could modulate H3 K4 methylation levels *in vivo* (Figure 3.9). These results are consistent with elevated histone H3 K4 methylation conferring resistance to replication stress in *htz1*Δ mutants. Our findings revealed fumarate could also promote resistance to replication stress through a second pathway in *htz1*Δ mutants that was H3 K4 methylation- or *JHD2*-independent (Figure 3.7 and Figure 3.8), implying that multiple mechanisms exist by which fumarate promoted growth during replication stress. Synthetic interaction analyses with intra-S phase checkpoint factors were consistent with the sensitivity to replication stress of *htz1*Δ mutants, and suppression of this sensitivity by fumarate, being primarily associated with defects in one or more events involved in processing and restart of stalled forks, rather than recognition of damage or activation of the intra-S phase checkpoint (Figure 3.10, Figure 3.11, Figure 3.12, Figure 3.13, Figure 3.14, Table 3.1).

In humans, fumarase has been described as a tumor suppressor where it's loss has been associated with stabilization of HIF1-α under normoxic conditions through inhibition of α-KG-dependent prolyl hydroxylases (Tomlinson *et al.* 2002; Isaacs *et al.* 2005; Koivunen *et al.* 2007; Gaude and Frezza 2014; Laurenti and Tennant 2016). However, a growing body of evidence points towards an additional integral role of this tumor suppressor in responses to DNA damage. In the past few

years, a direct link between fumarase deficiency and genome instability has emerged from studies in yeast as well as in mammalian cells. Yeast expressing Fum1p exclusively in mitochondria are sensitive to ionizing radiation, HU and DSBs created by expression of the HO endonuclease (Yogev *et al.* 2010; Leshets *et al.* 2018), and exhibit dramatically reduced stability of Sae2p, leading to defects in resection at HO-mediated DSBs (Leshets *et al.* 2018). Fum1p binds Sae2p *in vitro* and *in vivo* (Leshets *et al.* 2018), however, whether the catalytic activity of Fum1p, in addition to binding, is required to stabilize Sae2p has yet to be tested. In this study, we have demonstrated that Fum1p acted as an intra-S phase checkpoint response factor that became induced and enriched in the nucleus upon exposure to stress during DNA replication (Figure 3.1, see also (Yogev *et al.* 2010)), and that fumarate could suppress sensitivity to DNA replication stress in yeast lacking *SAE2* (Figure 3.14A), collectively implying Fum1p promotes genome integrity both through stabilizing Sae2p, and through the production of fumarate to modulate chromatin modification states. Interestingly, human fumarase also becomes enriched in chromatin extracts after exposure to ionizing radiation, and is recruited to DSBs created by the restriction endonuclease I-SceI (Jiang *et al.* 2015). Upon induction of a DSB in human cells, chromatin association of fumarase is facilitated by its interaction with H2A.Z, but whether CtIP (Sae2p) is also required is unknown. During DSB repair by NHEJ, chromatin-associated fumarase promotes association of the NHEJ factor KU70 by production of fumarate and inhibition of KDM2B, a histone demethylase that targets H3 K36 methylation (Jiang *et al.* 2015). In contrast, during the intra-S phase checkpoint response in budding yeast, sensitivity to replication stress in *htz1*Δ mutants was independent of *YKU70*, and fumarate promoted resistance to replication stress in *htz1*Δ mutants through a *YKU70*-independent pathway (Figure 3.14C) that involved inhibition of Jhd2p, a H3 K4-specific demethylase (Figure 3.6, Figure 3.7, Figure 3.8, Figure 3.9). As fumarate could also suppress the sensitivity to DNA replication stress of *htz1*Δ *sae2*Δ mutants, which contained *FUM1* but lacked these anticipated partners for targeting Fum1p to sites of damage (Figure 3.14A), our findings are consistent with a model (Figure 3.15) in which a critical role of fumarase during the DNA replication stress response is to modify chromatin composition by generating fumarate to inhibit Jhd2p, and potentially other dioxygenases (Figure 3.6, Figure 3.7, Figure 3.8, Figure 3.9).

Additional investigation will be required to decipher the mechanism(s) by which modulation of H3 K4 methylation by fumarate contributes to resistance to HU, but our data are consistent with a

role for this modification in facilitating processing and restart of stalled forks (Figure 3.14). While replication fork reversal during replication stress protects genome stability by facilitating replication restart, reversed forks resemble one end of a DSB, and are susceptible to excessive resection of nascent strands, resulting in genome instability (Thangavel *et al.* 2015; Zellweger *et al.* 2015; Giannattasio and Branzei 2017; Quinet *et al.* 2017). Thus, mechanisms induced during intra-S phase checkpoint activation also serve to limit resection during replication restart (Sogo *et al.* 2002; Rossi *et al.* 2015). Precedence exists for a role of H3 K4 methylation in intra-S phase checkpoint response and replication restart. In budding yeast, cells lacking *SET1* and expressing wild-type H3 or H3 K4R are similarly sensitive to replication stress, and *set1*Δ mutants exhibit a defect in recovery from exposure to HU as well as defects in recruiting YKu80p to DSBs (Faucher and Wellinger 2010). In mammals, SETD1A localizes to replication forks, and SETD1A-dependent H3 K4 methylation at forks stalled with HU protects such compromised forks from excessive Dna2-dependent resection via promoting histone mobilization by the chaperone FANCD2, and by negatively regulating the remodeler CHD4. This, in turn, promotes recruitment of RAD51, or RAD51 filament stability, at stalled or arrested forks in HU or MMS (Higgs *et al.* 2018). Additionally, SET1DA may play a role in the mammalian transcriptional response during DDR, but the impact of this effect is unclear (Hoshii *et al.* 2018; Arndt *et al.* 2018; Higgs *et al.* 2018). A second example for a role of H3 K4 methylation in fork restart during the intra-S phase checkpoint response can be found with the mammalian H3 K4-specific methyltransferases MLL2/3, which also function at stalled forks by enhancing recruitment of MRE11 and influencing fork processing in the absence of BRCA2 (Ray Chaudhuri *et al.* 2016; Higgs *et al.* 2018). In addition, other histone methyltransferases participate in responses to replication stress. The mammalian H3 K4- and K36-specific methyltransferase Metnase interacts with the 9-1-1 complex and participates in restarting stalled forks after arrest in HU, although Metnase itself is not required for RAD51 focus formation (De Haro *et al.* 2010). Moreover, recruitment of the endonuclease MUS81 to stalled forks is regulated by EZH2, a H3 K27-specific methyltransferase (Rondinelli *et al.* 2017). The relationship between these methyltransferases, H2A.Z, and fumarate at stalled forks in mammals awaits investigation.

Prior to the identification of H2A.Z as a binding partner of human fumarase (Jiang *et al.* 2015), Htz1p/H2A.Z had been identified as a participant in responses to DNA damage in yeast and human

cells (Mizuguchi *et al.* 2004; Dhillon *et al.* 2006; Kalocsay *et al.* 2009; Xu *et al.* 2012; Adkins *et al.* 2013), and yeast *HTZ1* had been found to exhibit synthetic genetic interactions with various DNA damage response factors including *MEC1*, *MRC1*, *RAD53*, and *EXO1* (Figure 3.12, Figure 3.14 and (Pan *et al.* 2006; Collins *et al.* 2007; Adkins *et al.* 2013)). During DSB repair, this histone variant is transiently incorporated around DSBs (Kalocsay *et al.* 2009), and Htz1p as well as the chromatin remodeling complexes SWR1C and INO80C, which regulate deposition of Htz1p onto chromatin, are involved in NHEJ, homologous recombination, and fork stability (Kobor *et al.* 2004; Papamichos-Chronakis *et al.* 2006, 2011; van Attikum *et al.* 2007; Papamichos-Chronakis and Peterson 2008; Xu *et al.* 2012; Adkins *et al.* 2013). Like in *htz1*Δ mutants, fumarate suppresses the sensitivity to replication stress of *swr1*Δ mutants (Figure 3.4), which are defective in incorporation of Htz1p into nucleosomes (Krogan *et al.* 2003; Mizuguchi *et al.* 2004; Kobor *et al.* 2004).

The chromatin remodeler INO80C is a target of the DRC; INO80C binds and is phosphorylated by Rad53p (Morrison *et al.* 2007; Chen *et al.* 2010; Poli *et al.* 2016), and participates in removal of Htz1p adjacent to DSBs (van Attikum *et al.* 2007; Lademann *et al.* 2017), which promotes Rad51p presynaptic filament formation for HR (Lademann *et al.* 2017). Together with Mec1p and the PAF1 complex, INO80C has also been implicated in replication fork progression and restart during collisions between the replication and transcription machinery through a mechanism that involves eviction of the initiating form (phosphorylated on Ser 5) of RNA PolII from DNA during replication stress in HU (Poli *et al.* 2016). Consistent with this observation, during recovery from HU, DSBs in *mec1* mutants are more likely to occur within genes induced by replication stress (Hoffman *et al.* 2015). How INO80C's substrate, nucleosomes containing Htz1p such as those found at transcriptional start sites, affect the efficiency of resolving such collisions is unknown. Interestingly, the PAF1 complex is also essential for monoubiquitination of H2B at promoters by Bre1p-Rad6p (Wood *et al.* 2003). Bre1p-Rad6p, in turn, is required for H3 K4 methylation by COMPASS/Set1p (Sun and Allis 2002; Dover *et al.* 2002; Ng *et al.* 2003; Wood *et al.* 2003; Krogan *et al.* 2003) and for association of COMPASS with RNA Pol II (Krogan *et al.* 2003). *htz1*Δ H3 K4R mutants exhibit synthetic growth defects (Figure 3.7 and (Venkatasubrahmanyam *et al.* 2007), and *set1*Δ and H3 K4R mutants exhibit growth defects in HU (Figure 3.7, Figure 3.8 and (Faucher and Wellinger 2010). In addition, fumarate promoted H3 K4 methylation (Figure 3.9) as

well as suppressed sensitivity of *htz1*Δ mutants to HU through a *JHD2*-dependent pathway (Figure 3.6). Thus, it is tempting to speculate that, by promoting H3 K4 methylation, fumarate could facilitate processing of such replication-transcription machinery collisions occurring in the *htz1*Δ mutants during replication stress.

In addition to having growth defects upon exposure to HU, *set1*Δ mutants display an increased rate of plasmid loss relative to wild-type in mini-chromosome maintenance assays (Faucher and Wellinger 2010; Rizzardi *et al.* 2012). Additionally, H3 K4me2 and me3 are enriched at origins of replication and H3 K4 methylation promotes efficient origin function (Rizzardi *et al.* 2012). As *htz1*Δ mutants show delays in origin firing (Dhillon *et al.* 2006), these observations collectively support a model in which high levels of H3 K4 methylation (by deletion of *JHD2* or inhibition of Jhd2p by elevated levels of cellular fumarate) could promote firing from inefficient or late origin to complement *htz1*Δ-dependent delays in replication during replication stress. Such a mechanism could involve instilling characteristics normally associated with early origins to late origins to advance timing of firing, or bypass of the Mrc1p-activated Rad53p inhibitory signal during DDR that normally blocks late origin firing in HU. However, we did not observe dramatic fumarate-dependent effects on cell cycle progression during replication stress in *htz1*Δ mutants (Figure 3.10), and this scenario would require late origin regulation in yeast to be somewhat different than in mammalian cells, which require SETD1A to prevent late origin firing after exposure to MMS during the DRC response (Higgs *et al.* 2018).

Thus, we instead favor a model in which fumarate confers resistance to replication stress primarily by bypassing a defect in replication fork processing and restart caused by the absence of *HTZ1* through upregulating histone methylation, in part, by inhibition of Jhd2p (Figure 3.15). However, another possible mechanism by which growth defects of *htz1*Δ mutants during replication stress could be suppressed by fumarate is by complementing defects in spindle assembly. In addition to inducing DNA replication stress, HU can cause defects in spindle formation (Liu *et al.* 2008). Moreover, *htz1*Δ mutants show defects in spindle assembly and sensitivity to benomyl (Krogan *et al.* 2004), but, like wild-type cells, arrest in HU with short mitotic spindles, a single nucleus and large buds (Dhillon and Kamakaka 2000). Whether or how fumarase and fumarate impact spindle assembly remains to be explored.

Future studies will also be required to reveal whether fumarase and fumarate can act in histone methylation independent pathway(s) to modulate cellular responses to DNA damage and replication stress. For example fumarate has the potential to regulate protein function (e.g. (Blatnik et al. 2008)) through reacting with cysteine residues to create a post-translational modification known as succination (Alderson *et al.* 2006). In fact, high levels of protein succination has been found in tumors with fumarase deficiency from patients with HLRCC (Bardella et al. 2011), but potential regulatory roles of protein succination on cysteine residues during responses to DNA damage largely await characterization.

Collectively, the results of this study and others (Yogev *et al.* 2010; Leshets *et al.* 2018) indicate that cellular responses to DNA replication stress are sensitive to fumarate, and imply that metabolism is intimately linked to the intra-S phase checkpoint response. Consistent with our findings, other studies have reported that addition of exogenous antagonists of α-KG including fumarate, succinate, or the oncometabolite R-2-HG as well as expression of tumor derived *FH*, *SDH* or *IDH* mutants cause a global increase of histone methylation levels (Xu *et al.* 2011; Xiao *et al.* 2012). Moreover, fumarate, succinate and 2-HG can modulate numerous cellular functions ranging from gene expression and silencing to DNA damage responses (Xu *et al.* 2011; Xiao *et al.* 2012; Jiang *et al.* 2015; Sulkowski *et al.* 2017; Janke *et al.* 2017). Thus, changes in metabolite availability through normal signal relay pathways, exogenous sources or genetic metabolic defects have the potential to impact genome integrity upon DNA replication stress by regulation of histone methylation, supporting a model in which metabolites broadly play crucial roles as chemical messengers in signaling pathways triggering cellular responses to various types of stress, the examples illustrated herein being DNA replication stress and DNA damage.

3.4 Future directions

3.4.1 Analyzing the effect of fumarate on H3 K4 methylation levels associated with DNA replication forks

We have shown that fumarate is a modulator of Jhd2p activity and H3 K4me3 levels using whole-cell extracts. However, whether DNA replication fork-associated H3 K4 methylation levels are also modulated by fumarate is not known. In Section 5.2.3, I will describe in more detail a method

to analyze proteins and histone PTMs associated with newly synthesized DNA in wild-type and *htz1*Δ mutants in the presence or absence of fumarate.

3.4.2 Analyzing the effect of overexpression or enhanced catalytic activity of Set1p on HU sensitivity of wild-type and *htz1*Δ mutants

If inhibition of Jhd2p by fumarate and increased levels of H3 K4 methylation is responsible for suppression of HU sensitivity of htz1Δ mutants, then overexpression of Set1p is expected to also confer resistance to *htz1*Δ mutants. We attempted to overexpress Set1p using a high copy number plasmid (2μ). However, a high variation was observed between independent clones (in two clones out of 10 tested clones, a slight resistance to HU was observed in *htz1*Δ mutants with overexpression of Set1p). As an alternative a low copy number plasmid or a Set1(Y1052F) mutant which has increased H3 K4 methyltransferase activity *in vitro* and *in vivo* (Takahashi *et al.* 2009) will be used to test whether high cellular levels of H3 K4 methylation can confer resistance to HU in *htz1*Δ mutants.

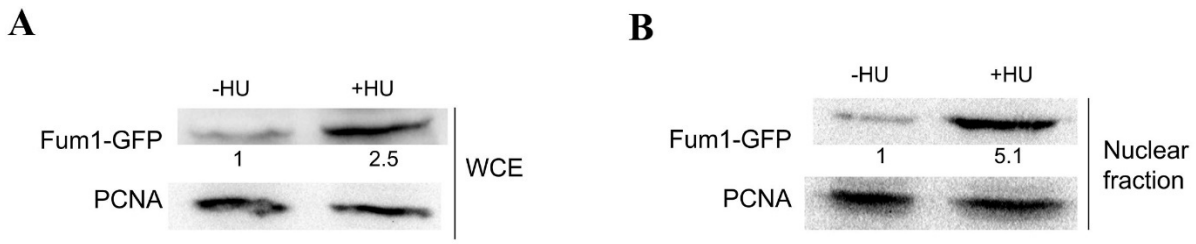

Figure 3.1 Expression of Fum1p is induced, and Fum1p becomes enriched in the nuclear fraction upon exposure to HU.

Yeast expressing Fum1-GFP were incubated in the absence or presence of 200 mM HU at 30oC for three hours. A) Whole cell extracts, or B) nuclear fractions were analyzed by immunoblotting using anti-GFP, and anti-PCNA antibodies. A representative immunoblot and fold enrichment of Fum1p from two independent experiments is shown. Levels of Fum1-GFPp were normalized to levels of PCNA (loading control), then expressed relative to signal that was observed in the absence of HU, which was set to 1.

$$\text{Fold enrichment of Fum1p} = \frac{(\text{Fum1p/PCNA})\text{indicated sample}}{(\text{Fum1p/PCNA})\text{no HU}}$$

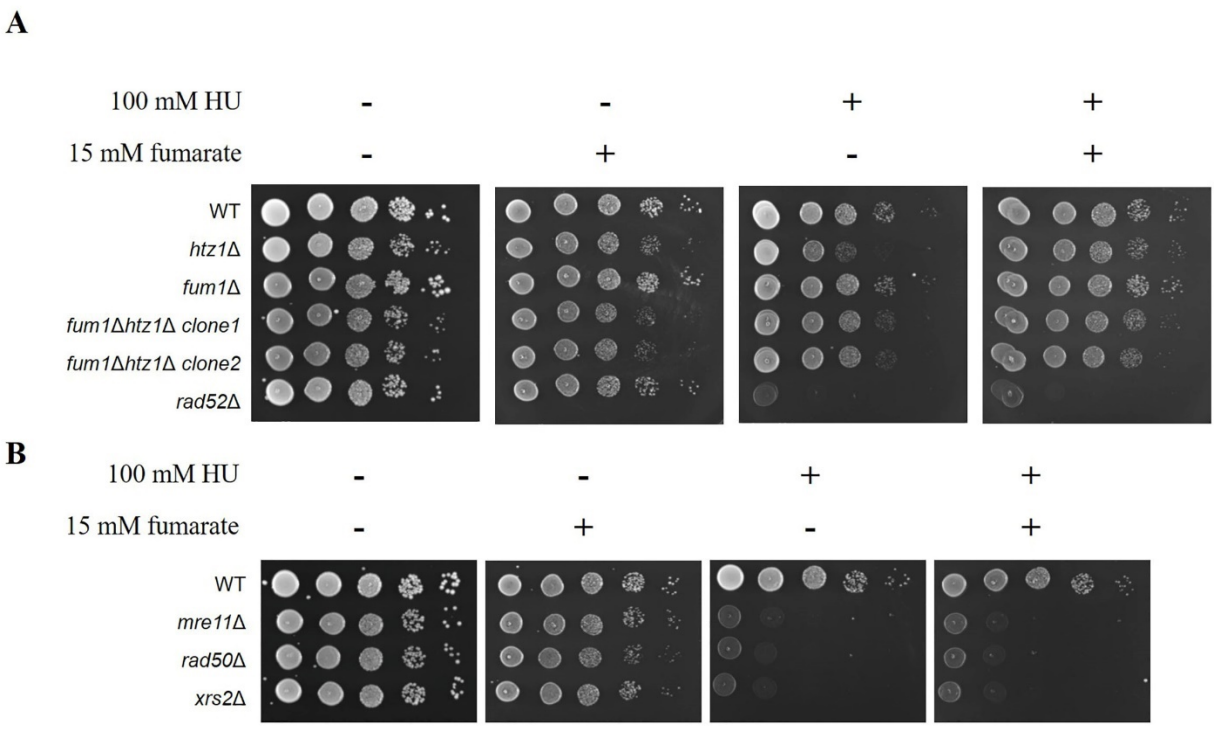

Figure 3.2 Fumarate can complement sensitivity of *htz1*Δ mutants to DNA replication stress.

A) Genetic interaction between *fum1*Δ and *htz1*Δ mutants. B) The effect of exogenous fumarate on DNA replication stress in *mre11*Δ, *rad50*Δ and *xrs2*Δ mutants. Cells with genotypes as indicated were grown overnight in rich (YPD) medium, then three µL of 10-fold serial dilutions were spotted onto YPD medium containing the indicated concentrations of fumarate and/or HU and incubated at 30°C for two days prior to imaging.

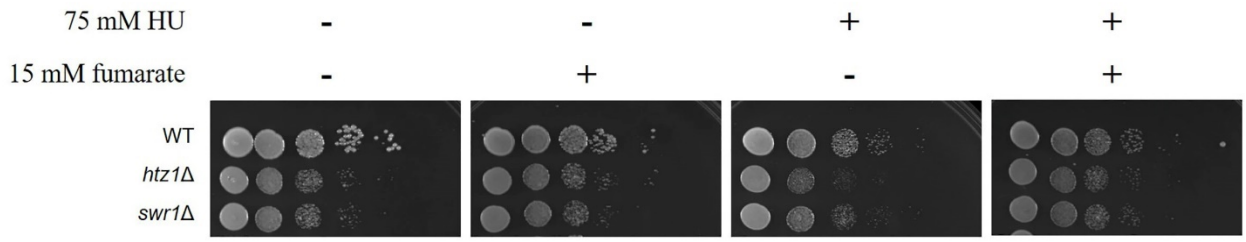

Figure 3.3 Exogenous fumarate suppresses sensitivity to DNA replication stress of *htz1*Δ and *swr1*Δ mutants.

Cells with indicated genotypes were grown overnight in rich medium (YPD), then three µL of 10-fold serial dilutions were spotted onto YPD medium containing 2×PBS and the indicated concentrations of fumarate and/or HU. Plates were incubated at 30°C for two days prior to imaging.

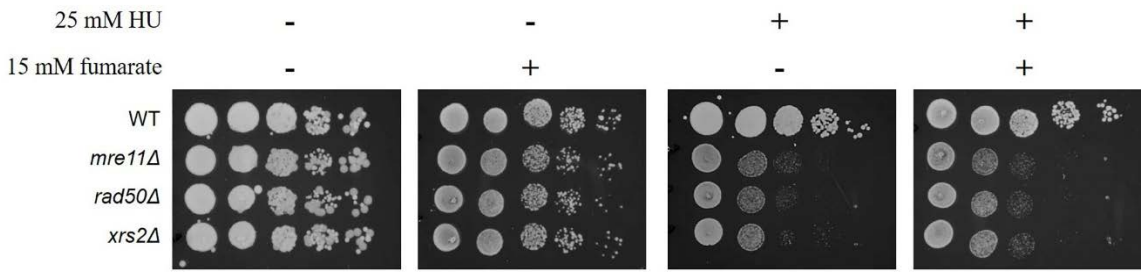

Figure 3.4 Sensitivity to DNA damage for mutants lacking components of the MRX complex is largely unaffected by exogenous fumarate.

Cells with indicated genotypes were grown overnight in rich medium (YPD), then three μL of 10-fold serial dilutions were spotted onto YPD medium containing 2×PBS and the indicated concentrations of fumarate and/or HU. Plates were incubated at 30°C for two days prior to imaging.

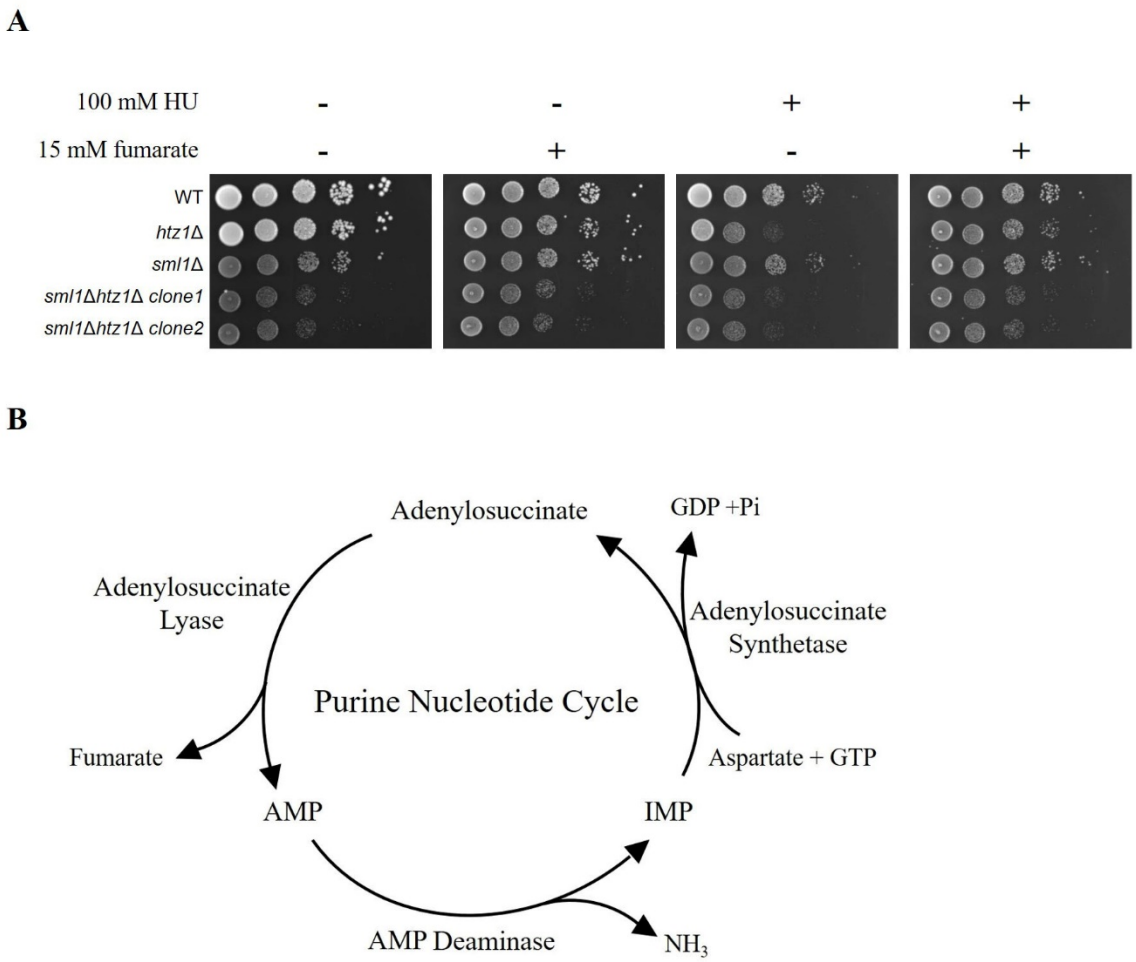

Figure 3.5 Fumarate-mediated suppression of sensitivity to DNA replication stress of *htz1*Δ mutants is independent of modulation of nucleotide pools.

A) Fumarate suppresses the sensitivity to DNA replication stress of *htz1*Δ mutants in the absence of an inhibitor of ribonucleotide reductase. B) Fumarate is a product in the purine nucleotide synthesis pathway. In purine nucleotide cycle, aspartate becomes converted to fumarate in a two-staged reaction, which is facilitated by hydrolysis of GTP. This two-stage reaction involves generation of adenylosuccinate from inosine monophosphate (IMP) and aspartate, which is then converted to fumarate and adenosine monophosphate (AMP). This reaction is followed by deamination of AMP to IMP by AMP deaminase. C) Fumarate suppresses the sensitivity to DNA replication stress of *htz1*Δ mutants in the absence of adenylosuccinate synthase (*ADE12*). Strains with genotypes as indicated in (A) and (C) were analyzed in serial dilution growth assays as described in Figure 3.2.

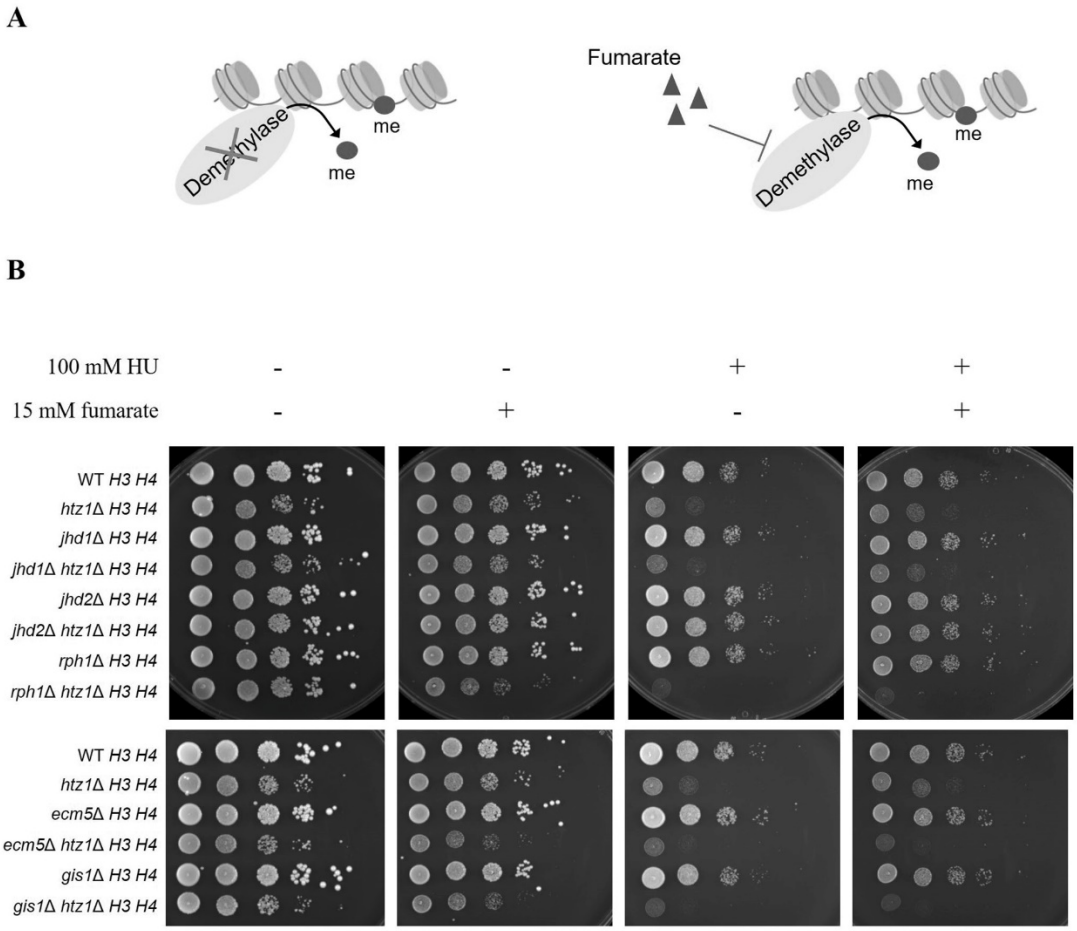

Figure 3.6 Loss of JmjC domain-containing histone demethylase Jhd2p suppresses the sensitivity to DNA replication stress of *htz1*Δ mutants.

A) Enhancing histone methylation by deletion of histone demethylase(s) or enzyme inhibition by fumarate. B) Genetic interaction analyses between *htz1*Δ mutants and histone demethylase mutants. Strains with indicated genotypes were analyzed in serial dilution growth assays as described in Figure 3.2.

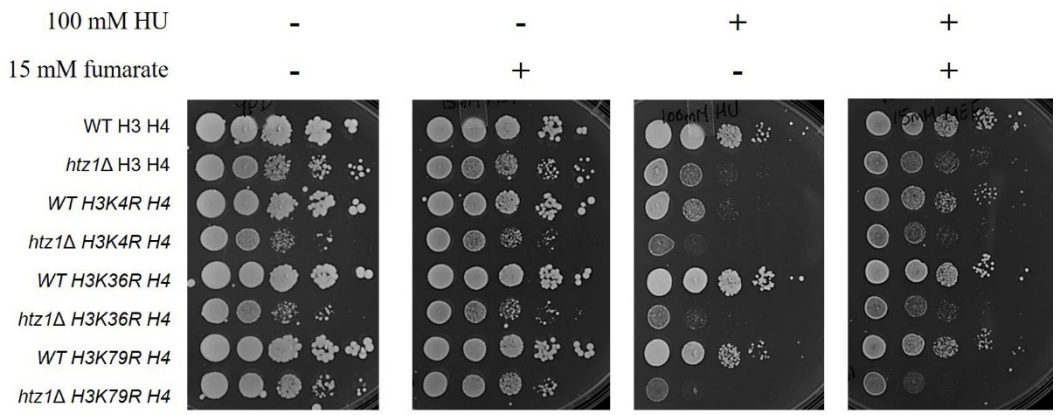

Figure 3.7 Fumarate-dependent suppression of sensitivity to DNA replication stress of strains expressing H3 mutants with lysine to arginine mutations at H3 K4, K36 or K79.

Strains with genotypes as indicated were analyzed in serial dilution growth assays as described in Figure 3.2.

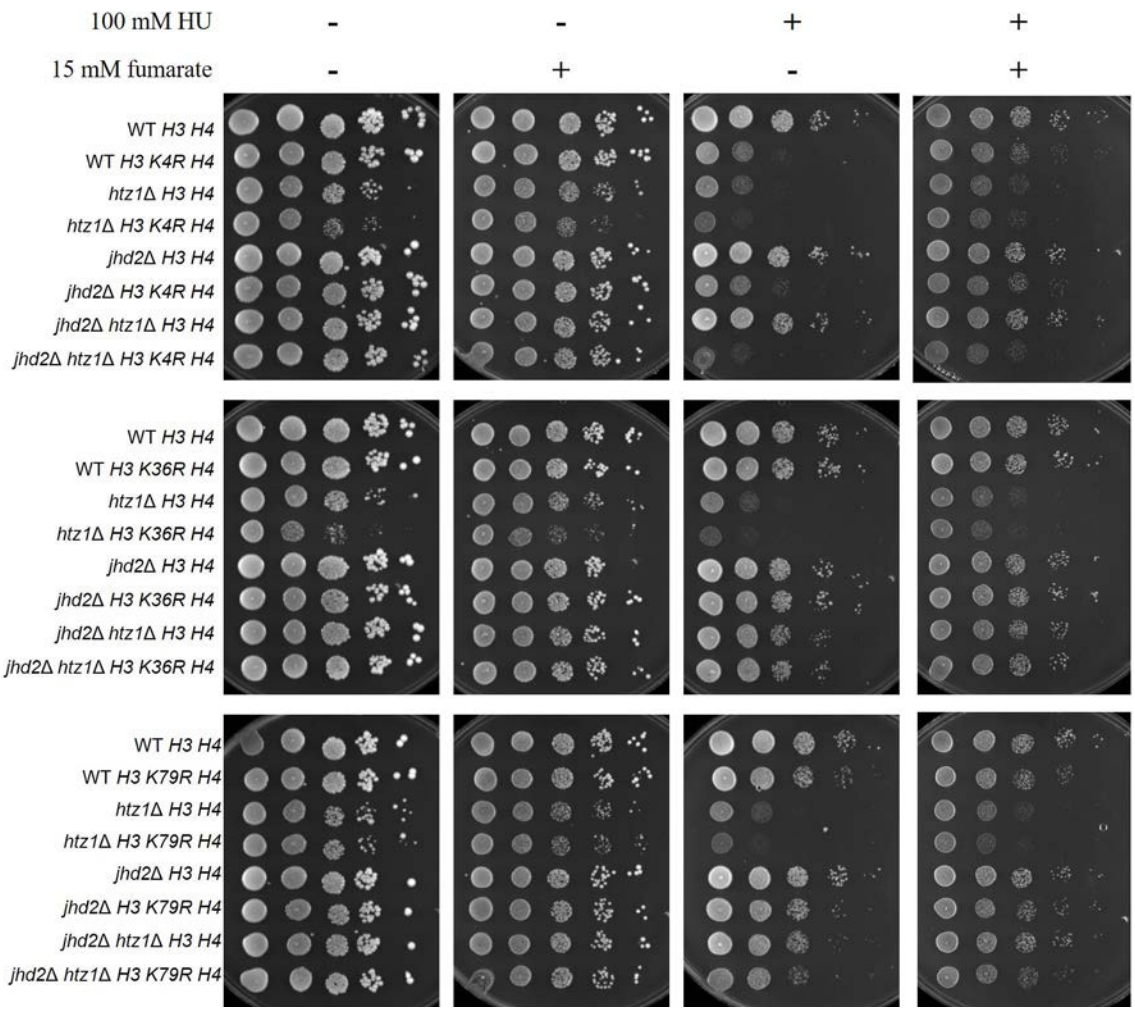

Figure 3.8 Impact of histone methylation, loss of *JHD2* and exogenous fumarate on sensitivity to DNA replication stress of *htz1*Δ mutants.

Strains with indicated genotypes were analyzed in serial dilution growth assays as described in Figure 3.2.

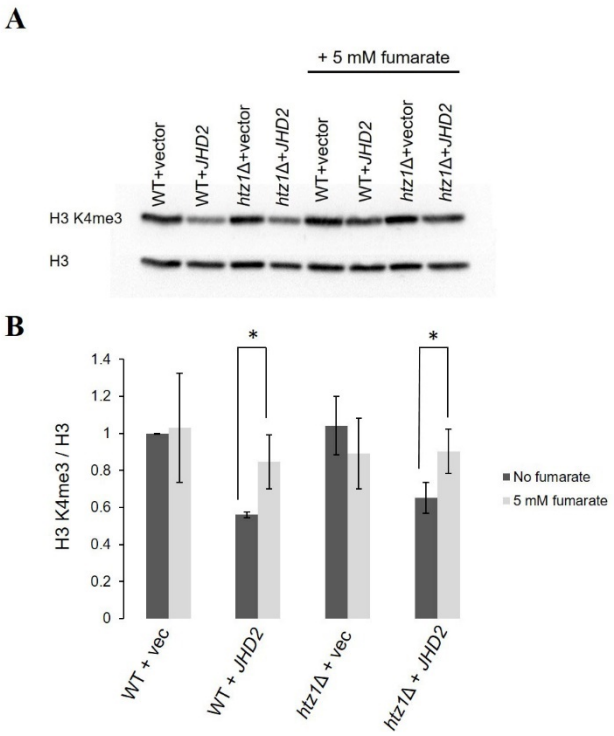

Figure 3.9 Fumarate modulates levels of *JDH2*-dependent H3 K4 methylation.

Wild-type yeast and *htz1*Δ mutants carrying an empty vector or a plasmid for overexpression of Jhd2p were grown logarithmically in selective medium with or without 5 mM fumarate. A) Whole cell extracts of strains with indicated genotypes were analyzed by immunoblotting against H3 K4me3 and H3 (loading control). B) Levels of H3 K4me3 were normalized to H3, and expressed relative to that observed in wild-type with vector (vec), which was set to 1 (Avg. +/- STD, n=3; representative independent experiment shown in A). The level of H3 K4me3 relative to H3 was calculated as $\frac{(\text{H3 K4me3/H3})_{\text{sample}}}{(\text{H3 K4me3/H3})_{\text{WT + vec}}}$. The statistical analysis was performed using Wilcoxon Rank Sum test and P-value < 0.05 is shown by *.

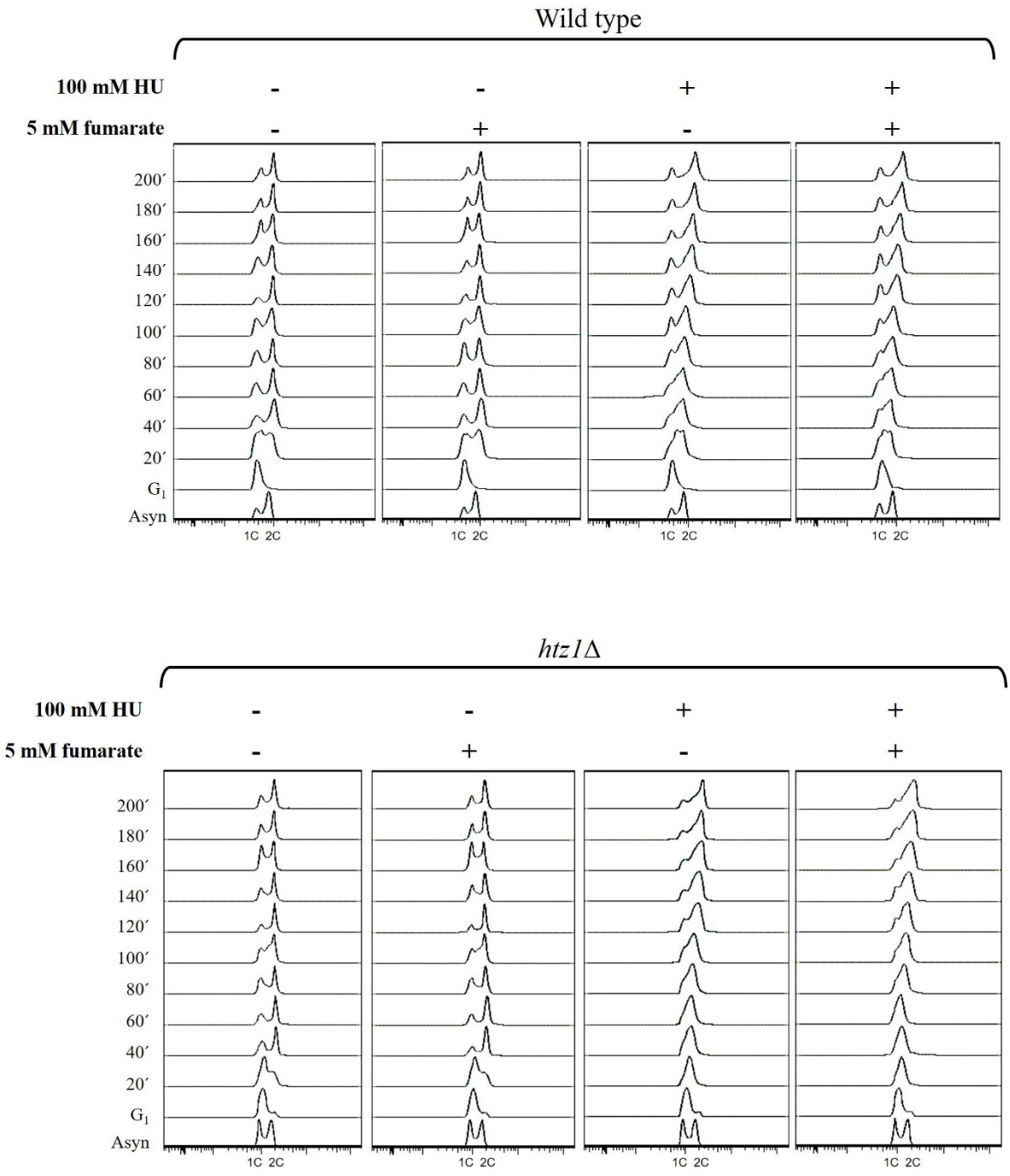

Figure 3.10 Analysis of cell cycle progression of wild-type yeast and *htz1*Δ mutants upon exposure to hydroxyurea and/or fumarate.

Cultures were grown logarithmically at 30ºC in rich (YPD) medium, then arrested in G_1 by the addition of α-factor, and incubated for three hours. Cultures were then released into YPD containing 2×PBS in the presence or absence of 100 mM HU and 5 mM fumarate as noted. Cells were collected during logarithmic growth, during G_1 arrest, and every 20 minutes after release from G_1, then stained with propidium iodide and analyzed by flow cytometry.

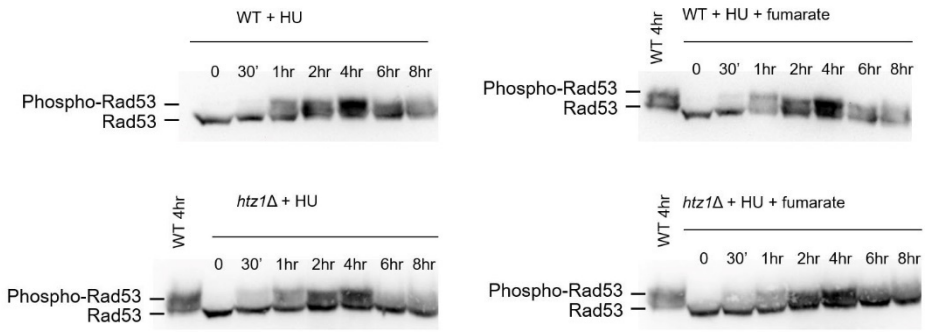

Figure 3.11 Intra-S phase checkpoint is activated upon exposure to hydroxyurea +/- fumarate.

Wild-type yeast and *htz1*Δ mutants were grown logarithmically at 30ºC in rich (YPD) medium, then arrested in G_1 by the addition of α-factor, then incubated for three hours. Cells were released from G_1 into YPD medium containing 2×PBS and 100 mM HU with or without 5 mM fumarate. Aliquots were collected at indicated timepoints from each culture, and whole cells extracts were analyzed by immunoblotting using anti-Rad53p. Whole cell extract from wild-type cells treated with HU for four hours were run on blots as a reference.

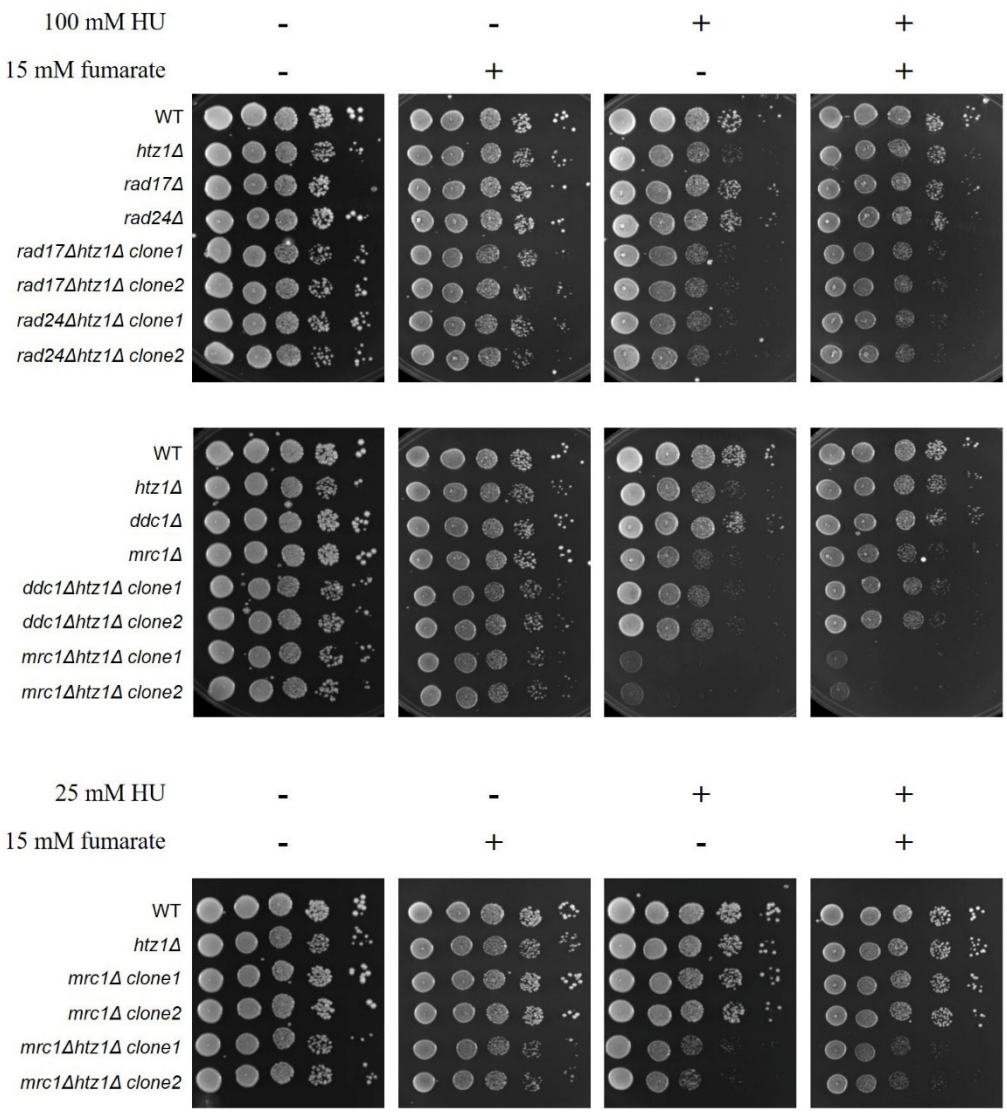

Figure 3.12 Fumarate-dependent suppression of sensitivity to DNA replication stress of *htz1*Δ mutants requires components of the intra-S phase checkpoint.

A) The 9-1-1 complex and the 9-1-1 loader Rad24p are required for fumarate to suppress the sensitivity to DNA replication stress of *htz1*Δ mutants. (A and B) *htz1*Δ mutants require the DRC mediator Mrc1p during DNA replication stress. Strains with genotypes as indicated were analyzed as described in Figure 3.2.

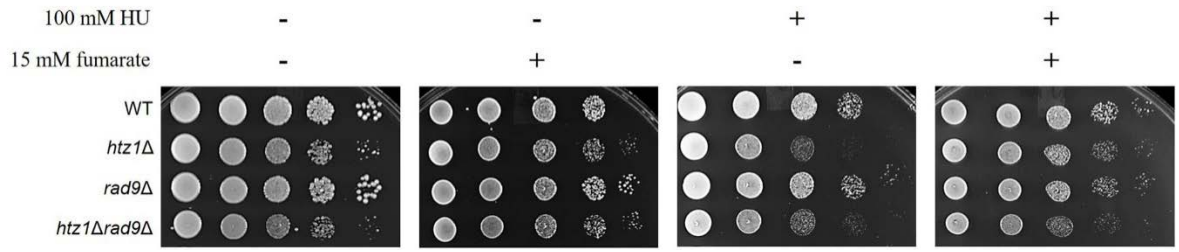

Figure 3.13 *htz1*Δ mutants do not require the DDC mediator Rad9p during DNA replication stress. Strains with genotypes as indicated were analyzed as described in Figure 3.2.

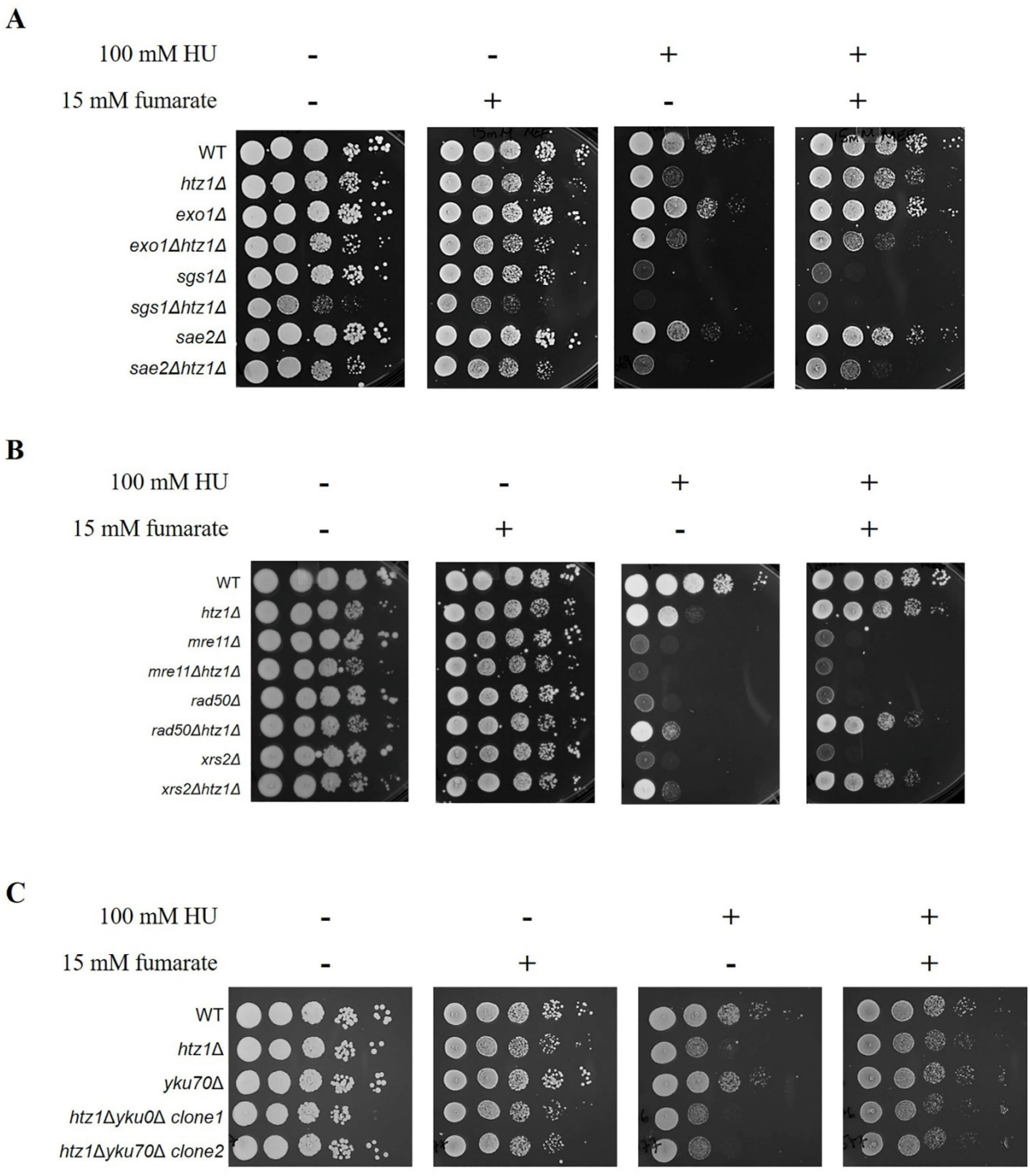

Figure 3.14 Impact of loss of *HTZ1* and exogenous fumarate on sensitivity to DNA replication stress of mutants with defects in DRC and processing and restart of aberrant replication forks.

A) Fumarate suppresses the sensitivity to DNA replication stress in cells lacking *EXO1*, or *SAE2* in the presence or absence *of HTZ1*. B) Loss of *HTZ1* confers resistance to DNA replication stress of cells lacking subunits of the MRX complex, and fumarate enhances this effect. C) Ku70p is not required for suppression of sensitivity of *htz1*Δ mutants to DNA replication stress by fumarate. Strains with genotypes as indicated were analyzed as described in Figure 3.2.

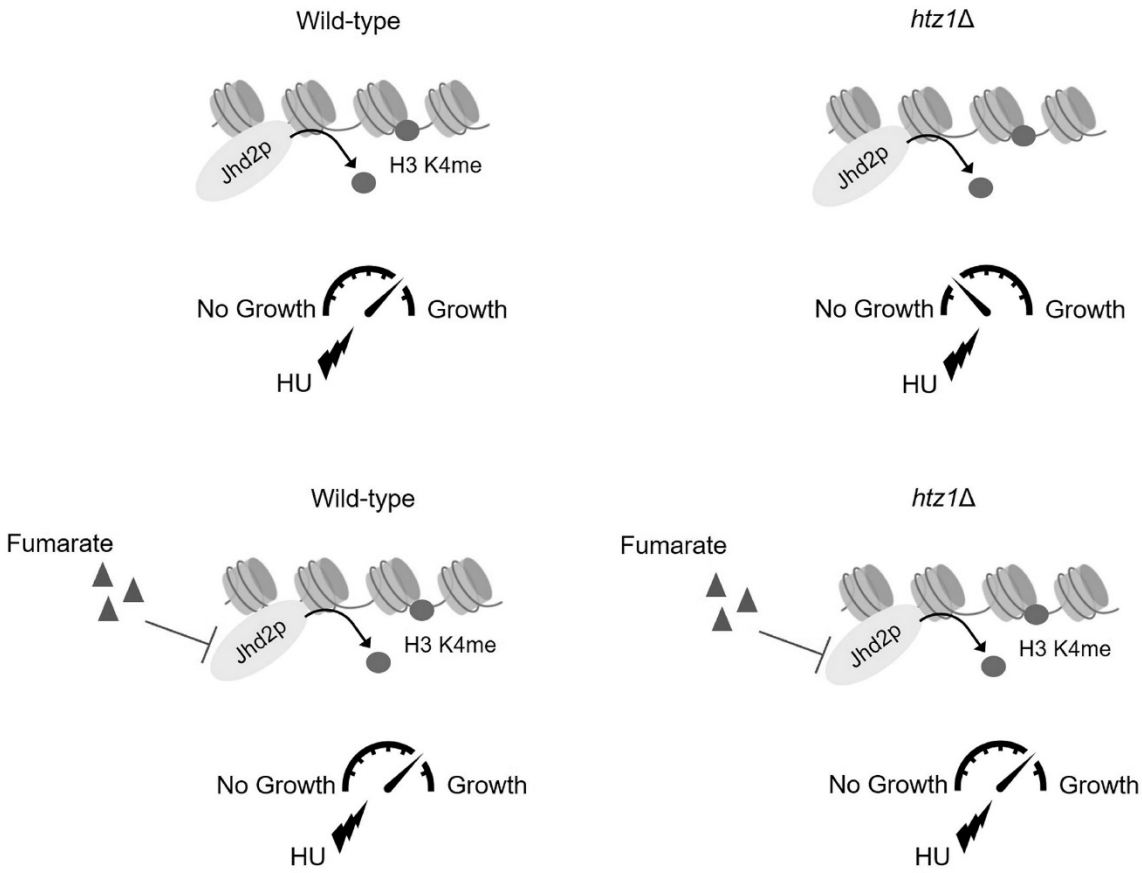

Figure 3.15 Fumarate promotes cell survival in *htz1*Δ mutants upon DNA replication stress by inhibition of the JmjC domain-containing histone demethylase Jhd2p.

Table 3.1 Summary of genetic interactions between *htz1*Δ mutants and DNA replication stress response components or histone demethylases.

Function	Mutant tested	Genetic interaction with *htz1*Δ on rich medium	Genetic interaction with *htz1*Δ on HU	Suppression of HU sensitivity by fumarate in wild-type background	Suppression of HU sensitivity by fumarate in *htz1*Δ background
Sensor of DNA replication stress	*rad17*Δ	None[1]	None	N/D[2]	No[3]
	*ddc1*Δ	None	None	N/D	No
	*rad24*Δ	None	None	N/D	No
Mediator of checkpoint signaling	*mrc1*Δ	None	-[4]	N/D	No
	*rad9*Δ	None	+[4]	N/D	N/D
DNA processing factor	*exo1*Δ	None	None	N/D	Yes[3]
	*sgs1*Δ	-	N/D	No	No
	*sae2*Δ	None	-	Yes	Yes
	*yku70*Δ	None	None	N/D	Yes
	*mre11*Δ	None	-	No	No
	*rad50*Δ	None	+	No	Yes
	*xrs2*Δ	None	+	No	Yes
	*rad52*Δ	Not tested[5]	Not tested	No	Not tested
Chromatin modifying enzyme	*jhd1*Δ	None	None	N/D	Yes
	*jhd2*Δ	+	+	N/D	N/D
	*rph1*Δ	None*[6]	-	N/D	No
	*gis1*Δ	None*	None	N/D	No
	*ecm5*Δ	None*	None	N/D	No
Other	*fum1*Δ	None	+	N/D	Yes
	*swr1*Δ	Not tested	Not tested	Yes	Not tested
	*sml1*Δ	-	+	N/D	Yes
	*ade12*Δ	None	-	N/D	Yes

CHAPTER 4. EFFECT OF FUMARATE ON RESPONSE TO DSBs UPON LOSS OF HTZ1 AND OTHER DNA DAMAGE RESPONSE FACTORS

4.1 Introduction

Double stranded DNA break (DSBs) is a deleterious form of DNA damage and a single unrepaired DSB can initate DNA damage checkpoint activation (Sandell and Zakian 1993; Lee *et al.* 1998; Pellicioli *et al.* 2001). HR and NHEJ are two major pathways for repair of DSBs. NHEJ is most efficienct on clean or minimally processed DNA ends, whereas in DNA repair by HR, DNA end resection is the first critical step (see Section 1.2.1 for a detailed discussion). In yeast, HR is the predominant pathway for DNA repair and mutants lacking components of the HR pathway including *RAD51*, *RAD52*, *MRE11*, *XRS2* or *RAD50* (see Section 1.2.1.2 for a review) are highly sensitive to irradiation or bleomycin (Game and Mortimer 1974). However, mutants lacking components of the NHEJ pathway including *YKU70*, *DNL4*, *LIF1* or *NEJ1* show little to no sensitivity to DNA damage (Game and Mortimer 1974; Gao *et al.* 2016). In a study by Zhang *et al.*, DSB induction by expression of the HO endonuclease was used in yeast strains lacking *HMLα*, the donor locus for *MAT***a,** to study the efficinecy of NHEJ vs. HR (Zhang *et al.* 2009). The study showed that in logarithmically growing cells, only 10% of the cells survived in *rad52*Δ mutants, whereas in *yku70*Δ mutants, all cells survived and formed colonies (Zhang *et al.* 2009), indicating that in cycling cells, HR is the main patway for DSB repair. Interestingly, in G_1-arrested cells where NHEJ is the predomiannt pathway for DSB repair, ~40% of cells were able to form colonies after HO induction in *rad52*Δ mutants (Zhang *et al.* 2009). Moreover, studies in *S. cerevisiae* in which more than 99% of the population is arrested in G_1, showed that mutants lacking *YKU70* or *YKU80* are highly sensitive to γ-radiation (Gao *et al.* 2016). These findings are consistent with NHEJ being a minor pathway for DNA repair in cycling cells in yeast and predominantly functioning in G_1. In G_1-arrested cells, NHEJ efficiently repairs DSBs, indicating that NHEJ is an efficient pathway for DNA repair in a cell-cycle specific manner (see Section 1.2.1.3 for a review of the role of cell cycle in DNA repair pathway choice) (Gao *et al.* 2016).

As discussed in Section 1.8, chromatin association of human FH is enhanced by its interaction with the histone variat H2A.Z in human cells (Jiang *et al.* 2015). Moreover, yeast fumarase has been shown to play a role in HR and DNA end resection by binding to and stabilizing Sae2p protein levels (Leshets *et al.* 2018). However, whether yeast fumarase is also involved in NHEJ is not known.

When added as substrates *in vitro*, nucleosomes containing canonical histone H2A are inhibitory for exonuclease activity of Exo1p, whereas H2A.Z-containing nucleosomes are permissible for Exo1p exonuclease activity, indicating that incorporation of H2A.Z promotes activity of Exo1p (Adkins *et al.* 2013). *In vivo*, Htz1p is traniently deposited near DSBs and loss of Htz1p causes defects in checkpoint activation upon DSB induction as measured by Rad53p phosphorylation (Kalocsay *et al.* 2009). Moreover, upon persistent induction of DSB, Htz1p promotes anchoring of DSBs to the nuclear periphery where unrepairble DSBs interact with the nuclear envelope (Kalocsay *et al.* 2009; Lisby *et al.* 2010; Freudenreich and Su 2016). In yeast, loss of Htz1p decreases the amount of DNA end resection following DSB induction (Kalocsay *et al.* 2009; Adkins *et al.* 2013; Lademann *et al.* 2017) (see Section 1.5.1.2 for a detailed discussion of the role of H2A.Z in DNA damage response). In addition, removal of Htz1p by INO80 complex (see Section 1.5.1.2 for a detailed review of deposition/removal of Htz1p by the SWR-C and INO80 complexes) promotes formation of Rad51p nucleoprotein filaments (Lademann *et al.* 2017). These observations imply that the dynamic chromatin association of Htz1p is critical for repair by HR in yeast. However, whether yeast Htz1p is also involved in DNA repair by NHEJ is not known. Here, we examined the role of Fum1p and Htz1p in NHEJ and analyzed the genetic interaction between *FUM1*, *HTZ1* and other DNA damage response factors. In addition, we explored how metabolite fumarate affects the sensitivity to DNA damage in mutants lacking Fum1p, Htz1p and other DNA damage response factors.

We showed that Fum1p and the histone variant Htz1p promote DNA repair by NHEJ. Consistent with a role for Fum1p and Htz1p in DNA damage response, deletion of *FUM1* or *HTZ1* caused sensitivity to zeocin, and *HTZ1* and *FUM1* showed negative synthetic genetic interaction in the presence of zeocin. Moreover, we showed a negative synthetic genetic interaction between *HTZ1* and multiple components of the HR pathway including *SGS1* and *SAE2*, which are involved in the DNA end resection pathway (see Section 1.2.1.2 and Figure 1.2 for a description of the role of

these factors in DNA end resection during HR). For multiple mutants, including cells lacking *FUM1*, *HTZ1* or other components of the DNA damage response like *RAD52*, *SAE2* and *SGS1*, sensitivity to induction of DSB by zeocin was complemented by exogenous fumarate. Our data also imply that suppression of sensitivity to DSBs in *htz1*Δ mutants by fumarate is likely independent of inhibition of JmjC domain containing histone demethylases by fumarate. Although exogenous fumarate did not largely affect RPA foci formation, it attenuated checkpoint activation as measured by analyzing phosphorylation of Rad53p. Future experiments are required to further investigate the mechanism by which exogenous fumarate confers resistance to zeocin in *htz1*Δ mutants, and other mutants with defects in DNA repair by HR (e.g. *rad52*Δ, *sgs1*Δ, *sae2*Δ or *fum1*Δ). Future experiments will be discussed in Section 4.3.2.

4.2 Results

4.2.1 Fumarase and Htz1p promote DNA repair by NHEJ

In mammalian cells, fumarase is recruited to the sites of DSBs through interaction with the histone variant H2A.Z (Jiang *et al.* 2015), and human fumarase and H2A.Z promote association of KU70 with DSB ends and DNA repair by NHEJ (Xu *et al.* 2012; Jiang *et al.* 2015). To test whether yeast Htz1p and Fum1p also contribute to NHEJ, we performed plasmid re-joining assays using strains with deletion of *HTZ1* or *FUM1*. The plasmid re-joining efficiency is a measure for the ability of cells to repair DSBs generated by restriction enzyme digestion (Wilson *et al.* 1997). The site of restriction enzyme digestion is selected in a manner to ensure no homology exists between regions surrounding the cut site and the yeast genome (e.g. at multiple cloning site of the plasmid). In this assay, yeast strains are transformed with a low copy number plasmid linearized by restriction digestion. To grow on selective media, the linearized plasmid needs to be re-circularized by NHEJ in order to be replicated and maintained in subsequent cell divisions. To normalize for differences in transformation efficiency between strains tested, a supercoiled form of the plasmid is also transformed into the cells in parallel. Therefore, the number of transformants obtained using the linearized plasmid relative to the supercoiled plasmid is a quantitative measure for the efficiency of repair of the DSB. To avoid repair of the plasmid by HR, the site of the DSB created by the restriction enzyme is chosen within regions of the plasmid with no homology to the yeast genome.

To measure plasmid re-joining efficiency in strains lacking *HTZ1* or *FUM1*, we linearized with pRS313 (*ARS4/CEN6/HIS3*) using XbaI or SmaI (to generate sticky ends or blunt ends, respectively). XbaI and SmaI have unique recognition sequences in pRS313 at the multiple cloning site. As a positive control, we used strains lacking *YKU70*, as Yku70p is required for repair by NHEJ (Chen *et al.* 2005; Faucher and Wellinger 2010). We also used *rad52*Δ mutants as a negative control as deletion of *RAD52*, while critical for repair by HR, has no significant effect on re-joining efficiency by NHEJ (Chen *et al.* 2005). As shown in Figure 4.1, and consistent with previous reports (Chen *et al.* 2005; Faucher and Wellinger 2010), plasmid re-joining efficiency in *rad52*Δ mutants was comparable to wild-type, whereas in *yku70*Δ mutants, plasmid re-joining efficiency decreased to about 10% of wild-type when either XbaI or SmaI were used to generate a DSB ($p=0.029$ for both XbaI and SmaI). The plasmid re-joining efficiency in *htz1*Δ decrease to about 50% of wild-type when either XbaI or SmaI were used to generate a DSB ($p=0.029$ and 0.05 for XbaI and SmaI, respectively). The plasmid re-joining efficiency for *fum1*Δ decreased to 45% and 35% relative to wild-type when XbaI or SmaI was used, respectively ($p=0.029$ and 0.027 for XbaI and SmaI, respectively). These results indicate that in yeast, like in human cells, Htz1p and Fum1p promote DNA repair by NHEJ.

4.2.2 Synthetic genetic interaction between *FUM1* and *HTZ1*

Chromatin association of human fumarase and production of fumarate promotes growth upon exposure to ionizing radiation (Jiang *et al.* 2015). To understand the role of fumarase and how the metabolite fumarate promote growth upon DSB induction, we tested the impact of deletion of yeast *FUM1* or addition of exogenous fumarate on growth upon induction of DSBs. To induce DSBs, we used a radiomimetic chemical named zeocin, which is commonly used to induce DSBs. As shown in Figure 4.2 (first vs. third panel), and consistent with previous reports where *htz1*Δ mutants show sensitivity to phleomycin (Morillo-Huesca *et al.* 2010), *htz1*Δ mutants were sensitive to zeocin. Deletion of *FUM1* also resulted in sensitivity to zeocin, consistent with previous studies in which mutants with defects in nuclear localization of Fum1p showed sensitivity to IR and DSB induction at *MAT* locus by expression of the HO endonuclease (Yogev *et al.* 2010).

*htz1*Δ *fum1*Δ mutants showed greater sensitivity to zeocin compared to *htz1*Δ and *fum1*Δ mutants indicating that deletion of *FUM1* exacerbated sensitivity of *htz1*Δ mutants to DSBs (Figure 4.2 first vs. third panel). This implied that Fum1p played a role in repair of DSBs and is consistent

with our data showing that Fum1p promoted DNA repair by NHEJ (Figure 4.1). Moreover, Fum1p promotes DNA end resection and repair by HR in *S. cerevisiae* by stabilizing Sae2p, the MRX associated endonuclease that is involved in initiation of DNA end resection (Lengsfeld *et al.* 2007; Cannavo and Cejka 2014) (See Section 1.2.1.2 and Figure 1.2).

Next, we tested the effect of fumarate on growth and sensitivity to DSB in mutants with deletion of *FUM1* or *HTZ1*. As shown in Figure 4.2 (first vs. second panel), and as previously reported in Chapter 3 (for example see Figure 3.2 and Figure 3.4), addition of fumarate causes a decrease in colony size in all strains tested. In the presence of zeocin, addition of fumarate, suppressed the sensitivity to DSB in *htz1*Δ mutants in strains containing or lacking *FUM1* (Figure 4.2 third vs. fourth panel). This implied that exogenous fumarate could suppress the sensitivity to zeocin in *htz1*Δ mutants and that this suppression does not require Fum1p. Exogenous fumarate also suppressed the sensitivity to zeocin in *fum1*Δ mutants and *rad52*Δ mutants indicating that exogenous fumarate could bypass defects in DNA damage response in the absence of Fum1p or Rad52p. As described above, Fum1p promotes DNA end resection while, Rad52p promotes formation of Rad51p nucleoprotein filaments, strand invasion and strand annealing during SDSA (Sugiyama *et al.* 1998; Pâques and Haber 1999; Davis and Symington 2001) (see sections 1.2.1.2.1 and 1.8 for a review of these processes and the roles of Rad51p and Rad52p in HR). Taken together, these data implied that fumarate bypassed defects in multiple steps of the DNA damage response or had caused fewer DNA lesion upon exposure to zeocin (see 4.3.2 for description of a hypothesis and proposed future experiments).

4.2.3 Suppression of sensitivity to zeocin in *htz1*Δ mutants by fumarate does not require NHEJ

As *htz1*Δ mutants showed defects in DNA repair by NHEJ (Figure 4.1), and the enzymatic activity of fumarase, as well as accumulation of fumarate after DSB induction promote repair by NHEJ in human cells (Jiang *et al.* 2015), we tested whether suppression of sensitivity to zeocin by fumarate required repair by NHEJ. We analyzed the genetic interaction between *HTZ1* and *YKU70* by comparing growth of *htz1*Δ, *yku70*Δ and *htz1*Δ *yku70*Δ mutants upon induction of DSBs by zeocin in the presence and absence of fumarate. As shown in Figure 4.3, while *htz1*Δ mutants showed growth defects upon exposure to zeocin (third vs. first panel), *yku*70Δ mutants did not (as compared to wild-type) (third vs. first panel). This is consistent with previous reports where

*yku70*Δ and *yku80*Δ showed no sensitivity to γ-radiation (Gao *et al.* 2016) and with NHEJ being a minor pathway for repair of DSBs in yeast (Zhang *et al.* 2009).

In support of this model, in zeocin-containing medium, *htz1*Δ *yku70*Δ double mutants grew similarly to *htz1*Δ mutants (Figure 4.3 third vs. first panel). Addition of exogenous fumarate suppressed the sensitivity to zeocin of *htz1*Δ mutants as well as *htz1*Δ *yku70*Δ mutants (Figure 4.3 third vs. first panel), indicating that Yku70p and DNA repair by NHEJ was not required for suppression of sensitivity to zeocin by fumarate.

4.2.4 RPA foci formation upon zeocin treatment was largely unaffected in the presence of fumarate

in vitro studies have shown that Exo1p (a component of the DNA end resection pathway described in Section 1.2.1.2 and Figure 1.2) has little exonuclease activity when presented with substrates with nucleosomes containing canonical histones. However, incorporation of H2A.Z into nucleosomes increases the exonuclease activity of Exo1p *in vitro* (Adkins *et al.* 2013). Moreover, in yeast, *htz1*Δ mutants have defects in DNA end resection as these mutants show decreased accumulation of ssDNA (Kalocsay *et al.* 2009; Lademann *et al.* 2017), indicating that Htz1p promotes DNA end resection. Therefore, we tested whether fumarate impacted DNA end resection upon DSB in wild-type or *htz1*Δ mutants by analyzing RPA foci formation. RPA is a heterotrimer of Rfa1p, Rfa2p and Rfa3p and binds to ssDNA generated during DNA end resection (Brill and Stillman 1991; Alani *et al.* 1992). RPA accumulates on ssDNA after induction of a DSB can be visualized as discrete foci (Gasior *et al.* 1998; Sugiyama and Kowalczykowski 2002). Binding of RPA to ssDNA promotes formation of Rad51p nucleofilaments (Sugiyama *et al.* 1997; Sugiyama and Kowalczykowski 2002) and is required for recruitment of Mec1p-Ddc2p to the sites of damage to promote checkpoint activation (Zou and Elledge 2003) (see Sections 1.2.1.2 and 1.2.1.4 for a detailed description).

We tested wild-type or *htz1*Δ mutants expressing Rfa1p C-terminally tagged with GFP for formation of RPA foci upon zeocin exposure by fluorescence microscopy. Wild-Type or *htz1*Δ mutants expressing Rfa1-GFP were exposed to zeocin with or without exogenous fumarate for four hours and RPA foci were analyzed before, and 30 min, one, two, three and four hours after treatment. As shown in Figure 4.4, about 10% of wild-type cells, and more than 20% of *htz1*Δ cells

showed discrete RPA foci prior to treatment with zeocin. Higher levels of RPA foci in the *htz1*Δ mutants could be due to high levels of ssDNA accumulated due to endogenous DNA damage or defects in replication forks. This is consistent with the observation that deletion of *HTZ1* in strains with mutations in *POL3* increases the rate of mutation (Van *et al.* 2015). *POL3* is an essential gene encoding the catalytic subunit of Polδ, a high fidelity DNA polymerase involved in lagging strand DNA synthesis (Garg and Burgers 2005; Swan *et al.* 2009). In addition, deletion of *HTZ1* increases genomic instability and causes defects in chromosome segregation (Krogan *et al.* 2004; Srivatsan *et al.* 2018).

An increase in the number of cells containing RPA foci was detected within 30 min of treatment in both wild-type and *htz1*Δ mutants and by three hours ~50% of cells contained RPA foci. Addition of fumarate did not largely impact the number of cells with RPA foci at any timepoints examined in wild-type. In contrast, a fumarate-dependent delay in increase of the number of RPA foci was observed in *htz1*Δ mutants after 30 min of exposure to zeocin. However, by one hour, the number of htz1Δ mutant cells with RPA foci was comparable to that observed in the absence of fumarate. These results implied that RPA foci formation upon induction of DSBs by zeocin was not greatly affected by fumarate in wild-type or *htz1*Δ mutants.

Components of the DNA end resection pathway are dispensable for suppression of sensitivity to zeocin in *htz1*Δ by fumarate

To further examine the relationship between fumarate, Htz1p and the DNA end resection pathway during HR, we repeated our growth assays in strains lacking *HTZ1,* and components of the DNA end resection pathway including *EXO1, SGS1* and *SAE2.* Sae2p promotes endonuclease activity of the Mre11p subunit of the MRX complex (Lengsfeld *et al.* 2007; Cannavo and Cejka 2014). MRX complex initiates DNA end resection by creating a nick near DNA ends (Garcia *et al.* 2011). Sgs1p is a helicase that functions with the exonuclease Dna2p in long-range DNA end resection, while Exo1p functions in a parallel pathway during long-range DNA end resection and has 5’ to 3’ exonuclease activity (Figure 4.5 A) (Zhu *et al.* 2008; Mimitou and Symington 2008) (see Section 1.2.1.2 and Figure 1.2 for a description of their function). As shown in Figure 4.5 B (first panel), and previously demonstrated in Figure 3.14 (first panel), *sgs1*Δ *htz1*Δ mutants show growth defects in rich medium (YPD) relative to *sgs1*Δ or *htz1*Δ mutants indicating that Sgs1 is critical for growth in the absence of Htz1p. In the presence of zeocin, *htz1*Δ, *sgs1*Δ and *sae2*Δ showed

growth defects while *exo1*Δ exhibited no sensitivity to zeocin as compared to wild-type (Figure 4.5 B first vs. third panel). This indicated that Exo1p has a minor role in DNA damage response upon DSB consistent with previous studies showing that *exo*1Δ mutants do not show sensitivity to IR (Mimitou and Symington 2010). *htz1*Δ *exo1*Δ mutants were as sensitive as *htz1*Δ mutants consistent with Htz1p and Exo1p functioning in the same pathway during DNA end resection (see 1.5.1.2 and (Adkins *et al.* 2013)). In contrast, *htz1*Δ *sae2*Δ and *htz1*Δ *sgs1*Δ showed increased sensitivity to zeocin as compared to *htz1*Δ, *sae2*Δ, and *sgs1*Δ mutants or wild-type indicating a negative synthetic genetic interaction (Figure 4.5 B first vs. third panel). This observation indicated that Htz1p, Sae2p, and Sgs1p function in parallel pathways in DNA damage response and loss of Htz1p exacerbates genotoxic effects caused by loss of Sae2p or Sgs1p. Addition of fumarate suppressed the sensitivity to zeocin in *htz1*Δ, *sgs1*Δ, *sae2*Δ, *htz1*Δ *exo1*Δ, *htz1*Δ *sae2*Δ and *htz1*Δ *sgs1*Δ mutants (Figure 4.5 B second vs. fourth panel). This indicates that fumarate could bypass the defect caused by loss of components of the DNA end resection pathways (see 4.3.2 for description of a hypothesis and proposed future experiments).

4.2.5 Exogenous fumarate attenuated checkpoint activation and promoted checkpoint adaptation upon DSB

Upon induction of DSB, two checkpoint kinases are recruited to sites of DSB, Tel1p and Mec1p (Lowndes and Murguia 2000; Mantiero *et al.* 2007). Both Tel1p and Mec1p can activate the DNA damage checkpoint by phosphorylation of Rad53p (Sanchez *et al.* 1996; Sun *et al.* 1996; Lowndes and Murguia 2000). Tel1p is recruited to DSBs by association with the Xrs2p subunit of the MRX complex (Nakada *et al.* 2003). Mec1p and its associated factor, Ddc2p, bind to RPA-coated ssDNA at the sites of DNA break (Paciotti *et al.* 2000; Rouse and Jackson 2000, 2002; Seeber *et al.* 2016; Deshpande *et al.* 2017) (see Section 1.2.1.4 for a more detailed discussion).

To further understand the role of fumarate during DNA damage response to DSBs, we examined activation and deactivation of DNA damage checkpoint by analyzing Rad53p phosphorylation (see Section 1.2.1.4). Logarithmically growing wild-type yeast and *htz1*Δ mutants were treated with zeocin in the presence or absence of exogenous fumarate for 16 hours and samples were collected before, and every two hours after treatment. Phosphorylation of Rad53p was analyzed by immunoblotting. As shown in Figure 4.6, phosphorylation of Rad53p was detectable by a shift in Rad53p mobility in immunoblots. Within two hours of treatment with zeocin in the absence of

fumarate, phosphorylation of Rad53p was strongly induced in both wild-type an *htz1*Δ mutants. However, in the presence of fumarate, at the two-hour timepoint, phosphorylation of Rad53p was delayed (as compared to the two-hour time point in the absence of fumarate) in both wild-type and *htz1*Δ mutants. Phosphorylation of Rad53p in the presence of fumarate reached a maximum only after 6-8 hours of zeocin treatment indicating that exposure to fumarate caused a delay in checkpoint activation. Moreover, in wild-type cells, phosphorylation of Rad53p was retained even after 16 hours in the absence of fumarate, whereas when fumarate was added, phosphorylation of Rad53p is significantly reduced by 10 hours, implying checkpoint adaptation may have been accelerated. In *htz1*Δ mutants exposed to fumarate, checkpoint activation ad deactivation was not as evident as in wild-type cells making it hard to fully interpret the data. Further investigation is required to compare DNA checkpoint activation and deactivation in the presence and absence of fumarate in *htz1*Δ mutants.

4.2.6 Dot1p and Rad9p were not required for suppression of sensitivity to zeocin in *htz1*Δ mutants by fumarate

Upon DSB induction in wild-type, we observed an attenuated checkpoint activation when exogenous fumarate was added (see Section 4.2.5 and Figure 4.6). Phosphorylation of Rad53p upon DSB requires the mediator Rad9p (Sun *et al.* 1998). Rad9p contains a tandem tudor domain that binds to H3 K79 methylation. The interaction between H3 K79 methylation and Rad9p promotes recruitment of Rad9p to the sites of damage where it is phosphorylated by Mec1p (Giannattasio *et al.* 2005; Wysocki *et al.* 2005). Rad53p binds to Mec1p-phosphorylated Rad9p and increased local concentration of Rad53p at DSBs promotes autophosphorylation and activation of Rad53p (Sun *et al.* 1998) (see Section1.2.1.4).

To further understand the role of fumarate in checkpoint activation, we examined the role for H3 K79 methylation fumarate-mediated suppression of sensitivity to zeocin. We tested whether fumarate-mediated suppression of sensitivity to zeocin in *htz1*Δ mutants required Dot1p, the histone methyltransferase for H3 K79 methylation, or Rad9p by repeating the growth assays using single and double mutants lacking *DOT1*, *RAD9* and/or *HTZ1*. As shown in Figure 4.7 (first vs. third panel), *dot1*Δ mutants were slightly sensitive to zeocin compared to wild-type, whereas *rad9*Δ mutants showed greater sensitivity to zeocin. This observation is consistent with either a H3 K79 methylation-independent role for Rad9p in DNA damage response, or a second H3 K79

methylation-independent mechanism for recruitment of Rad9p to DSBs. Consistent with this interpretation, in budding yeast, γ-H2A is required for recruitment and phosphorylation of Rad9p and Rad53p in G_1 (Javaheri *et al.* 2006). Similarly, in *S. pombe*, γ-H2A can be co-immunoprecipitated with Crb2 (ortholog of Rad9p) and γ-H2A promotes formation of Crb2 foci upon exposure to IR (Nakamura *et al.* 2004).

While the growth of *dot1*Δ *htz1*Δ mutants on rich medium (YPD) was comparable to *htz1*Δ mutants in rich medium (YPD) (Figure 4.7 first panel), *dot1*Δ *htz1*Δ mutants showed greater sensitivity to zeocin as compared to *htz1*Δ or *dot1*Δ mutants (Figure 4.7 first vs. third panel), indicating that Htz1p is important for growth upon DSB induction in the absence of Dot1p. Similarly, growth of *rad9*Δ *htz1*Δ mutants in rich medium (YPD) was comparable to that of *htz1*Δ mutants (Figure 4.7 first panel). However, on zeocin-containing medium, *rad9*Δ *htz1*Δ mutants showed enhanced sensitivity relative to *htz1*Δ or *rad9*Δ mutants (Figure 4.7 first vs. third panel), indicating that Htz1p is important for growth upon DSB induction in the absence of Rad9p. These results also imply that Dot1p and Rad9p act in pathway parallel to that of Htz1p and are consistent with the negative synthetic genetic interaction between *htz1*Δ and other components of the DNA damage checkpoint (e.g. *htz1 rad53* and *htz1 mec1* are synthetically lethal (Pan *et al.* 2006; Bandyopadhyay *et al.* 2010)).

Although addition of fumarate to the rich medium (YPD) did not dramatically impact the growth of *dot1*Δ, *rad9*Δ, *dot1*Δ *htz1*Δ, or *rad9*Δ *htz1*Δ mutants, fumarate greatly reduced the sensitivity of these mutants to zeocin (Figure 4.7 third vs. fourth panel). In the presence of fumarate and zeocin, *dot1*Δ *htz1*Δ, or *rad9*Δ *htz1*Δ grew with similar efficiency as *htz1*Δ mutants (Figure 4.7 fourth panel), implying that fumarate complements the negative synthetic genetic interaction between *htz1*Δ and *dot1*Δ or *htz1*Δ and *rad9*Δ. Moreover, these data implied that Dot1p and Rad9p were not required for fumarate-mediated suppression of sensitivity of *htz1*Δ mutants to DSBs.

4.2.7 Deletion of JmjC domain-containing histone demethylases does not suppress the sensitivity to zeocin in *htz1*Δ mutants in S288C background

In Figure 3.6 and Section 3.2.4, we showed that deletion of *JHD2* can suppress the HU sensitivity caused by deletion of *HTZ1* in a H3 K4 methylation-dependent manner. In addition, increasing evidence from studies in human cells have described JmjC domain containing histone

demethylases in DNA damage response (see Section 1.5.1.4 for a more detailed discussion). To test the relationship between JmjC domain-containing proteins in yeast, Htz1p and fumarate upon induction of DSBs by zeocin, we examined the sensitivity of strains with deletion of JmjC domain-containing histone demethylases to zeocin, with or without deletion of *HTZ1* and in the presence or absence of fumarate.

As shown in Figure 4.8 (first panel), *jhd1*Δ, *jhd2*Δ, *rph1*Δ, *ecm5*Δ and *gis1*Δ mutants grew as well as wild-type on rich medium (YPD). However, *rph1*Δ *htz1*Δ and *gis1*Δ *htz1*Δ showed a slight growth defect on rich medium as compared to wild-type or *htz1*Δ mutants, indicating that Htz1p promotes growth in the absence of Rph1p or Gis1p. Upon treatment with zeocin, *rph1*Δ mutants showed a slight growth defect relative to wild-type (Figure 4.8 third panel). This implied that Rph1p plays a role in DNA damage response upon DSB. Addition of exogenous fumarate suppressed the sensitivity to DNA damage in *rph1*Δ mutants (Figure 4.8 fourth panel) implying that fumarate could complement the defect in DNA damage response caused by loss of *RPH1*.

*rph1*Δ *htz1*Δ mutants were also more sensitive to zeocin compared to *htz1*Δ or *rph1*Δ mutants (Figure 4.8 third panel) indicating that Rph1p promotes growth upon induction of DSBs by exposure to zeocin in the absence of Htz1p. Similar to *rph1*Δ mutants, addition of exogenous fumarate suppressed the sensitivity to zeocin in *rph1*Δ *htz1*Δ mutants (Figure 4.8 fourth panel). Taken together, these results point to a role for Rph1p in DNA damage response. Future experiments are required to determine the pathway and the exact role of Rph1p in this process.

Deletion of other JmjC domain-containing proteins did not cause sensitivity to zeocin in the S288C background. In strains lacking Htz1p, deletion of *JHD1*, *JHD2*, *ECM5* or *GIS1* did not exacerbate or relieve the sensitivity to zeocin (Figure 4.8 third panel). Moreover, addition of fumarate restored the growth in all of these double mutants indicating that *JHD1*, *JHD2*, *ECM5* or *GIS1* were not required for fumarate-mediated suppression of sensitivity to zeocin (Figure 4.8 fourth panel). Taken together, these results implied that fumarate-mediated suppression of sensitivity to zeocin in the *htz1*Δ mutant, could not be recapitulated by deletion of any of the JmjC domain-containing histone demethylases, and that no single histone demethylase was required for this suppression.

4.2.8 Individual histone methylation sites were not required for fumarate-mediated suppression of the sensitivity to zeocin in *htz1*Δ mutants

To further examine the role of histone methylation in fumarate-mediated suppression of sensitivity to DBS, we repeated the growth assays in strains expressing wild-type H3/H4 or histone H3 mutants in which lysine methylation sites H3 K4, H3 K36 and H3 K79 had been mutated to arginine plus H4. As reported previously (see Figure 3.7 and Section 3.2.4), *htz1*Δ strains expressing H3 K4R or H3 K36R showed a synthetic growth defect on rich medium (YPD) (Figure 4.8 first panel). *htz1*Δ mutants expressing H3 K79R also showed a slight growth defect on rich medium as compared to wild-type or *htz1*Δ mutants (Figure 4.8 first panel).

Upon zeocin treatment, *htz1*Δ mutants expressing H3 K4R or H3 K36R mutants showed severe growth sensitivity relative to wild-type and *htz1*Δ mutants (Figure 4.8 third panel). These results indicate that H3 K4 methylation and H3 K36 methylation are critical for survival upon induction of DSBs by zeocin in the absence of Htz1p. The molecular mechanism by which H3 K4 methylation plays a role in DSB is not well known and the relationship between Htz1p and H3 K4 methylation in response to DSB remains to be determined.

A study by Jha and Strahl has pointed out to a role for methylation of H3 K36 in checkpoint activation (measured by analyzing phosphorylation of Rad53p) upon induction of DSBs (Jha and Strahl 2014). Moreover, mutants lacking Set2p, the sole histone methyltransferase responsible for H3 K36 methylation in *S. cerevisiae*, showed defects in DNA end resection as well as in plasmid re-ligation assay indication that H3 K36 methylation is important for both HR and NHEJ pathways (Jha and Strahl 2014). Results from our studies and others have implicated a role of Htz1p in NHEJ (Figure 4.1) as well as in DNA end resection (Kalocsay *et al.* 2009) (Adkins *et al.* 2013; Lademann *et al.* 2017). Therefore, both H3 K36 methylation and Htz1p are involved in similar pathways following induction of DSBs. However, the exact relationship between the two chromatin modifications in DNA damage response remains to be determined.

*htz1*Δ mutants expressing H3 K79R showed increased sensitivity to zeocin compared to *htz1*Δ mutants and wild-type cells expressing H3 K79R (Figure 4.8 third panel). This is consistent with previous studies that showed negative synthetic genetic interaction between *htz1*Δ mutants and mutants with defects in components of the DNA damage checkpoint activation including *mec1*

and *rad53* mutants (Pan *et al.* 2006; Bandyopadhyay *et al.* 2010). Moreover, we showed that loss of *RAD9* also exacerbated sensitivity of *htz1*Δ mutants to zeocin (Figure 4.7). Taken together, our findings as well as other studies indicate that proper checkpoint activation is critical for survival in the absence of Htz1p upon induction of DSBs. Addition of fumarate to zeocin-containing medium suppressed the sensitivity to DNA damage in *htz1*Δ mutants, as well as *htz1*Δ mutants expressing H3 K4R, H3 K36R or H3 K79R. These results indicated that individual histone methylation events were not necessary for fumarate-mediated suppression of sensitivity to zeocin in *htz1*Δ mutants.

4.2.9 Varying effects of fumarate and loss of *FUM1* on sensitivity to UV and camptothecin in *htz1*Δ mutants.

Exposure to UV can create lesions, including pyrimidine dimers and (6-4) photoproducts, throughout the cell cycle. These lesions are repaired by multiple pathways, depending on their location and their presence during different points in the cell cycle, including Nucleotide Excision Repair, NER, through either transcription-coupled NER or Global Genome NER pathways (Waters *et al.* 2015). However, if UV lesions are present in S phase, they can result in arrest of replication forks and uncoupling of the replicative helicase from DNA polymerase (Byun *et al.* 2005), in contrast to HU in which the fork remains intact and travels slowly (Sogo *et al.* 2002). Such UV lesions can be repaired by multiple post-replicative repair strategies that are error prone, involving specialized translesion synthesis DNA polymerases, or error free, involving template switching, fork regression and gap-filling (Boiteux *et al.* 2013). To test the impact of loss of *HTZ1* and exposure to fumarate on sensitivity to UV, we compared growth of *htz1*Δ mutants to wild-type yeast in untreated cells versus after exposing cells to UV, and with or without adding exogenous fumarate. As shown in Figure 4.10 A (top row, first versus third panel), *htz1*Δ mutants were sensitive to exposure to UV (see also (Deng *et al.* 2005)). This UV sensitivity could be suppressed by expression of *HTZ1* exogenously (Figure S9A top row, first versus third panels), but not via deletion of *FUM1* (Figure 4.10 A top row, first versus third panels) or the addition of exogenous fumarate (Figure 4.10 A top row, third versus fourth panels). Loss of *FUM1* also did not alter sensitivity to UV relative to wild-type (Figure 4.10 A bottom row, first versus third panels), nor did exposure to exogenous fumarate (Figure 4.10 A, third versus fourth panels).

We next evaluated the impact of fumarate and *FUM1* on sensitivity to camptothecin (CPT). CPT is a topoisomerase I inhibitor that causes ssDNA nicks by stabilizing TopI cleavage complexes and preventing them from re-ligating DNA. This then results in replication-dependent formation of DSBs on the leading strand when forks collide with the TopI cleavage complexes (Covey *et al.* 1989; Hsiang *et al.* 1989; Strumberg *et al.* 2000). Thus, CPT activates the *RAD9*-dependent (Lancelot *et al.* 2007) DDC branch of the intra-S phase checkpoint, in contrast to the DRC-related pathway implicated in relation to HU discussed above. As shown in Figure S9B (top row, panels one and three) *htz1*Δ mutants were hypersensitive to CPT (see also (Deng *et al.* 2005), and this sensitivity was suppressed by the addition of exogenously expressed *HTZ1*. In contrast to what had been observed for HU, this sensitivity was increased by loss of *FUM1*. Cells lacking both *FUM1* and *HTZ1* were hypersensitive to CPT relative to either single mutant or wild-type, but this sensitivity could be partially suppressed by the addition of exogenous fumarate (Figure 4.10 B first versus third and fourth rows). Together, these results imply that *FUM1* and fumarate influence repair of multiple forms of DNA damage, but not all repair pathways (see Section 4.3).

4.3 Discussion

4.3.1 Summary

Here, using a plasmid re-joining assay, we demonstrated that fumarase and Htz1p promote DNA repair by NHEJ (Figure 4.1). Moreover, deletion of *FUM1* caused sensitivity to zeocin and this sensitivity was enhanced in the absence of Htz1p (Figure 4.2) indicating that fumarase is important for survival after induction of DSBs in the absence of Htz1p. Fumarase has previously been shown to play a role DNA repair by HR by binding to and stabilizing Sae2p (Leshets *et al.* 2018). Therefore, it is possible that fumarase promotes DNA repair by HR by stabilizing Sae2p protein levels and promoting DNA end resection. Our data also shows that fumarase promotes NHEJ (Figure 4.1). However, the molecular mechanism by which it plays a role in NHEJ is not known. It is possible that Fumarase also promotes survival in *htz1*Δ mutants by promoting DNA repair by NHEJ.

As discussed previously, a study by Adkins *et al.*, demonstrated that H2A.Z nucleosomes are permissible for exonuclease activity of Exo1p, whereas canonical histone-containing nucleosomes are not (Adkins *et al.* 2013). These results imply that H2A.Z and Exo1p may function in the same

pathway in DNA end resection. Consistent with the study by Adkins *et al.*, our results showed that sensitivity of *htz1*Δ *exo1*Δ mutants to zeocin was comparable to that of *htz1*Δ mutants (Figure 4.5). Moreover, *exo1*Δ *sgs1*Δ mutants were highly sensitive to induction of DSB at the *MAT* locus by expression of the HO endonuclease and show little to no DNA end resection (Mimitou and Symington 2008). In our studies, in the presence of zeocin, *htz1*Δ mutants showed negative synthetic genetic interaction with *sgs1*Δ mutants (Figure 4.5). These data demonstrate that yeast Htz1p and Exo1p function in a common DNA end resection pathway that works in parallel with the Dna2p/Sgs1p to promote DNA end resection.

In contrast to our observation upon DNA replication stress where deletion of *FUM1* suppressed the sensitivity to DNA damage in *htz1*Δ mutants (see Section 3.2.1 and Figure 3.2), in the presence of zeocin, *fum1*Δ and *htz1*Δ mutants showed a negative synthetic genetic interaction (Figure 4.2). These data showed that fumarase and Htz1p have distinct roles in DNA damage response upon DNA replication stress vs. DSBs. Although intracellular fumarate accumulates upon loss of Fum1p (Lin *et al.* 2011), addition of exogenous fumarate suppressed the sensitivity of *fum1*Δ mutants to zeocin (Figure 4.2). Moreover, exogenous fumarate suppressed the sensitivity of *htz1*Δ mutants to zeocin, as well as multiple other components of the DNA damage response pathway including *rad52*Δ, *sgs1*Δ, *sae2*Δ and *rad9*Δ mutants (Figure 4.2, Figure 4.3, Figure 4.5 and Figure 4.7).

To better understand the role of the metabolite fumarate in DNA damage response to DSBs, we tested the requirement for multiple pathways in fumarate-mediated suppression of sensitivity to zeocin in *htz1*Δ mutants and showed that exogenous fumarate could bypass the requirement for NHEJ pathway (Figure 4.3), the DNA end resection pathway components (Figure 4.5) as well as the DNA damage checkpoint mediator Rad9p (Figure 4.7). Moreover, fumarate did not greatly impact RPA foci formation upon zeocin treatment in wild-type or *htz1*Δ mutants at later timepoints (Figure 4.4). However, in wild-type, we observed a delay in DNA damage checkpoint activation and an early checkpoint deactivation as measured by phosphorylation of Rad53p upon treatment with zeocin and fumarate compared to zeocin only (Figure 4.6). As we have demonstrated, that treatment with fumarate in the presence of zeocin, causes no gross defects in RPA foci formation (Figure 4.4), the delay in Rad53p phosphorylation when fumarate is added could reflect a defect in recruitment of the DNA damage checkpoint kinase Mec1p or its associated factor Ddc2p to RPA-coated ssDNA (see Section 1.2.1.4). Alternatively, the attenuated Rad53p phosphorylation

could reflect lower levels of DSB had been induced (in wild-type or *htz1*Δ mutants) in the presence of fumarate compared to the absence of fumarate (see Section 4.3.2 for proposed future directions to test this hypothesis).

We also showed that suppression of sensitivity to zeocin by fumarate did not require Jhd1p, Jhd2p, Rph1p, Ecm5p, Gis1p or H3 K4, H3 K36, or H3 K79 methylation (Figure 4.8 and Figure 4.9). These results are consistent with fumarate-mediated suppression of sensitivity to DSB being distinct from its function in inhibition of JmjC domain-containing histone demethylases. Future experiments are required to understand the molecular mechanism by which fumarate could promote growth upon exposure to zeocin. Below, I will outline some future directions and experiments that could be performed to gain a better understanding of the role of fumarate in DNA damage response or other cellular processes.

4.3.2 Future directions

As shown in Figure 4.6, in wild-type, phosphorylation of Rad53p was delayed when fumarate was present during zeocin treatment and diminishes early as compared to the absence of fumarate. However, RPA foci formation remained largely normal under these conditions. A defect in DNA damage checkpoint activation, including decreased or delayed recruitment of the mediator Rad9p, the kinase Mec1p or its associated partner Ddc2p could cause such a delay. However, this defect in checkpoint activation would be unlikely to suppress the sensitivity of *htz1*Δ mutants or other DNA damage response factors (*rad52*Δ, *sgs1*Δ, *rad9*Δ, *sae2*Δ) to zeocin as these mutants show a negative synthetic genetic interaction with factors involved in DNA damage checkpoint activation. For example, deletion of *HTZ1* is synthetically lethal with loss of *RAD53* (Pan *et al.* 2006), and shows a negative synthetic genetic interaction with loss of *MEC1* (Pan *et al.* 2006; Bandyopadhyay *et al.* 2010). Similarly, deletion of *SGS1* is also synthetically lethal with loss of *RAD53* (Pan *et al.* 2006) or with a temperature sensitive mutant of *RFA1* (gene encoding a subunit of RPA (see Section 1.2.1.2)) (Ruff *et al.* 2016). Moreover, sensitivity to zeocin caused by loss of Rad52p was also suppressed by addition of fumarate (see Figure 4.2). Rad52p is involved in multiple steps during HR including formation of Rad51p nucleofilaments as well as during post-synapsis steps of HR in SDSA (see Section 1.2.1.2.1 for a more detailed description of the role of Rad52p in HR). Furthermore, our data showed that suppression of sensitivity to DSB in *htz1*Δ mutants by fumarate does not require NHEJ or factors involved in early steps of HR (see Figure 4.2 and Figure 4.5). To

facilitate suppression of sensitivity to DNA damage tested mutants, multiple steps of DNA repair by HR would need to be regulated by fumarate. An alternative hypothesis that could explain the suppression of sensitivity to zeocin in multiple mutants lacking different components of the DNA repair process is that fumarate had reduced the amount of DSBs induced by zeocin. Zeocin is a glycopeptide from the bleomycin family. Therefore, it is possible that fumarate had reduced the intracellular concentration of zeocin by regulation of expression or activity of factors involved in drug resistance in yeast. To test this hypothesis, I propose analyzing of the expression levels of genes involved in resistance to bleomycin upon treatment with fumarate using qRT-PCR or western blot. Several genetic screens have identified genes involved in resistance to bleomycin including *AGP2* (a transporter for bleomycin, which is structurally similar to zeocin) (Aouida *et al.* 2004a), *IMP2* (gene encoding a transcriptional co-activator, deletion of *IMP2* causes sensitivity to bleomycin) (Aouida *et al.* 2004b), and *ZEO1* (zeocin resistance gene, high expression of *ZEO1* confers resistance to zeocin) (Green *et al.* 2003). If an increased expression of Imp2p, Zeo1p or decreased expression of Agp2p is detected upon treatment with fumarate, it would support a model in which treatment with fumarate decreases the effective concentration of zeocin and the amount of DSBs induced by zeocin through enhancing its export or decreasing its uptake by the cell. Since RPA foci formation upon zeocin treatment is not greatly impacted when exogenous fumarate is added, we favor a model in which the effect of fumarate is not immediate but rather a delayed response.

To test whether the suppression of sensitivity to DSB in *htz1*Δ (and other mutants) by exogenous fumarate upon DSB induction is specific to zeocin, cells could be exposed to IR in the presence and absence of fumarate. The results of our studies on the effect of fumarate on sensitivity to DNA damaging agents, showed that, in contrast to zeocin, sensitivity of *rad52*Δ mutants and components of the MRX complex to HU cannot be complemented by fumarate (see Figure 3.2, Figure 3.4 and Figure 4.2). Moreover, sensitivity to CPT in *htz1*Δ or *htz1*Δ *fum1*Δ mutants was not suppressed by fumarate either. These results imply that the mechanism by which fumarate confers resistance to zeocin is specific to this DNA damaging agent.

An alternative model that could also result in decreased amount of DSBs induced by zeocin, is that exogenous fumarate had caused a modification of zeocin structure that decreased its efficiency in intercalating DNA and induction of DSBs. Fumarate can modify activity of proteins by succination

of cysteine residues (Blatnik *et al.* 2008) (see Section 3.3). However, it is unlikely for zeocin to be directly succinated as it lacks any thiol group. Measurement of the intracellular concentration of zeocin with and without fumarate added to the growth medium by GC-MS could determine whether intracellular concentration of zeocin is affected by addition of fumarate.

It is also possible for activity of a protein such as pump to be modified by succination when exogenous fumarate is added. A mass spectroscopy analysis could reveal succinated proteins in the presence of exogenous fumarate. If any drug resistance pump is identified, further experiments can determine how succination regulates the activity of the target(s).

To further gain insights into changes in the DNA damage response, chromatin association of DNA repair factors at different steps of the DNA damage response could be analyzed. Since fumarate can bypass the requirement for individual DNA end resection factors (including Sae2p or Sgs1p (see Figure 4.5)), it could be informative to analyze chromatin association of factors involved in early steps of HR upon DSB induction in the presence or absence of fumarate. Chromatin association of components of the MRX complex, Exo1p, Dna2p, Sgs1p, components of the RPA heterotrimer, Rad51p and Rad52p could be analyzed by ChIP using a locus-specific induction of a DSB (for example using inducible expression of the HO endonuclease and analyzing chromatin association of DNA repair factors at the *MAT* locus). This could shed light on changes in chromatin association of DNA repair factors and determine which step(s) during the DNA damage response is modified in the presence of fumarate.

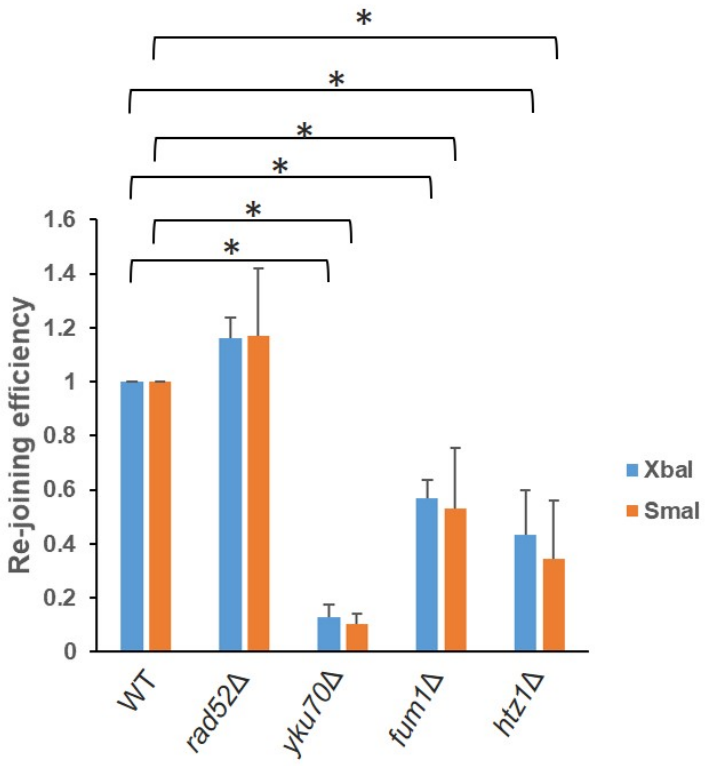

Figure 4.1 Fumarase and Htz1p promote DNA repair by NHEJ.

Strains with indicated genotypes were transformed with pAK54 (pRS313) linearized with XbaI or SmaI or with circular plasmid and grown on selective media for three days. The number of colonies were counted, and the efficiency of plasmid re-joining was calculated as shown below. Average and standard deviation of three independent experiments was reported as relative to wild-type. The statistical analysis was performed using Wilcoxon Rank Sum test and P-value ≤ 0.05 is shown by *.

$$\text{Plasmid re-joining efficiency}=\left(\frac{\text{number of colonies using linearized plasmid}}{\text{number of colonies using circular plasmid}}\right)_{\text{mutant}}/\left(\frac{\text{number of colonies using linearized plasmid}}{\text{number of colonies using circular plasmid}}\right)_{\text{WT}}$$

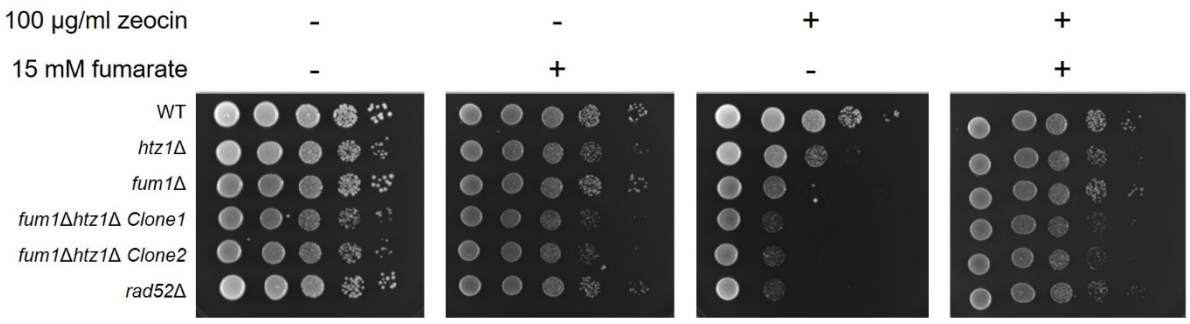

Figure 4.2 Genetic interaction between *fum1*Δ and *htz1*Δ and the effect of fumarate on sensitivity to DSB in mutants lacking *FUM1* or *HTZ1*.

Strains with genotypes as indicated were grown on rich medium (YPD) containing 2×PBS with or without zeocin or fumarate at indicated concentrations and were grown at 30°C for two days prior to imaging.

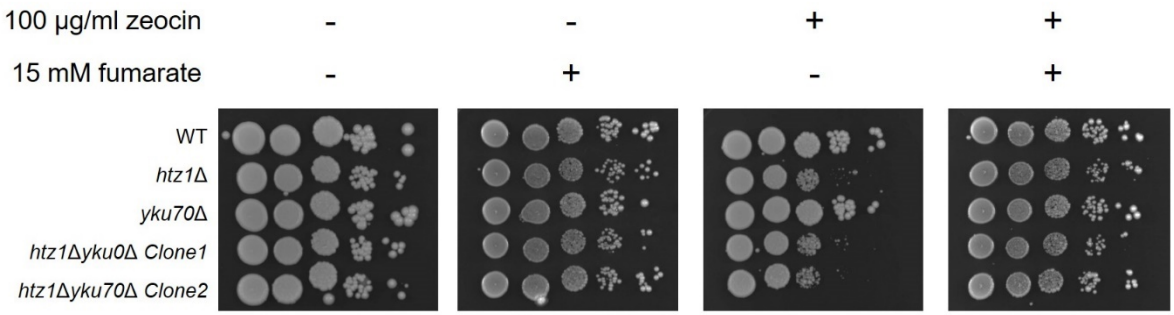

Figure 4.3 Genetic interaction between *yku70*Δ and *htz1*Δ mutants and the effect of fumarate on sensitivity to DSBs induced by zeocin upon deletion of *YKU70*.

Strains with indicated genotypes were grown on rich medium (YPD) containing or lacking zeocin and fumarate at indicated concentrations as described in Figure 4.2.

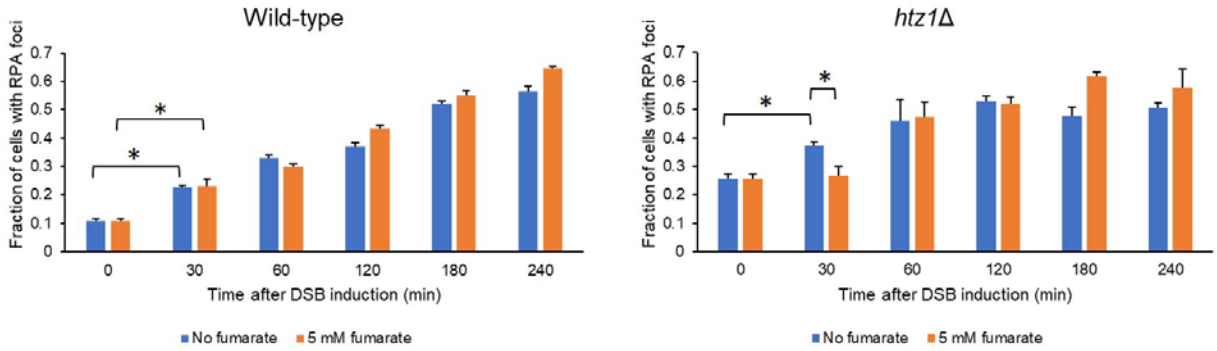

Figure 4.4 Analysis of RPA foci in wild-type and *htz1*Δ mutants treated with zeocin in the presence or absence of fumarate.

Logarithmically growing wild-type and *htz1*Δ mutants expressing Rfa1p-GFP were treated with zeocin with or without fumarate as described in Section 2.9. RPA foci formation was analyzed before addition of 20µg/mL zeocin and 30 min, one hour, two hours, three hours and four hours after addition of zeocin and/or fumarate by fluorescence microscopy. Average and standard deviation of the fraction of cells showing discrete RPA foci in the presence or absence of fumarate is shown for each time-point for two independent experiment. At least 100 cells were counted for each sample. The statistical analysis was performed for 0 and 30 min timepoints using Student t test and statistical significance at 95% confidence level is shown by *.

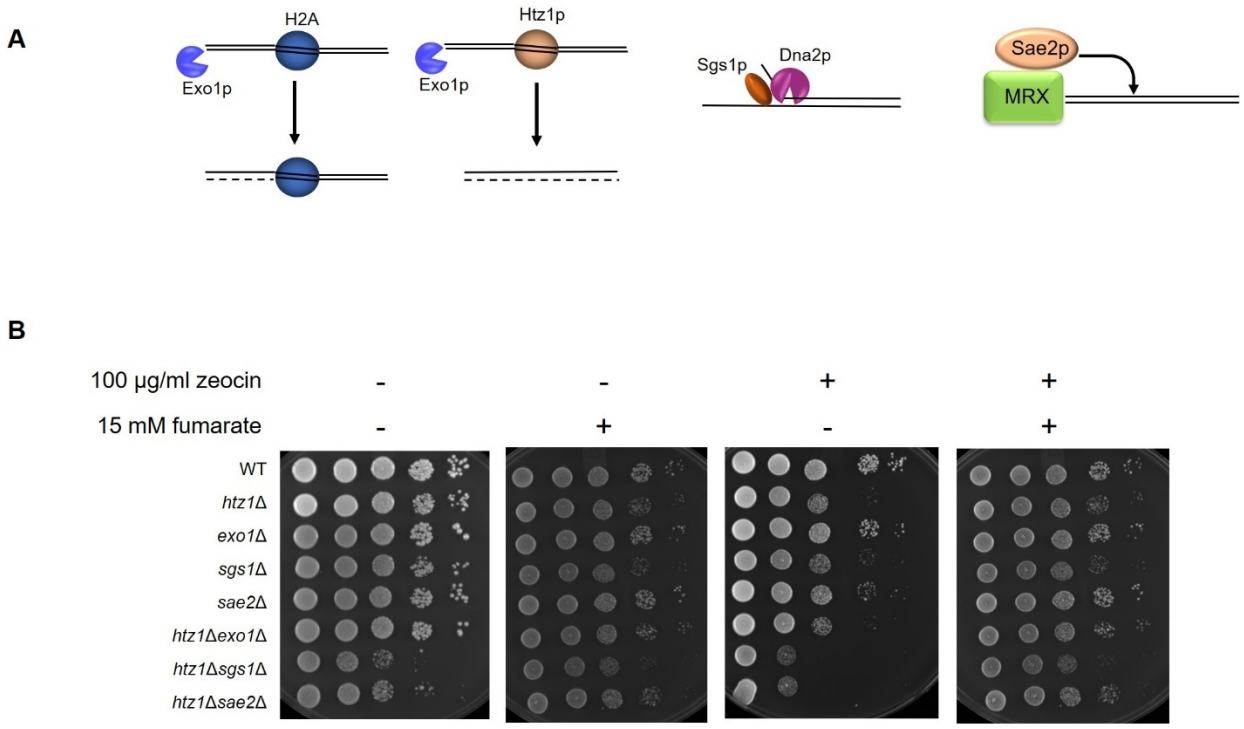

Figure 4.5 Genetic interaction between *htz1*Δ and mutants with deletion of factors involved in DNA end resection and the effect of fumarate on sensitivity to zeocin.

A) Role of Htz1p, and components of the DNA end resection pathway. Htz1p-containing nucleosomes are permissible for exonuclease activity of Exo1p. Dna2p/Sgs1p function in a pathway parallel to Exo1p. Sae2p initiates DNA end resection by stimulating the endonuclease activity of Mre11p in MRX complex.

B) Strains with indicated genotypes were grown on rich medium (YPD) containing indicated concentratons of zeocin and fumarate as described in Figure 4.2.

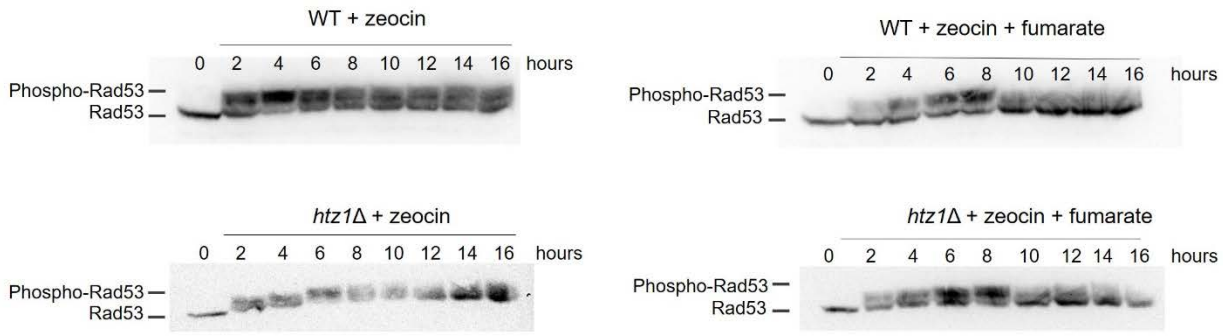

Figure 4.6 Effect of fumarate on Rad53p phosphorylation upon induction of DSBs by zeocin.

Logarithmically growing wild-type and *htz1*Δ strains were treated with 100µg/mL zeocin for 16 hours in the presence or absence of 5 mM fumarate. Whole cell extracts were prepared before and every two hours after treatment and used for immunoblotting with anti-Rad53p antibody as described in Section 2.6.2.

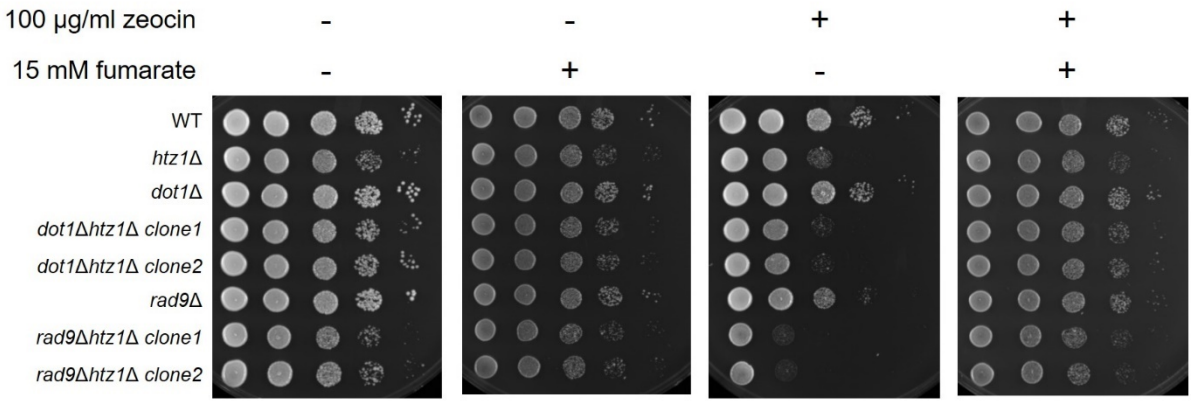

Figure 4.7 Genetic interaction between *htz1*Δ mutants and *dot1*Δ or *rad9*Δ mutants and the effect of fumarate on sensitivity to zeocin.

Strains with indicated genotypes were grown on rich medium (YPD) containing indicated concentrations of zeocin and fumarate as described in Figure 4.2.

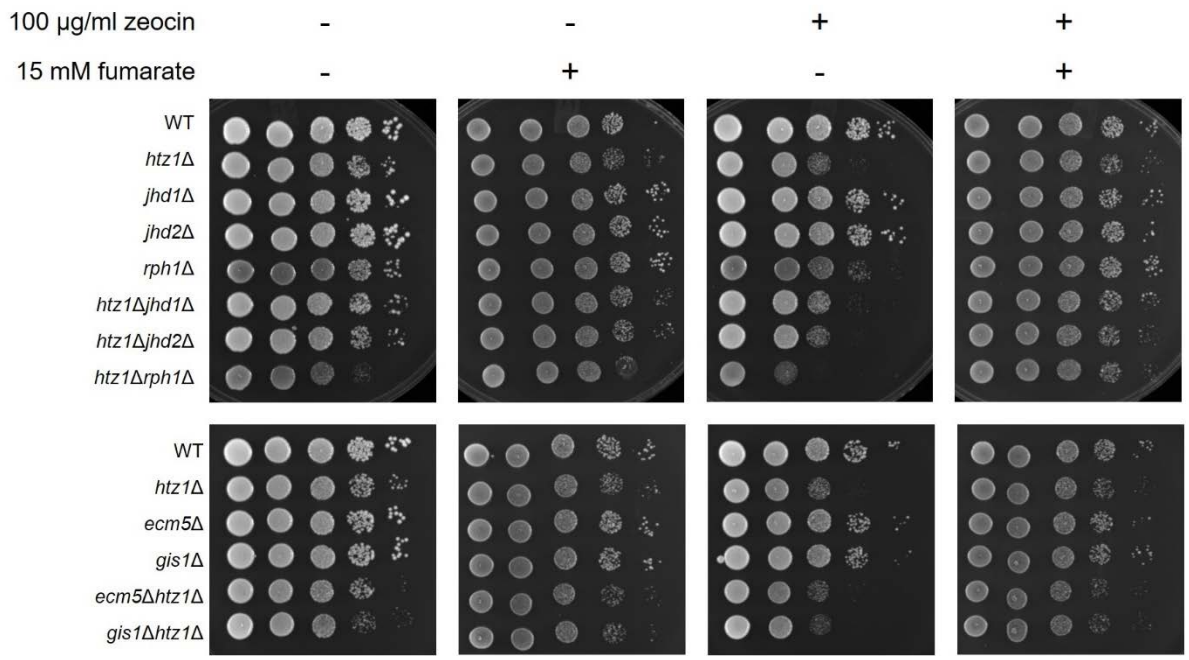

Figure 4.8 Effect of deletion of histone demethylases and exogenous fumarate on sensitivity of *htz1*Δ mutants to zeocin in S288C background.

Strains with indicated genotypes were grown on rich medium (YPD) containing indicated concentrations of zeocin and fumarate as described in Figure 3.2.

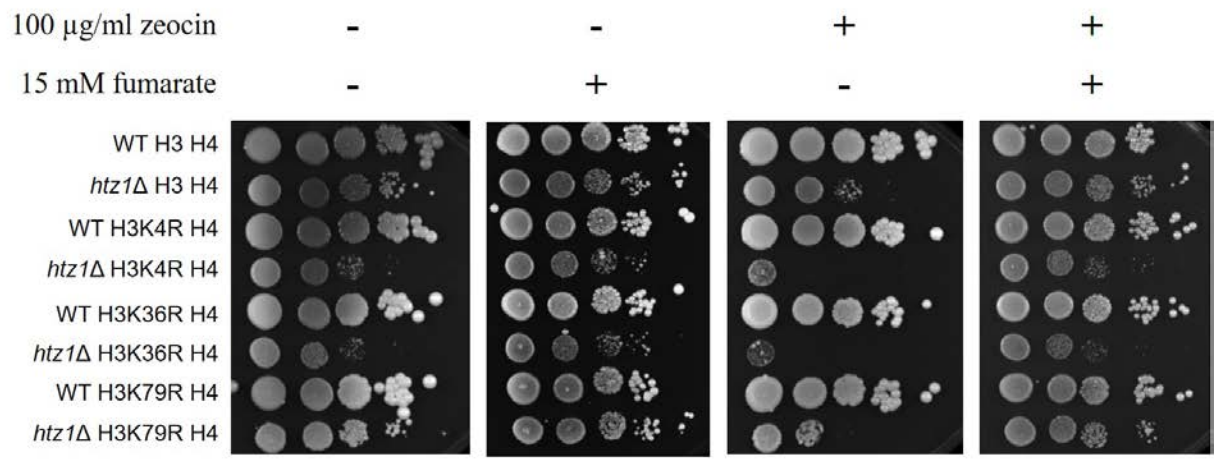

Figure 4.9 Genetic interaction between *htz1*Δ mutants and H3 K4R, K36R and K79R mutants and the effect of fumarate on sensitivity to zeocin.

Strains with indicated genotypes were grown on rich medium (YPD) containing indicated concentrations of zeocin and fumarate as described in Figure 4.2.

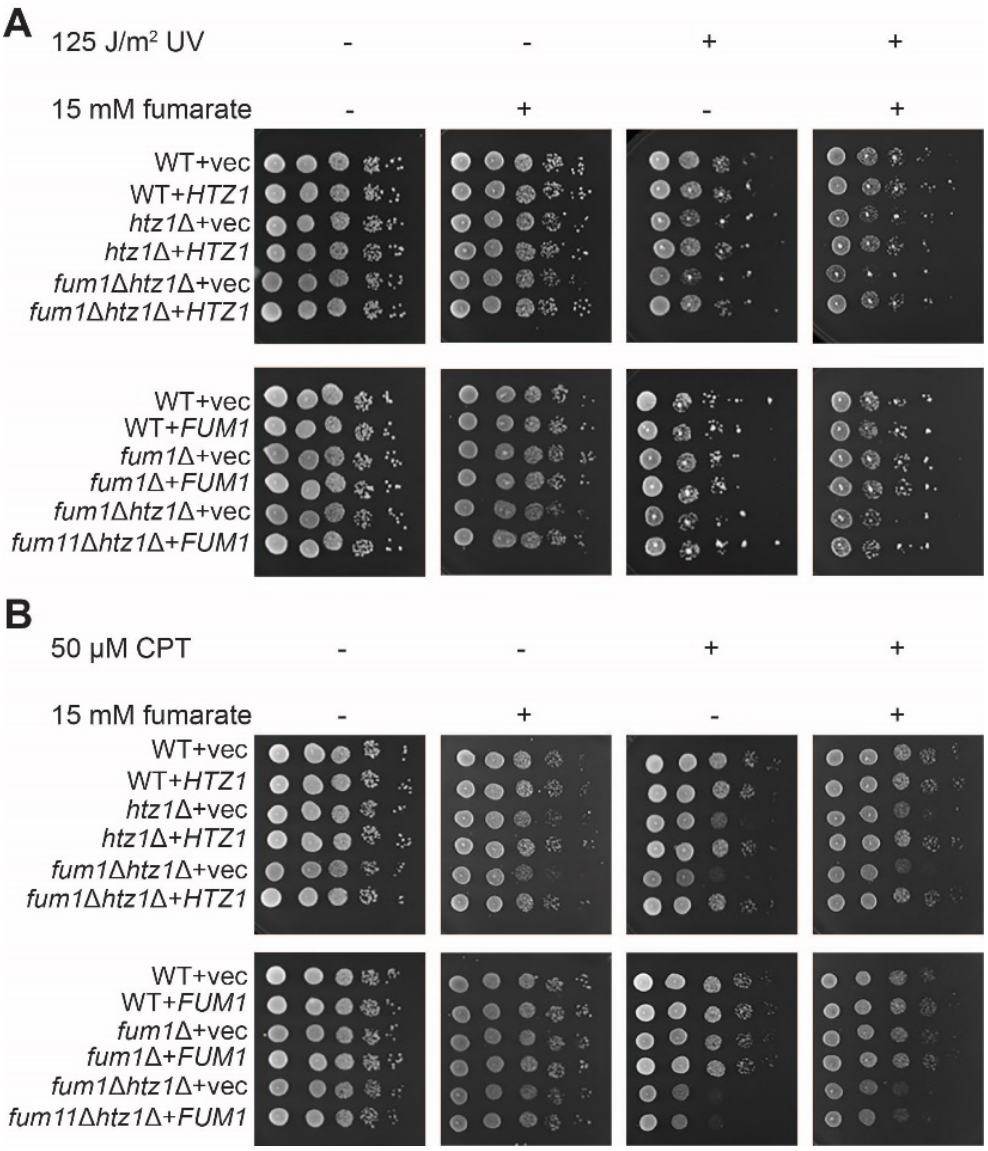

Figure 4.10 Sensitivity of *htz1*Δ and *htz1*Δ *fum1*Δ mutants to DNA damage caused by UV or camptothecin and the effect of fumarate.

Cells with genotypes as indicated were grown overnight in selective medium (medium lacking leucine or uracil), then three μL of 10-fold serial dilutions were spotted onto YPD medium containing 2×PBS with or without the indicated concentrations of fumarate and exposed to UV (A) or camptothecin, CPT, (B) and incubated at 30°C for two days prior to imaging.

CHAPTER 5. CONCLUSIONS AND FUTURE DIRECTION

5.1 Discussion

The results of this work (Chapter 3 and Chapter 4) sheds light on the role of the metabolic enzyme fumarase and the metabolite fumarate upon different types of DNA damage (DNA replication stress is discussed in Chapter 3 and DSB is discussed in Chapter 4). In addition, the genetic interaction between the *htz1*Δ mutants and mutants with defects in different DNA repair pathways presented here improves our understanding of the relationship between chromatin modifications and the DNA damage response factors. This work has also uncovered previously unknown roles for histone modifying enzymes in DNA damage response in *S. cerevisiae*.

5.1.1 Role of fumarase and the metabolite fumarate upon DNA replication stress

In Chapter 3, we report that *S. cerevisiae* fumarase, Fum1p, acts as a response factor during DNA replication stress, and fumarate enhances survival of yeast lacking Htz1p. We observed that exposure to DNA replication stress led to upregulation as well as nuclear enrichment of Fum1p and raising levels of fumarate in cells via deletion of *FUM1* or addition of exogenous fumarate suppressed the sensitivity to DNA replication stress of *htz1*Δ mutants. This suppression was independent of modulating nucleotide pool levels and repair by NHEJ as shown by experiments using mutants lacking *YKU70*. Rather, our results are consistent with fumarate conferring resistance to DNA replication stress in *htz1*Δ mutants by inhibiting the H3 K4-specific histone demethylase Jhd2p and increasing global levels of H3 K4 methylation. Whether H3 K4 methylation is enriched at replication forks and how this modification changes upon treatment with fumarate is not known (see Section 5.2.3 for proposed future experiments to analyze H3 K4 methylation at DNA replication forks). In our experiments, deletion of *JHD2* phenocopied high cellular levels of fumarate and suppressed the HU sensitivity of *htz1*Δ mutants in a H3 K4 methylation-dependent manner. Although the timing of checkpoint activation and deactivation remained largely unaffected by fumarate upon DNA replication stress, sensors and mediators of the DNA replication checkpoint including Mrc1p, Rad9p, Rad17p, Rad24p and Ddc1p were required for fumarate-dependent resistance to replication stress in the *htz1*Δ mutants, whereas

factors involved in processing of regressed replication forks including Sae2p, Rad50p and Xrs2p were not. Whether timing or the level of association of the above-mentioned factors involved in DNA replication checkpoint is impacted by changes in fumarate availability or histone methylation levels has not been examined yet. Analyzing changes in association of DNA replication checkpoint factors associated with replication forks upon increased fumarate levels can be achieved as described later in Section 5.2.3. Together, our findings imply that metabolic enzymes and metabolites aid in processing replicative intermediates by affecting chromatin modification states, thereby promoting genome integrity.

5.1.2 Role of fumarase and the metabolite fumarate upon DSB

In Chapter 4, we showed that Htz1p and Fum1p promoted DNA repair by NHEJ. Consistent with a role for Htz1p in NHEJ, the growth defect of *htz1*Δ *yku70*Δ mutants upon treatment with zeocin was comparable to that of *htz1*Δ mutants. These findings are consistent with Htz1p and Yku70p functioning in the same pathway in response to DSBs. However, the exact step in which Htz1p plays a role in during NHEJ still remains unknown. Moreover, whether the catalytic activity of Fum1p is required for its role in DNA repair by NHEJ remains to be explored. Whether fumarase, fumarate or Htz1p promote association of NHEJ factors like Yku70p or Lig4p can be determined by chromatin immunoprecipitation (ChIP) experiments. Wild-type, *fum1*Δ and *htz1*Δ mutants expressing an inducible HO endonuclease could be used to analyze association of the above mentioned NHEJ factors around the *MAT* locus following generation of a DSB by expression of HO.

We also studied the genetic interaction between *htz1*Δ mutants and mutants with deletions in different components of the DNA damage response pathway to DSBs including factors involved in the DNA end resection pathway and components of the DNA damage checkpoint signaling pathway. Consistent with a role for Htz1p in the Exo1p-dependent pathway of DNA end resection, *htz1*Δ *exo1*Δ mutants showed no greater sensitivity to zeocin compared to *htz1*Δ mutants whereas *htz1*Δ *sgs1*Δ and *htz1*Δ *sae2*Δ mutants showed a negative synthetic genetic interaction. These data demonstrate that Htz1p, Sgs1p and Sae2p function in different steps and pathways of DNA end resection. Moreover, consistent with previous reports of negative synthetic genetic interaction of *htz1*Δ and components of the DNA damage checkpoint, *htz1*Δ *rad9*Δ and *htz1*Δ *dot1*Δ mutants

showed negative synthetic genetic interaction in the presence of zeocin. These results imply that proper checkpoint activation is critical for survival upon DSB in the absence of Htz1p.

Although RPA foci formation was not greatly affected by fumarate, DNA damage checkpoint activation (as measured by phosphorylation of Rad53p) was delayed and the duration of the time in which DNA damage checkpoint had remained active was reduced upon treatment with fumarate in wild-type. There are at least three possible events that can cause a delay in checkpoint activation: 1) a defect in recruitment of the Mec1p-Ddc2 to RPA coated ssDNA regions; 2) a defect in phosphorylation and activation of the DNA damage checkpoint mediator Rad9p or the effector kinase Rad53p; or 3) reduced number of DSB sites induced upon treatment with zeocin (see Section 4.3.2 for further discussion and proposed future experiment to test this hypothesis) when fumarate is added. Since suppression of *htz1*Δ sensitivity to zeocin by fumarate did not require Rad9p, Dot1p or H3 K79 methylation, fumarate-mediated suppression of sensitivity to zeocin is unlikely to promote growth upon zeocin by modulation of Mec1p or Rad9p recruitment or activity.

5.2 Future directions

5.2.1 Identification of proteins that physically interact with fumarase upon DNA damage

Our work has shown that expression of fumarase is induced and that fumarase becomes enriched in the nucleus upon DNA replication stress (see Section 3.2.1 and Figure 3.1) Moreover, we have shown that yeast fumarase promotes DNA repair by NHEJ (see Section 4.2.1 and Figure 4.1). However, the exact role it plays during the DNA damage response and the repair of DNA damage is not known. *in vitro* binding assays as well as co-immunoprecipitation experiments have shown that Fum1p binds to Sae2p in the presence or absence of DNA damage (induced by addition of HU) and that this interaction increases the stability of Sae2p (Leshets *et al.* 2018). Consistent with its role in stabilization of Sae2p, expression of Fum1p exclusively in the mitochondria, which prevents its nuclear localization (Yogev *et al.* 2010), causes sensitivity to the DNA damaging agent MMS (methyl methane sulfonate, an alkylating agent) and this sensitivity can be suppressed by overexpression of Sae2p (Leshets *et al.* 2018). Whether Fum1p interacts with Htz1p or other DNA damage response factors in yeast is unknown. A co-immunoprecipitation of Fum1p coupled with a mass spectroscopy (Co-IP/MS) in the presence or absence of DNA damaging agents including HU (to determine Fum1p's interacting partners upon DNA replication stress) or zeocin (to

determine Fum1p's interacting partners during response to DSBs) could identify proteins that fumarase interacts with during DNA damage response. Elucidating the binding partners of fumarase will help gain a better understanding of how fumarase promotes repair and identify the pathway(s) or mechanism(s) by which functions.

5.2.2 Identification of succinated proteins upon increased intracellular levels of fumarate

Fumarate can react with thiol groups in cysteine residues of proteins resulting in a protein modification named succination. Protein succination can impact protein function as this modification has previously been shown to inactivate the enzyme GAPDH irreversibly (Blatnik *et al.* 2008). Moreover, FH deficiency causes accumulation of fumarate (also see Section 3.3) and high levels of protein succination is detected in FH deficient mouse embryonic fibroblasts, renal cysts and HLRCC tumors (Bardella *et al.* 2011; Ternette *et al.* 2013). Therefore, it is possible that high cellular levels of fumarate upon deletion of *FUM1* or addition of exogenous fumarate promotes growth upon DNA damage (induced by HU or zeocin) by modifying protein(s) involved in DNA damage response (including in HR or NHEJ pathway) and thereby affecting their function. A mass spectroscopy analysis of succinated proteins (as described in (Ternette *et al.* 2013)) in *fum1*Δ mutants or upon addition of fumarate could potentially identify relevant protein targets. If any targets are identified, further analysis would be required to understand how succination affects protein function (e.g. activation, inactivation, degradation or change in localization) or binding to other proteins or DNA and how such changes can impact the DNA damage response (e.g. recruitment of DNA repair factors, chromatin modifications or chromatin accessibility) and promote growth upon DNA damage.

5.2.3 Determining changes in H3 K4 methylation levels associated with DNA replication forks upon increased intracellular levels of fumarate

We have established that loss of the JmjC domain-containing histone demethylase Jhd2p, which target H3 K4 methylation, can suppress the sensitivity of *htz1*Δ mutants to DNA replication stress by HU (see Figure 3.6 and Section 3.2.4). We have also shown that suppression of sensitivity to HU in *htz1*Δ mutants by deletion of *JHD2* was H3 K4 methylation-dependent (see Figure 3.8 and Section 3.2.5). Moreover, our analysis of the global levels of H3 K4 me3 showed that fumarate, an inhibitor of α-KG dependent enzymes, could modulate the activity of Jhd2p and increase the levels of H3 K4me3 (relative to H3) in both wild-type and *htz1*Δ mutants (see Figure 3.9 and

Section 3.2.6). However, whether fumarate directly modulates H3 K4me3, me2 or me1 at DNA replication forks is unknown.

Using a method for identification of proteins associated with nascent DNA (iPOND), active and stalled forks could be isolated and proteins associated with the forks could be analyzed (Sirbu *et al.* 2011). In iPOND, a thymidine analog, EdU, is used to label nascent DNA for a short period of time. Next, click chemistry is used to add biotin to the EdU-labeled DNA which allows purification of proteins associated with EdU-labeled DNA using streptavidin beads (Sirbu *et al.* 2011). I propose pulse-labeling of wild-type and *htz1*Δ, *fum1*Δ or *fum1*Δ *htz1*Δ mutants with EdU followed by HU treatment in the presence or absence of fumarate prior to performing click chemistry reaction. Purification of proteins associated with EdU-labeled DNA followed by a quantitative immunoblot for H3 K4me3, me2 or me1 could determine changes in the levels of H3 K4 methylation associated with DNA replication stress in the presence or absence of fumarate. Based on our previous results showing increased global levels of H3 K4me3 in the presence of fumarate (Figure 3.9 and Section 3.2.6), we expect a higher level of H3 K4me3 to be associated with nascent DNA in the presence of fumarate. In addition, immunoblotting for other DNA replication-associated proteins or DNA repair factors, including Mrc1p and components of the 9-1-1 complex that were required for suppression of HU sensitivity of *htz1*Δ by fumarate (see Figure 3.12 and Section 1.3), could also clarify how loss of Htz1p or high cellular levels of fumarate affects the response to DNA replication stress.

5.2.4 Analysis of gene expression changes associated with high cellular levels of fumarate

As discussed previously in sections 5.2.3 and 3.2.6, we have demonstrated that fumarate is a modulator of Jhd2p activity. H3 K4me3 is associated with actively transcribed regions and Jhd2p and Set1p activity regulate gene expression as large scale analyses of gene expression changes by RNA-seq show a common set of genes that are differentially expressed in *jhd2*Δ or *set1*Δ mutants as compared to wild-type (Ramakrishnan *et al.* 2016). Some of the genes identified to be differentially expressed in *jhd2*Δ and *set1*Δ mutants were involved in glycogen and serine metabolism, highlighting the link between H3 K4 methylation and metabolic pathways (Ramakrishnan *et al.* 2016). The extent to which high cellular levels of fumarate in *fum1*Δ mutants or upon addition of exogenous fumarate affects gene expression by regulation of H3 K4 methylation and the implications of such changes in DNA damage response is not known.

Analyzing gene expression changes associated with high cellular levels of fumarate in *fum1*Δ mutants or in the presence of exogenous fumarate compared to wild-type and no fumarate conditions by RNA-seq (in the presence or absence of DNA damage by HU or zeocin) could identify target genes for which expression is modulated by fumarate. Whether such changes are dependent on modulation of H3 K4 methylation can be determined by repeating the experiments in a *set1*Δ mutants or mutants expressing H3 K4R.

5.3 Perspectives

Chromatin modifications play a central role in various cellular functions including gene expression, DNA replication and genome integrity. Changes in environmental conditions including environmental stress (for example, temperature, oxygen concentration and osmotic stress) and nutrient availability can regulate cellular function by utilizing signal transduction pathways as well as metabolic pathways to regulate gene expression, cell cycle progression, cellular differentiation and cell shape. Increasing evidence implies that changes in metabolite availability can modulate cellular functions by regulation of chromatin-associated functions. Here, we present evidence that the metabolic enzyme fumarase is involved in genome integrity and that changes in availability of the metabolite fumarate impacts cellular growth in genotoxic environments by regulation of the activity of a chromatin modifying enzyme. Studying the link between metabolism, chromatin and genome integrity will improve our understanding of how changes in environmental conditions induce changes in cellular functions in a manner that could provide plasticity to epigenetic states.

REFERENCES

Adams A., D. E. Gottschling, C. Kaiser, and T. Stearns, 1998 Methods in yeast genetics : a Cold Spring Harbor Laboratory course manual. Cold Spring Harbor Laboratory Press, Cold Spring Harbor, N.Y.

Adkins N. L., H. Niu, P. Sung, and C. L. Peterson, 2013 Nucleosome dynamics regulates DNA processing. Nat. Struct. Mol. Biol. 20: 836–842. doi:10.1038/nsmb.2585

Ait Saada A., A. Teixeira-Silva, I. Iraqui, A. Costes, J. Hardy, *et al.*, 2017 Unprotected Replication Forks Are Converted into Mitotic Sister Chromatid Bridges. Mol. Cell 66: 398–410.e4. doi:10.1016/J.MOLCEL.2017.04.002

Akiba T., K. Hiraga, and S. Tuboi, 1984 Intracellular distribution of fumarase in various animals. J. Biochem. 96: 189–95. doi:10.1093/oxfordjournals.jbchem.a134812

Alani E., R. Thresher, J. D. Griffith, and R. D. Kolodner, 1992 Characterization of DNA-binding and strand-exchange stimulation properties of y-RPA, a yeast single-strand-DNA-binding protein. J. Mol. Biol. 227: 54–71. doi:10.1016/0022-2836(92)90681-9

Alatwi H. E., and J. A. Downs, 2015 Removal of H2A.Z by INO80 promotes homologous recombination. EMBO Rep. 16: 986–994. doi:10.15252/embr.201540330

Alcasabas A. A., A. J. Osborn, J. Bachant, F. Hu, P. J. H. Werler, *et al.*, 2001 Mrc1 transduces signals of DNA replication stress to activate Rad53. Nat. Cell Biol. 3: 958–965. doi:10.1038/ncb1101-958

Alderson N. L., Y. Wang, M. Blatnik, N. Frizzell, M. D. Walla, *et al.*, 2006 S-(2-Succinyl)cysteine: A novel chemical modification of tissue proteins by a Krebs cycle intermediate. Arch. Biochem. Biophys. 450: 1–8. doi:10.1016/J.ABB.2006.03.005

Alexander J. L., and T. L. Orr-Weaver, 2016 Replication fork instability and the consequences of fork collisions from rereplication. Genes Dev. 30: 2241–2252. doi:10.1101/gad.288142.116

Aouida M., N. Pagé, A. Leduc, M. Peter, and D. Ramotar, 2004a A genome-wide screen in Saccharomyces cerevisiae reveals altered transport as a mechanism of resistance to the anticancer drug bleomycin. Cancer Res. 64: 1102–9.

Aouida M., O. Tounekti, A. Leduc, O. Belhadj, L. Mir, *et al.*, 2004b Isolation and characterization of Saccharomyces cerevisiae mutants with enhanced resistance to the anticancer drug bleomycin. Curr. Genet. 45: 265–272. doi:10.1007/s00294-004-0492-x

Aparicio T., R. Baer, and J. Gautier, 2014 DNA double-strand break repair pathway choice and cancer. DNA Repair (Amst). 19: 169–75. doi:10.1016/j.dnarep.2014.03.014

Arndt K., A. Kranz, J. Fohgrub, A. Jolly, A. S. Bledau, *et al.*, 2018 SETD1A protects HSCs from activation-induced functional decline in vivo. Blood 131: 1311–1324. doi:10.1182/blood-2017-09-806844

Attikum H. van, O. Fritsch, B. Hohn, and S. M. Gasser, 2004 Recruitment of the INO80 Complex by H2A Phosphorylation Links ATP-Dependent Chromatin Remodeling with DNA Double-Strand Break Repair. Cell 119: 777–788. doi:10.1016/j.cell.2004.11.033

Attikum H. van, O. Fritsch, S. M. Gasser, A. Bird, D. Yu, *et al.*, 2007 Distinct roles for SWR1 and INO80 chromatin remodeling complexes at chromosomal double-strand breaks. EMBO J. 26: 4113–4125. doi:10.1038/sj.emboj.7601835

Bacal J., M. Moriel-Carretero, B. Pardo, A. Barthe, S. Sharma, *et al.*, 2018 Mrc1 and Rad9 cooperate to regulate initiation and elongation of DNA replication in response to DNA damage. EMBO J. e99319. doi:10.15252/embj.201899319

Baker Brachmann C., A. Davies, G. J. Cost, E. Caputo, J. Li, *et al.*, 1998 Designer deletion strains derived fromSaccharomyces cerevisiae S288C: A useful set of strains and plasmids for PCR-mediated gene disruption and other applications. Yeast 14: 115–132. doi:10.1002/(SICI)1097-0061(19980130)14:2<115::AID-YEA204>3.0.CO;2-2

Bandyopadhyay S., M. Mehta, D. Kuo, M.-K. Sung, R. Chuang, *et al.*, 2010 Rewiring of genetic networks in response to DNA damage. Science 330: 1385–9. doi:10.1126/science.1195618

Bannister A. J., and T. Kouzarides, 2011 Regulation of chromatin by histone modifications. Cell Res. 21: 381–95. doi:10.1038/cr.2011.22

Bardella C., M. El-Bahrawy, N. Frizzell, J. Adam, N. Ternette, *et al.*, 2011 Aberrant succination of proteins in fumarate hydratase-deficient mice and HLRCC patients is a robust biomarker of mutation status. J. Pathol. 225: 4–11. doi:10.1002/path.2932

Barnes L. B., and S. H. Bishop, 1975 Adenylosuccinate lyase from human erythrocytes. Int. J. Biochem. 6: 497–503. doi:10.1016/0020-711X(75)90030-0

Bartkova J., Z. Hořejší, K. Koed, A. Krämer, F. Tort, *et al.*, 2005 DNA damage response as a candidate anti-cancer barrier in early human tumorigenesis. Nature 434: 864–870. doi:10.1038/nature03482

Bernstein K. A., E. Shor, I. Sunjevaric, M. Fumasoni, R. C. Burgess, *et al.*, 2009 Sgs1 function in the repair of DNA replication intermediates is separable from its role in homologous recombinational repair. EMBO J. 28: 915–925. doi:10.1038/emboj.2009.28

Bernstein K. A., S. Gangloff, and R. Rothstein, 2010 The RecQ DNA helicases in DNA repair. Annu. Rev. Genet. 44: 393–417. doi:10.1146/annurev-genet-102209-163602

Bilousova G., A. Marusyk, C. C. Porter, R. D. Cardiff, and J. DeGregori, 2005 Impaired DNA replication within progenitor cell pools promotes leukemogenesis. PLoS Biol. 3: e401. doi:10.1371/journal.pbio.0030401

Biswas D., S. Takahata, H. Xin, R. Dutta-Biswas, Y. Yu, *et al.*, 2008 A role for Chd1 and Set2 in negatively regulating DNA replication in Saccharomyces cerevisiae. Genetics 178: 649–59. doi:10.1534/genetics.107.084202

Bjergbaek L., J. A. Cobb, M. Tsai-Pflugfelder, and S. M. Gasser, 2005 Mechanistically distinct roles for Sgs1p in checkpoint activation and replication fork maintenance. EMBO J. 24: 405–17. doi:10.1038/sj.emboj.7600511

Black J. C., C. Van Rechem, and J. R. Whetstine, 2012 Histone lysine methylation dynamics: establishment, regulation, and biological impact. Mol. Cell 48: 491–507. doi:10.1016/j.molcel.2012.11.006

Black J. C., A. L. Manning, C. Van Rechem, J. Kim, B. Ladd, *et al.*, 2013 KDM4A lysine demethylase induces site-specific copy gain and rereplication of regions amplified in tumors. Cell 154: 541–55. doi:10.1016/j.cell.2013.06.051

Blatnik M., S. R. Thorpe, and J. W. Baynes, 2008 Succination of proteins by fumarate: mechanism of inactivation of glyceraldehyde-3-phosphate dehydrogenase in diabetes. Ann. N. Y. Acad. Sci. 1126: 272–5. doi:10.1196/annals.1433.047

Boiteux S., S. Jinks-Robertson, L. H. Hartwell, and G. F. Crouse, 2013 DNA repair mechanisms and the bypass of DNA damage in Saccharomyces cerevisiae. Genetics 193: 1025–64. doi:10.1534/genetics.112.145219

Bonner W. M., C. E. Redon, J. S. Dickey, A. J. Nakamura, O. A. Sedelnikova, *et al.*, 2008 GammaH2AX and cancer. Nat. Rev. Cancer 8: 957–67. doi:10.1038/nrc2523

Bottomley M. J., 2004 Structures of protein domains that create or recognize histone modifications. EMBO Rep. 5: 464–9. doi:10.1038/sj.embor.7400146

Boulton S. J., and S. P. Jackson, 1996 Saccharomyces cerevisiae Ku70 potentiates illegitimate DNA double- strand break repair and serves as a barrier to error-prone DNA repair pathways. EMBO J. 15: 5093–5103. doi:10.1002/J.1460-2075.1996.TB00890.X

Brahma S., M. I. Udugama, J. Kim, A. Hada, S. K. Bhardwaj, *et al.*, 2017 INO80 exchanges H2A.Z for H2A by translocating on DNA proximal to histone dimers. Nat. Commun. 8: 15616. doi:10.1038/ncomms15616

Breiling A., and F. Lyko, 2015 Epigenetic regulatory functions of DNA modifications: 5-methylcytosine and beyond. Epigenetics Chromatin 8: 24. doi:10.1186/s13072-015-0016-6

Bressan D. A., B. K. Baxter, and J. H. Petrini, 1999 The Mre11-Rad50-Xrs2 protein complex facilitates homologous recombination-based double-strand break repair in Saccharomyces cerevisiae. Mol. Cell. Biol. 19: 7681–7.

Briggs S. D., M. Bryk, B. D. Strahl, W. L. Cheung, J. K. Davie, *et al.*, 2001 Histone H3 lysine 4 methylation is mediated by Set1 and required for cell growth and rDNA silencing in Saccharomyces cerevisiae. Genes Dev. 15: 3286–3295. doi:10.1101/gad.940201

Brill S. J., and B. Stillman, 1991 Replication factor-A from Saccharomyces cerevisiae is encoded by three essential genes coordinately expressed at S phase. Genes Dev. 5: 1589–600.

Bruce K., F. A. Myers, E. Mantouvalou, P. Lefevre, I. Greaves, *et al.*, 2005 The replacement histone H2A.Z in a hyperacetylated form is a feature of active genes in the chicken. Nucleic Acids Res. 33: 5633–5639. doi:10.1093/nar/gki874

Byun T. S., M. Pacek, M. Yee, J. C. Walter, and K. A. Cimprich, 2005 Functional uncoupling of MCM helicase and DNA polymerase activities activates the ATR-dependent checkpoint. Genes Dev. 19: 1040–52. doi:10.1101/gad.1301205

Cadet J., T. Douki, D. Gasparutto, and J.-L. Ravanat, 2003 Oxidative damage to DNA: formation, measurement and biochemical features. Mutat. Res. Mol. Mech. Mutagen. 531: 5–23. doi:10.1016/J.MRFMMM.2003.09.001

Cai L., B. M. Sutter, B. Li, and B. P. Tu, 2011 Acetyl-CoA Induces Cell Growth and Proliferation by Promoting the Acetylation of Histones at Growth Genes. Mol. Cell 42: 426–437. doi:10.1016/J.MOLCEL.2011.05.004

Cannavo E., P. Cejka, and S. C. Kowalczykowski, 2013 Relationship of DNA degradation by Saccharomyces cerevisiae Exonuclease 1 and its stimulation by RPA and Mre11-Rad50-Xrs2 to DNA end resection. Proc. Natl. Acad. Sci. 110: E1661–E1668. doi:10.1073/pnas.1305166110

Cannavo E., and P. Cejka, 2014 Sae2 promotes dsDNA endonuclease activity within Mre11–Rad50–Xrs2 to resect DNA breaks. Nature 514: 122–125. doi:10.1038/nature13771

Capuano F., M. Mülleder, R. Kok, H. J. Blom, and M. Ralser, 2014 Cytosine DNA Methylation Is Found in *Drosophila melanogaster* but Absent in *Saccharomyces cerevisiae*, *Schizosaccharomyces pombe* , and Other Yeast Species. Anal. Chem. 86: 3697–3702. doi:10.1021/ac500447w

Cejka P., E. Cannavo, P. Polaczek, T. Masuda-Sasa, S. Pokharel, *et al.*, 2010 DNA end resection by Dna2–Sgs1–RPA and its stimulation by Top3–Rmi1 and Mre11–Rad50–Xrs2. Nature 467: 112–116. doi:10.1038/nature09355

Cejka P., 2015 DNA End Resection: Nucleases Team Up with the Right Partners to Initiate Homologous Recombination. J. Biol. Chem. 290: 22931–8. doi:10.1074/jbc.R115.675942

Cervera A. M., J.-P. Bayley, P. Devilee, and K. J. McCreath, 2009 Inhibition of succinate dehydrogenase dysregulates histone modification in mammalian cells. Mol. Cancer 8: 89. doi:10.1186/1476-4598-8-89

Chabes A., V. Domkin, and L. Thelander, 1999 Yeast Sml1, a protein inhibitor of ribonucleotide reductase. J. Biol. Chem. 274: 36679–83. doi:10.1074/JBC.274.51.36679

Chan C. Y., A. Galli, and R. H. Schiestl, 2008 Pol3 is involved in nonhomologous end-joining in Saccharomyces cerevisiae. DNA Repair (Amst). 7: 1531–1541. doi:10.1016/J.DNAREP.2008.05.008

Chen L., K. Trujillo, W. Ramos, P. Sung, and A. E. Tomkinson, 2001 Promotion of Dnl4-catalyzed DNA end-joining by the Rad50/Mre11/Xrs2 and Hdf1/Hdf2 complexes. Mol. Cell 8: 1105–15. doi:10.1016/S1097-2765(01)00388-4

Chen S., A. A. Davies, D. Sagan, and H. D. Ulrich, 2005 The RING finger ATPase Rad5p of Saccharomyces cerevisiae contributes to DNA double-strand break repair in a ubiquitin-independent manner. Nucleic Acids Res. 33: 5878–86. doi:10.1093/nar/gki902

Chen S.-H., and H. Zhou, 2009 Reconstitution of Rad53 activation by Mec1 through adaptor protein Mrc1. J. Biol. Chem. 284: 18593–604. doi:10.1074/jbc.M109.018242

Chen S., C. P. Albuquerque, J. Liang, R. T. Suhandynata, and H. Zhou, 2010 A proteome-wide analysis of kinase-substrate network in the DNA damage response. J. Biol. Chem. 285: 12803–12. doi:10.1074/jbc.M110.106989

Chen X., and A. E. Tomkinson, 2011 Yeast Nej1 is a key participant in the initial end binding and final ligation steps of nonhomologous end joining. J. Biol. Chem. 286: 4931–40. doi:10.1074/jbc.M110.195024

Chen X., H. Niu, W.-H. Chung, Z. Zhu, A. Papusha, *et al.*, 2011 Cell cycle regulation of DNA double-strand break end resection by Cdk1-dependent Dna2 phosphorylation. Nat. Struct. Mol. Biol. 18: 1015–1019. doi:10.1038/nsmb.2105

Chen J., A. Miller, A. L. Kirchmaier, and J. M. K. Irudayaraj, 2012 Single-molecule tools elucidate H2A.Z nucleosome composition. J. Cell Sci. 125: 2954–64. doi:10.1242/jcs.101592

Chowdhury D., M.-C. Keogh, H. Ishii, C. L. Peterson, S. Buratowski, *et al.*, 2005 γ-H2AX Dephosphorylation by Protein Phosphatase 2A Facilitates DNA Double-Strand Break Repair. Mol. Cell 20: 801–809. doi:10.1016/J.MOLCEL.2005.10.003

Christianson T. W., R. S. Sikorski, M. Dante, J. H. Shero, and P. Hieter, 1992 Multifunctional yeast high-copy-number shuttle vectors. Gene 110: 119–122. doi:10.1016/0378-1119(92)90454-W

Clémenson C., and M.-C. Marsolier-Kergoat, 2009 DNA damage checkpoint inactivation: Adaptation and recovery. DNA Repair (Amst). 8: 1101–1109. doi:10.1016/j.dnarep.2009.04.008

Clerici M., D. Mantiero, I. Guerini, G. Lucchini, and M. P. Longhese, 2008 The Yku70-Yku80 complex contributes to regulate double-strand break processing and checkpoint activation during the cell cycle. EMBO Rep. 9: 810–8. doi:10.1038/embor.2008.121

Cloos P. A. C., J. Christensen, K. Agger, and K. Helin, 2008 Erasing the methyl mark: histone demethylases at the center of cellular differentiation and disease. Genes Dev. 22: 1115–40. doi:10.1101/gad.1652908

Cobb J. A., L. Bjergbaek, K. Shimada, C. Frei, and S. M. Gasser, 2003 DNA polymerase stabilization at stalled replication forks requires Mec1 and the RecQ helicase Sgs1. EMBO J. 22: 4325–36. doi:10.1093/emboj/cdg391

Cobb J. A., T. Schleker, V. Rojas, L. Bjergbaek, J. A. Tercero, *et al.*, 2005 Replisome instability, fork collapse, and gross chromosomal rearrangements arise synergistically from Mec1 kinase and RecQ helicase mutations. Genes Dev. 19: 3055–69. doi:10.1101/gad.361805

Collins S. R., K. M. Miller, N. L. Maas, A. Roguev, J. Fillingham, *et al.*, 2007 Functional dissection of protein complexes involved in yeast chromosome biology using a genetic interaction map. Nature 446: 806–810. doi:10.1038/nature05649

Colosio A., C. Frattini, G. Pellicanò, S. Villa-Hernández, and R. Bermejo, 2016 Nucleolytic processing of aberrant replication intermediates by an Exo1-Dna2-Sae2 axis counteracts fork collapse-driven chromosome instability. Nucleic Acids Res. 44: 10676–10690. doi:10.1093/nar/gkw858

Covey J. M., C. Jaxel, K. W. Kohn, and Y. Pommier, 1989 Protein-linked DNA strand breaks induced in mammalian cells by camptothecin, an inhibitor of topoisomerase I. Cancer Res. 49: 5016–22.

Daganzo S. M., J. P. Erzberger, W. M. Lam, E. Skordalakes, R. Zhang, *et al.*, 2003 Structure and function of the conserved core of histone deposition protein Asf1. Curr. Biol. 13: 2148–58. doi:10.1016/J.CUB.2003.11.027

Daley J. M., P. L. Palmbos, D. Wu, and T. E. Wilson, 2005 Nonhomologous End Joining in Yeast. Annu. Rev. Genet. 39: 431–451. doi:10.1146/annurev.genet.39.073003.113340

Dang L., D. W. White, S. Gross, B. D. Bennett, M. A. Bittinger, *et al.*, 2009 Cancer-associated IDH1 mutations produce 2-hydroxyglutarate. Nature 462: 739–744. doi:10.1038/nature08617

Davis A. P., and L. S. Symington, 2001 The yeast recombinational repair protein Rad59 interacts with Rad52 and stimulates single-strand annealing. Genetics 159: 515–25.

Deng C., J. A. Brown, D. You, and J. M. Brown, 2005 Multiple endonucleases function to repair covalent topoisomerase I complexes in Saccharomyces cerevisiae. Genetics 170: 591–600. doi:10.1534/genetics.104.028795

Desany B. A., A. A. Alcasabas, J. B. Bachant, and S. J. Elledge, 1998 Recovery from DNA replicational stress is the essential function of the S-phase checkpoint pathway. Genes Dev. 12: 2956–70.

Deshpande I., A. Seeber, K. Shimada, J. J. Keusch, H. Gut, *et al.*, 2017 Structural Basis of Mec1-Ddc2-RPA Assembly and Activation on Single-Stranded DNA at Sites of Damage. Mol. Cell 68: 431–445.e5. doi:10.1016/J.MOLCEL.2017.09.019

Dhillon N., and R. T. Kamakaka, 2000 A Histone Variant, Htz1p, and a Sir1p-like Protein, Esc2p, Mediate Silencing at HMR. Mol. Cell 6: 769–780. doi:10.1016/S1097-2765(00)00076-9

Dhillon N., M. Oki, S. J. Szyjka, O. M. Aparicio, and R. T. Kamakaka, 2006 H2A.Z functions to regulate progression through the cell cycle. Mol. Cell. Biol. 26: 489–501. doi:10.1128/MCB.26.2.489-501.2006

Doerfler L., and K. H. Schmidt, 2014 Exo1 phosphorylation status controls the hydroxyurea sensitivity of cells lacking the Pol32 subunit of DNA polymerases delta and zeta. DNA Repair (Amst). 24: 26–36. doi:10.1016/j.dnarep.2014.10.004

Dover J., J. Schneider, M. A. Tawiah-Boateng, A. Wood, K. Dean, *et al.*, 2002 Methylation of histone H3 by COMPASS requires ubiquitination of histone H2B by Rad6. J. Biol. Chem. 277: 28368–71. doi:10.1074/jbc.C200348200

Downs J. A., N. F. Lowndes, and S. P. Jackson, 2000 A role for Saccharomyces cerevisiae histone H2A in DNA repair. Nature 408: 1001–1004. doi:10.1038/35050000

Downs J. A., S. Allard, O. Jobin-Robitaille, A. Javaheri, A. Auger, *et al.*, 2004 Binding of Chromatin-Modifying Activities to Phosphorylated Histone H2A at DNA Damage Sites. Mol. Cell 16: 979–990. doi:10.1016/J.MOLCEL.2004.12.003

Duncker B. P., K. Shimada, M. Tsai-Pflugfelder, P. Pasero, and S. M. Gasser, 2002 An N-terminal domain of Dbf4p mediates interaction with both origin recognition complex (ORC) and Rad53p and can deregulate late origin firing. Proc. Natl. Acad. Sci. U. S. A. 99: 16087–92. doi:10.1073/pnas.252093999

Edelheit O., A. Hanukoglu, and I. Hanukoglu, 2009 Simple and efficient site-directed mutagenesis using two single-primer reactions in parallel to generate mutants for protein structure-function studies. BMC Biotechnol. 9: 61. doi:10.1186/1472-6750-9-61

Edmunds J. W., L. C. Mahadevan, and A. L. Clayton, 2008 Dynamic histone H3 methylation during gene induction: HYPB/Setd2 mediates all H3K36 trimethylation. EMBO J. 27: 406–20. doi:10.1038/sj.emboj.7601967

Ellison V., and B. Stillman, 2003 Biochemical Characterization of DNA Damage Checkpoint Complexes: Clamp Loader and Clamp Complexes with Specificity for 5′ Recessed DNA, (James E. Haber, Ed.). PLoS Biol. 1: e33. doi:10.1371/journal.pbio.0000033

Emerson C. H., and A. A. Bertuch, 2016 Consider the workhorse: Nonhomologous end-joining in budding yeast. Biochem. Cell Biol. 94: 396–406. doi:10.1139/bcb-2016-0001

Fan J., K. A. Krautkramer, J. L. Feldman, and J. M. Denu, 2015 Metabolic regulation of histone post-translational modifications. ACS Chem. Biol. 10: 95–108. doi:10.1021/cb500846u

Fang J., G. J. Hogan, G. Liang, J. D. Lieb, and Y. Zhang, 2007 The Saccharomyces cerevisiae Histone Demethylase Jhd1 Fine-Tunes the Distribution of H3K36me2. Mol. Cell. Biol. 27: 5055–5065. doi:10.1128/MCB.00127-07

Faucher D., and R. J. Wellinger, 2010 Methylated H3K4, a transcription-associated histone modification, is involved in the DNA damage response pathway. PLoS Genet. 6: e1001082. doi:10.1371/journal.pgen.1001082

Fieuw A., C. Kumps, A. Schramm, F. Pattyn, B. Menten, *et al.*, 2012 Identification of a novel recurrent 1q42.2-1qter deletion in high risk MYCN single copy 11q deleted neuroblastomas. Int. J. Cancer 130: 2599–2606. doi:10.1002/ijc.26317

Fingerman I. M., H.-C. Li, and S. D. Briggs, 2007 A charge-based interaction between histone H4 and Dot1 is required for H3K79 methylation and telomere silencing: identification of a new trans-histone pathway. Genes Dev. 21: 2018–29. doi:10.1101/gad.1560607

Foster S. S., A. Balestrini, and J. H. J. Petrini, 2011 Functional interplay of the Mre11 nuclease and Ku in the response to replication-associated DNA damage. Mol. Cell. Biol. 31: 4379–89. doi:10.1128/MCB.05854-11

Franco A. A., W. M. Lam, P. M. Burgers, and P. D. Kaufman, 2005 Histone deposition protein Asf1 maintains DNA replisome integrity and interacts with replication factor C. Genes Dev. 19: 1365–75. doi:10.1101/gad.1305005

Freudenreich C. H., and X. A. Su, 2016 Relocalization of DNA lesions to the nuclear pore complex. FEMS Yeast Res. 16. doi:10.1093/FEMSYR/FOW095

Fuchs S. M., K. O. Kizer, H. Braberg, N. J. Krogan, and B. D. Strahl, 2012 RNA polymerase II carboxyl-terminal domain phosphorylation regulates protein stability of the Set2 methyltransferase and histone H3 di- and trimethylation at lysine 36. J. Biol. Chem. 287: 3249–56. doi:10.1074/jbc.M111.273953

Furuya K., M. Poitelea, L. Guo, T. Caspari, and A. M. Carr, 2004 Chk1 activation requires Rad9 S/TQ-site phosphorylation to promote association with C-terminal BRCT domains of Rad4TOPBP1. Genes Dev. 18: 1154–64. doi:10.1101/gad.291104

Gadaleta M., E. Noguchi, M. C. Gadaleta, and E. Noguchi, 2017 Regulation of DNA Replication through Natural Impediments in the Eukaryotic Genome. Genes (Basel). 8: 98. doi:10.3390/genes8030098

Galli A., C. Y. Chan, L. Parfenova, T. Cervelli, and R. H. Schiestl, 2015 Requirement of POL3 and POL4 on non-homologous and microhomology-mediated end joining in rad50/xrs2 mutants of Saccharomyces cerevisiae. Mutagenesis 30: 841–9. doi:10.1093/mutage/gev046

Game J. C., and R. K. Mortimer, 1974 A genetic study of X-ray sensitive mutants in yeast. Mutat. Res. Mol. Mech. Mutagen. 24: 281–292. doi:10.1016/0027-5107(74)90176-6

Game J. C., M. S. Williamson, and C. Baccari, 2005 X-ray survival characteristics and genetic analysis for nine Saccharomyces deletion mutants that show altered radiation sensitivity. Genetics 169: 51–63. doi:10.1534/genetics.104.028613

Gao S., S. Honey, B. Futcher, and A. P. Grollman, 2016 The non-homologous end-joining pathway of S. cerevisiae works effectively in G1-phase cells, and religates cognate ends correctly and non-randomly. DNA Repair (Amst). 42: 1–10. doi:10.1016/j.dnarep.2016.03.013

Garcia V., S. E. L. Phelps, S. Gray, and M. J. Neale, 2011 Bidirectional resection of DNA double-strand breaks by Mre11 and Exo1. Nature 479: 241–244. doi:10.1038/nature10515

Garg P., and P. M. J. Burgers, 2005 DNA Polymerases that Propagate the Eukaryotic DNA Replication Fork. Crit. Rev. Biochem. Mol. Biol. 40: 115–128. doi:10.1080/10409230590935433

Gasior S. L., A. K. Wong, Y. Kora, A. Shinohara, and D. K. Bishop, 1998 Rad52 associates with RPA and functions with Rad55 and Rad57 to assemble meiotic recombination complexes. Genes Dev. 12: 2208–2221. doi:10.1101/gad.12.14.2208

Gaude E., and C. Frezza, 2014 Defects in mitochondrial metabolism and cancer. Cancer Metab. 2: 10. doi:10.1186/2049-3002-2-10

Gévry N., H. M. Chan, L. Laflamme, D. M. Livingston, and L. Gaudreau, 2007 p21 transcription is regulated by differential localization of histone H2A.Z. Genes Dev. 21: 1869–81. doi:10.1101/gad.1545707

Ghodke I., and K. Muniyappa, 2016 Genetic and biochemical evidences reveal novel insights into the mechanism underlying Saccharomyces cerevisiae Sae2-mediated abrogation of DNA replication stress. J. Biosci. 41: 615–641.

Giannattasio M., F. Lazzaro, P. Plevani, and M. Muzi-Falconi, 2005 The DNA Damage Checkpoint Response Requires Histone H2B Ubiquitination by Rad6-Bre1 and H3 Methylation by Dot1. J. Biol. Chem. 280: 9879–9886. doi:10.1074/jbc.M414453200

Giannattasio M., and D. Branzei, 2017 S-phase checkpoint regulations that preserve replication and chromosome integrity upon dNTP depletion. Cell. Mol. Life Sci. 74: 2361–2380. doi:10.1007/s00018-017-2474-4

Gilbert C. S., C. M. Green, and N. F. Lowndes, 2001 Budding Yeast Rad9 Is an ATP-Dependent Rad53 Activating Machine. Mol. Cell 8: 129–136. doi:10.1016/S1097-2765(01)00267-2

Gnügge R., and L. S. Symington, 2017 Keeping it real: MRX-Sae2 clipping of natural substrates. Genes Dev. 31: 2311–2312. doi:10.1101/gad.310771.117

Goldstein A. L., and J. H. McCusker, 1999 Three new dominant drug resistance cassettes for gene disruption in Saccharomyces cerevisiae. Yeast 15: 1541–53. doi:10.1002/(SICI)1097-0061(199910)15:14<1541::AID-YEA476>3.0.CO;2-K

Gorgoulis V. G., L.-V. F. Vassiliou, P. Karakaidos, P. Zacharatos, A. Kotsinas, *et al.*, 2005 Activation of the DNA damage checkpoint and genomic instability in human precancerous lesions. Nature 434: 907–913. doi:10.1038/nature03485

Gorisch S. M., M. Wachsmuth, K. F. Tóth, P. Lichter, and K. Rippe, 2005 Histone acetylation increases chromatin accessibility. J. Cell Sci. 118: 5825–5834. doi:10.1242/jcs.02689

Greaves I. K., D. Rangasamy, P. Ridgway, and D. J. Tremethick, 2007 H2A.Z contributes to the unique 3D structure of the centromere. Proc. Natl. Acad. Sci. U. S. A. 104: 525–30. doi:10.1073/pnas.0607870104

Green R., G. Lesage, A.-M. Sdicu, P. Ménard, and H. Bussey, 2003 A synthetic analysis of the Saccharomyces cerevisiae stress sensor Mid2p, and identification of a Mid2p-interacting protein, Zeo1p, that modulates the PKC1-MPK1 cell integrity pathway. Microbiology 149: 2487–2499. doi:10.1099/mic.0.26471-0

Gross S., R. A. Cairns, M. D. Minden, E. M. Driggers, M. A. Bittinger, *et al.*, 2010 Cancer-associated metabolite 2-hydroxyglutarate accumulates in acute myelogenous leukemia with isocitrate dehydrogenase 1 and 2 mutations. J. Exp. Med. 207: 339–44. doi:10.1084/jem.20092506

Guthrie C., and G. R. Fink, 1991 Guide to yeast genetics and molecular biology. Academic Press.

Haber J. E., 2012 Mating-type genes and MAT switching in Saccharomyces cerevisiae. Genetics 191: 33–64. doi:10.1534/genetics.111.134577

Hammel M., Y. Yu, S. Fang, S. P. Lees-Miller, and J. A. Tainer, 2010 XLF regulates filament architecture of the XRCC4·ligase IV complex. Structure 18: 1431–42. doi:10.1016/j.str.2010.09.009

Hammel M., M. Rey, Y. Yu, R. S. Mani, S. Classen, *et al.*, 2011 XRCC4 protein interactions with XRCC4-like factor (XLF) create an extended grooved scaffold for DNA ligation and double strand break repair. J. Biol. Chem. 286: 32638–50. doi:10.1074/jbc.M111.272641

Haro L. P. De, J. Wray, E. A. Williamson, S. T. Durant, L. Corwin, *et al.*, 2010 Metnase promotes restart and repair of stalled and collapsed replication forks. Nucleic Acids Res. 38: 5681–91. doi:10.1093/nar/gkq339

Hashimoto Y., A. Ray Chaudhuri, M. Lopes, and V. Costanzo, 2010 Rad51 protects nascent DNA from Mre11-dependent degradation and promotes continuous DNA synthesis. Nat. Struct. Mol. Biol. 17: 1305–1311. doi:10.1038/nsmb.1927

Hauer M. H., and S. M. Gasser, 2017 Chromatin and nucleosome dynamics in DNA damage and repair. Genes Dev. 31: 2204–2221. doi:10.1101/gad.307702.117

Hays S. L., A. A. Firmenich, P. Massey, R. Banerjee, and P. Berg, 1998 Studies of the interaction between Rad52 protein and the yeast single-stranded DNA binding protein RPA. Mol. Cell. Biol. 18: 4400–6. doi:10.1128/MCB.18.7.4400

Hegnauer A. M., N. Hustedt, K. Shimada, B. L. Pike, M. Vogel, *et al.*, 2012 An N-terminal acidic region of Sgs1 interacts with Rpa70 and recruits Rad53 kinase to stalled forks. EMBO J. 31: 3768–83. doi:10.1038/emboj.2012.195

Herrmann G., T. Lindahl, and P. Schär, 1998 Saccharomyces cerevisiae LIF1: a function involved in DNA double-strand break repair related to mammalian XRCC4. EMBO J. 17: 4188–98. doi:10.1093/emboj/17.14.4188

Heyer W.-D., K. T. Ehmsen, and J. Liu, 2010 Regulation of homologous recombination in eukaryotes. Annu. Rev. Genet. 44: 113–39. doi:10.1146/annurev-genet-051710-150955

Higgs M. R., J. J. Reynolds, A. Winczura, A. N. Blackford, V. Borel, *et al.*, 2015 BOD1L Is Required to Suppress Deleterious Resection of Stressed Replication Forks. Mol. Cell 59: 462–477. doi:10.1016/J.MOLCEL.2015.06.007

Higgs M. R., K. Sato, J. J. Reynolds, S. Begum, R. Bayley, *et al.*, 2018 Histone Methylation by SETD1A Protects Nascent DNA through the Nucleosome Chaperone Activity of FANCD2. Mol. Cell 71: 25–41.e6. doi:10.1016/j.molcel.2018.05.018

Hoffman E. A., A. McCulley, B. Haarer, R. Arnak, and W. Feng, 2015 Break-seq reveals hydroxyurea-induced chromosome fragility as a result of unscheduled conflict between DNA replication and transcription. Genome Res. 25: 402–412. doi:10.1101/gr.180497.114

Hoshii T., P. Cifani, Z. Feng, C.-H. Huang, R. Koche, *et al.*, 2018 A Non-catalytic Function of SETD1A Regulates Cyclin K and the DNA Damage Response. Cell 172: 1007–1021.e17. doi:10.1016/j.cell.2018.01.032

House N. C. M., M. R. Koch, and C. H. Freudenreich, 2014 Chromatin modifications and DNA repair: beyond double-strand breaks. Front. Genet. 5: 296. doi:10.3389/fgene.2014.00296

Hsiang Y. H., M. G. Lihou, and L. F. Liu, 1989 Arrest of replication forks by drug-stabilized topoisomerase I-DNA cleavable complexes as a mechanism of cell killing by camptothecin. Cancer Res. 49: 5077–82.

Huertas P., F. Cortés-Ledesma, A. A. Sartori, A. Aguilera, and S. P. Jackson, 2008 CDK targets Sae2 to control DNA-end resection and homologous recombination. Nature 455: 689–692. doi:10.1038/nature07215

Huh W.-K., J. V. Falvo, L. C. Gerke, A. S. Carroll, R. W. Howson, *et al.*, 2003 Global analysis of protein localization in budding yeast. Nature 425: 686–691. doi:10.1038/nature02026

Hustedt N., S. M. Gasser, and K. Shimada, 2013 Replication checkpoint: tuning and coordination of replication forks in s phase. Genes (Basel). 4: 388–434. doi:10.3390/genes4030388

Ingvarsdottir K., C. Edwards, M. G. Lee, J. S. Lee, D. C. Schultz, *et al.*, 2007 Histone H3 K4 demethylation during activation and attenuation of GAL1 transcription in Saccharomyces cerevisiae. Mol. Cell. Biol. 27: 7856–64. doi:10.1128/MCB.00801-07

Ira G., A. Pellicioli, A. Balijja, X. Wang, S. Fiorani, *et al.*, 2004 DNA end resection, homologous recombination and DNA damage checkpoint activation require CDK1. Nature 431: 1011–1017. doi:10.1038/nature02964

Iraqui I., Y. Chekkal, N. Jmari, V. Pietrobon, K. Fréon, *et al.*, 2012 Recovery of Arrested Replication Forks by Homologous Recombination Is Error-Prone, (S. Jinks-Robertson, Ed.). PLoS Genet. 8: e1002976. doi:10.1371/journal.pgen.1002976

Isaacs J. S., Y. J. Jung, D. R. Mole, S. Lee, C. Torres-Cabala, *et al.*, 2005 HIF overexpression correlates with biallelic loss of fumarate hydratase in renal cancer: Novel role of fumarate in regulation of HIF stability. Cancer Cell 8: 143–153. doi:10.1016/J.CCR.2005.06.017

Jackson S. P., and J. Bartek, 2009 The DNA-damage response in human biology and disease. Nature 461: 1071–1078. doi:10.1038/nature08467

Janke R., A. T. Iavarone, and J. Rine, 2017 Oncometabolite D-2-Hydroxyglutarate enhances gene silencing through inhibition of specific H3K36 histone demethylases. Elife 6: e22451. doi:10.7554/eLife.22451

Javaheri A., R. Wysocki, O. Jobin-Robitaille, M. Altaf, J. Côté, *et al.*, 2006 Yeast G1 DNA damage checkpoint regulation by H2A phosphorylation is independent of chromatin remodeling. Proc. Natl. Acad. Sci. U. S. A. 103: 13771–6. doi:10.1073/pnas.0511192103

Jha D. K., and B. D. Strahl, 2014 An RNA polymerase II-coupled function for histone H3K36 methylation in checkpoint activation and DSB repair. Nat. Commun. 5: 3965. doi:10.1038/ncomms4965

Jiang Y., X. Qian, J. Shen, Y. Wang, X. Li, *et al.*, 2015 Local generation of fumarate promotes DNA repair through inhibition of histone H3 demethylation. Nat. Cell Biol. 17. doi:10.1038/ncb3209

Jossen R., and R. Bermejo, 2013 The DNA damage checkpoint response to replication stress: A Game of Forks. Front. Genet. 4: 26. doi:10.3389/fgene.2013.00026

Kalocsay M., N. J. Hiller, and S. Jentsch, 2009 Chromosome-wide Rad51 Spreading and SUMO-H2A.Z-Dependent Chromosome Fixation in Response to a Persistent DNA Double-Strand Break. Mol. Cell 33: 335–343. doi:10.1016/j.molcel.2009.01.016

Karanam K., R. Kafri, A. Loewer, and G. Lahav, 2012 Quantitative live cell imaging reveals a gradual shift between DNA repair mechanisms and a maximal use of HR in mid S phase. Mol. Cell 47: 320–9. doi:10.1016/j.molcel.2012.05.052

Karniely S., and O. Pines, 2005 Single translation--dual destination: mechanisms of dual protein targeting in eukaryotes. EMBO Rep. 6: 420–5. doi:10.1038/sj.embor.7400394

Katou Y., Y. Kanoh, M. Bando, H. Noguchi, H. Tanaka, *et al.*, 2003 S-phase checkpoint proteins Tof1 and Mrc1 form a stable replication-pausing complex. Nature 424: 1078–1083. doi:10.1038/nature01900

Kelly T. J., S. Qin, D. E. Gottschling, and M. R. Parthun, 2000 Type B histone acetyltransferase Hat1p participates in telomeric silencing. Mol. Cell. Biol. 20: 7051–8. doi:10.1128/MCB.20.19.7051-7058.2000

Keogh M.-C., J.-A. Kim, M. Downey, J. Fillingham, D. Chowdhury, *et al.*, 2006 A phosphatase complex that dephosphorylates γH2AX regulates DNA damage checkpoint recovery. Nature 439: 497–501. doi:10.1038/nature04384

Khalil A. A., 2007 Biomarker discovery: A proteomic approach for brain cancer profiling. Cancer Sci. 98: 201–213. doi:10.1111/j.1349-7006.2007.00374.x

Khoury-Haddad H., N. Guttmann-Raviv, I. Ipenberg, D. Huggins, A. D. Jeyasekharan, *et al.*, 2014 PARP1-dependent recruitment of KDM4D histone demethylase to DNA damage sites promotes double-strand break repair. Proc. Natl. Acad. Sci. U. S. A. 111: E728. doi:10.1073/PNAS.1317585111

Kim S. T., D. S. Lim, C. E. Canman, and M. B. Kastan, 1999 Substrate specificities and identification of putative substrates of ATM kinase family members. J. Biol. Chem. 274: 37538–43. doi:10.1074/JBC.274.53.37538

Kim T., and S. Buratowski, 2007 Two Saccharomyces cerevisiae JmjC domain proteins demethylate histone H3 Lys36 in transcribed regions to promote elongation. J. Biol. Chem. 282: 20827–35. doi:10.1074/jbc.M703034200

Kirchmaier A. L., and J. Rine, 2006 Cell cycle requirements in assembling silent chromatin in Saccharomyces cerevisiae. Mol. Cell. Biol. 26: 852–62. doi:10.1128/MCB.26.3.852-862.2006

Kish A., and J. DiRuggiero, 2008 Rad50 Is Not Essential for the Mre11-Dependent Repair of DNA Double-Strand Breaks in Halobacterium sp. Strain NRC-1. J. Bacteriol. 190: 5210–5216. doi:10.1128/JB.00292-08

Kiuru M., R. Lehtonen, J. Arola, R. Salovaara, H. Järvinen, *et al.*, 2002 Few FH mutations in sporadic counterparts of tumor types observed in hereditary leiomyomatosis and renal cell cancer families. Cancer Res. 62: 4554–7.

Knox C., E. Sass, W. Neupert, and O. Pines, 1998 Import into mitochondria, folding and retrograde movement of fumarase in yeast. J. Biol. Chem. 273: 25587–93. doi:10.1074/JBC.273.40.25587

Kobor M. S., S. Venkatasubrahmanyam, M. D. Meneghini, J. W. Gin, J. L. Jennings, *et al.*, 2004 A Protein Complex Containing the Conserved Swi2/Snf2-Related ATPase Swr1p Deposits Histone Variant H2A.Z into Euchromatin, (Peter Becker, Ed.). PLoS Biol. 2: e131. doi:10.1371/journal.pbio.0020131

Koivunen P., M. Hirsilä, A. M. Remes, I. E. Hassinen, K. I. Kivirikko, *et al.*, 2007 Inhibition of hypoxia-inducible factor (HIF) hydroxylases by citric acid cycle intermediates: possible links between cell metabolism and stabilization of HIF. J. Biol. Chem. 282: 4524–32. doi:10.1074/jbc.M610415200

Komata M., M. Bando, H. Araki, and K. Shirahige, 2009 The direct binding of Mrc1, a checkpoint mediator, to Mcm6, a replication helicase, is essential for the replication checkpoint against methyl methanesulfonate-induced stress. Mol. Cell. Biol. 29: 5008–19. doi:10.1128/MCB.01934-08

Kondo T., K. Matsumoto, and K. Sugimoto, 1999 Role of a complex containing Rad17, Mec3, and Ddc1 in the yeast DNA damage checkpoint pathway. Mol. Cell. Biol. 19: 1136–43.

Krakoff I. H., N. C. Brown, and P. Reichard, 1968 Inhibition of ribonucleoside diphosphate reductase by hydroxyurea. Cancer Res. 28: 1559–65.

Krejci L., S. Van Komen, Y. Li, J. Villemain, M. S. Reddy, *et al.*, 2003 DNA helicase Srs2 disrupts the Rad51 presynaptic filament. Nature 423: 305–309. doi:10.1038/nature01577

Krogan N. J., M.-C. Keogh, N. Datta, C. Sawa, O. W. Ryan, *et al.*, 2003 A Snf2 Family ATPase Complex Required for Recruitment of the Histone H2A Variant Htz1. Mol. Cell 12: 1565–1576. doi:10.1016/S1097-2765(03)00497-0

Krogan N. J., K. Baetz, M.-C. Keogh, N. Datta, C. Sawa, *et al.*, 2004 Regulation of chromosome stability by the histone H2A variant Htz1, the Swr1 chromatin remodeling complex, and the histone acetyltransferase NuA4. Proc. Natl. Acad. Sci. U. S. A. 101: 13513–8. doi:10.1073/pnas.0405753101

Krogh B. O., and L. S. Symington, 2004 Recombination proteins in yeast. Annu. Rev. Genet. 38: 233–71. doi:10.1146/annurev.genet.38.072902.091500

Kwon D.-W., and S. H. Ahn, 2011 Role of yeast JmjC-domain containing histone demethylases in actively transcribed regions. Biochem. Biophys. Res. Commun. 410: 614–619. doi:10.1016/J.BBRC.2011.06.039

Lademann C. A., J. Renkawitz, B. Pfander, and S. Jentsch, 2017 The INO80 Complex Removes H2A.Z to Promote Presynaptic Filament Formation during Homologous Recombination. Cell Rep. 19: 1294–1303. doi:10.1016/j.celrep.2017.04.051

Lambert S., K. Mizuno, J. Blaisonneau, S. Martineau, R. Chanet, *et al.*, 2010 Homologous Recombination Restarts Blocked Replication Forks at the Expense of Genome Rearrangements by Template Exchange. Mol. Cell 39: 346–359. doi:10.1016/j.molcel.2010.07.015

Lancelot N., G. Charier, J. Couprie, I. Duband-Goulet, B. Alpha-Bazin, *et al.*, 2007 The checkpoint Saccharomyces cerevisiae Rad9 protein contains a tandem tudor domain that recognizes DNA. Nucleic Acids Res. 35: 5898–912. doi:10.1093/nar/gkm607

Laukka T., C. J. Mariani, T. Ihantola, J. Z. Cao, J. Hokkanen, *et al.*, 2016 Fumarate and Succinate Regulate Expression of Hypoxia-inducible Genes via TET Enzymes. J. Biol. Chem. 291: 4256–65. doi:10.1074/jbc.M115.688762

Launonen V., O. Vierimaa, M. Kiuru, J. Isola, S. Roth, *et al.*, 2001 Inherited susceptibility to uterine leiomyomas and renal cell cancer. Proc. Natl. Acad. Sci. U. S. A. 98: 3387–92. doi:10.1073/pnas.051633798

Laurenti G., and D. A. Tennant, 2016 Isocitrate dehydrogenase (IDH), succinate dehydrogenase (SDH), fumarate hydratase (FH): three players for one phenotype in cancer? Biochem. Soc. Trans. 44: 1111–1116. doi:10.1042/BST20160099

Lazzaro F., V. Sapountzi, M. Granata, A. Pellicioli, M. Vaze, *et al.*, 2008 Histone methyltransferase Dot1 and Rad9 inhibit single-stranded DNA accumulation at DSBs and uncapped telomeres. EMBO J. 27: 1502–12. doi:10.1038/emboj.2008.81

Lee S. E., J. K. Moore, A. Holmes, K. Umezu, R. D. Kolodner, *et al.*, 1998 Saccharomyces Ku70, Mre11/Rad50, and RPA Proteins Regulate Adaptation to G2/M Arrest after DNA Damage. Cell 94: 399–409. doi:10.1016/S0092-8674(00)81482-8

Lee C.-S., K. Lee, G. Legube, and J. E. Haber, 2014 Dynamics of yeast histone H2A and H2B phosphorylation in response to a double-strand break. Nat. Struct. Mol. Biol. 21: 103–9. doi:10.1038/nsmb.2737

Lehtonen R., M. Kiuru, S. Vanharanta, J. Sjöberg, L.-M. Aaltonen, *et al.*, 2004 Biallelic inactivation of fumarate hydratase (FH) occurs in nonsyndromic uterine leiomyomas but is rare in other tumors. Am. J. Pathol. 164: 17–22. doi:10.1016/S0002-9440(10)63091-X

Lengsfeld B. M., A. J. Rattray, V. Bhaskara, R. Ghirlando, and T. T. Paull, 2007 Sae2 Is an Endonuclease that Processes Hairpin DNA Cooperatively with the Mre11/Rad50/Xrs2 Complex. Mol. Cell 28: 638–651. doi:10.1016/j.molcel.2007.11.001

Leroy C., S. E. Lee, M. B. Vaze, F. Ochsenbien, R. Guerois, *et al.*, 2003 PP2C Phosphatases Ptc2 and Ptc3 Are Required for DNA Checkpoint Inactivation after a Double-Strand Break. Mol. Cell 11: 827–835. doi:10.1016/S1097-2765(03)00058-3

Leshets M., D. Ramamurthy, M. Lisby, N. Lehming, and O. Pines, 2018 Fumarase is involved in DNA double-strand break resection through a functional interaction with Sae2. Curr. Genet. 1–16. doi:10.1007/s00294-017-0786-4

Li X., and W.-D. Heyer, 2008 Homologous recombination in DNA repair and DNA damage tolerance. Cell Res. 18: 99–113. doi:10.1038/cr.2008.1

Li X., and W.-D. Heyer, 2009 RAD54 controls access to the invading 3’-OH end after RAD51-mediated DNA strand invasion in homologous recombination in Saccharomyces cerevisiae. Nucleic Acids Res. 37: 638–46. doi:10.1093/nar/gkn980

Li X., L. Liu, S. Yang, N. Song, X. Zhou, *et al.*, 2014 Histone demethylase KDM5B is a key regulator of genome stability. Proc. Natl. Acad. Sci. U. S. A. 111: 7096–101. doi:10.1073/pnas.1324036111

Li D., B. Guo, H. Wu, L. Tan, and Q. Lu, 2015 TET Family of Dioxygenases: Crucial Roles and Underlying Mechanisms. Cytogenet. Genome Res. 146: 171–80. doi:10.1159/000438853

Liang G., R. J. Klose, K. E. Gardner, and Y. Zhang, 2007 Yeast Jhd2p is a histone H3 Lys4 trimethyl demethylase. Nat. Struct. Mol. Biol. 14: 243–245. doi:10.1038/nsmb1204

Lin A.-P., S. L. Anderson, K. I. Minard, and L. McAlister-Henn, 2011 Effects of excess succinate and retrograde control of metabolite accumulation in yeast tricarboxylic cycle mutants. J. Biol. Chem. 286: 33737–46. doi:10.1074/jbc.M111.266890

Lisby M., J. H. Barlow, R. C. Burgess, and R. Rothstein, 2004 Choreography of the DNA Damage Response: Spatiotemporal Relationships among Checkpoint and Repair Proteins. Cell 118: 699–713. doi:10.1016/J.CELL.2004.08.015

Lisby M., T. Teixeira, E. Gilson, and V. Géli, 2010 The fate of irreparable DNA double-strand breaks and eroded telomeres at the nuclear periphery. Nucleus 1: 158–61. doi:10.4161/nucl.1.2.11173

Liu H., F. Liang, F. Jin, and Y. Wang, 2008 The Coordination of Centromere Replication, Spindle Formation, and Kinetochore–Microtubule Interaction in Budding Yeast, (O. Cohen-Fix, Ed.). PLoS Genet. 4: e1000262. doi:10.1371/journal.pgen.1000262

Lopes M., C. Cotta-Ramusino, A. Pellicioli, G. Liberi, P. Plevani, *et al.*, 2001 The DNA replication checkpoint response stabilizes stalled replication forks. Nature 412: 557–561. doi:10.1038/35087613

Lopez-Mosqueda J., N. L. Maas, Z. O. Jonsson, L. G. DeFazio-Eli, J. Wohlschlegel, *et al.*, 2010 Damage-induced phosphorylation of Sld3 is important to block late origin firing. Nature 467: 479–483. doi:10.1038/nature09377

Lou H., M. Komata, Y. Katou, Z. Guan, C. C. Reis, *et al.*, 2008 Mrc1 and DNA polymerase epsilon function together in linking DNA replication and the S phase checkpoint. Mol. Cell 32: 106–17. doi:10.1016/j.molcel.2008.08.020

Lowndes N. F., and J. R. Murguia, 2000 Sensing and responding to DNA damage. Curr. Opin. Genet. Dev. 10: 17–25. doi:10.1016/S0959-437X(99)00050-7

Luger K., A. W. Mäder, R. K. Richmond, D. F. Sargent, and T. J. Richmond, 1997 Crystal structure of the nucleosome core particle at 2.8 Å resolution. Nature 389: 251–260. doi:10.1038/38444

Luk E., A. Ranjan, P. C. FitzGerald, G. Mizuguchi, Y. Huang, *et al.*, 2010 Stepwise Histone Replacement by SWR1 Requires Dual Activation with Histone H2A.Z and Canonical Nucleosome. Cell 143: 725–736. doi:10.1016/J.CELL.2010.10.019

Lydeard J. R., S. Jain, M. Yamaguchi, and J. E. Haber, 2007 Break-induced replication and telomerase-independent telomere maintenance require Pol32. Nature 448: 820–823. doi:10.1038/nature06047

Majka J., and P. M. J. Burgers, 2003 Yeast Rad17/Mec3/Ddc1: a sliding clamp for the DNA damage checkpoint. Proc. Natl. Acad. Sci. U. S. A. 100: 2249–54. doi:10.1073/pnas.0437148100

Majka J., A. Niedziela-Majka, and P. M. J. Burgers, 2006 The Checkpoint Clamp Activates Mec1 Kinase during Initiation of the DNA Damage Checkpoint. Mol. Cell 24: 891–901. doi:10.1016/j.molcel.2006.11.027

Malkova A., E. L. Ivanov, and J. E. Haber, 1996 Double-strand break repair in the absence of RAD51 in yeast: a possible role for break-induced DNA replication. Proc. Natl. Acad. Sci. U. S. A. 93: 7131–6.

Mantiero D., M. Clerici, G. Lucchini, and M. P. Longhese, 2007 Dual role for Saccharomyces cerevisiae Tel1 in the checkpoint response to double-strand breaks. EMBO Rep. 8: 380–7. doi:10.1038/sj.embor.7400911

Mazin A. V, A. A. Alexeev, and S. C. Kowalczykowski, 2003 A novel function of Rad54 protein. Stabilization of the Rad51 nucleoprotein filament. J. Biol. Chem. 278: 14029–36. doi:10.1074/jbc.M212779200

Mazouzi A., G. Velimezi, and J. I. Loizou, 2014 DNA replication stress: Causes, resolution and disease. Exp. Cell Res. 329: 85–93. doi:10.1016/J.YEXCR.2014.09.030

Melo J. A., J. Cohen, and D. P. Toczyski, 2001 Two checkpoint complexes are independently recruited to sites of DNA damage in vivo. Genes Dev. 15: 2809–21. doi:10.1101/gad.903501

Meneghini M. D., M. Wu, and H. D. Madhani, 2003 Conserved Histone Variant H2A.Z Protects Euchromatin from the Ectopic Spread of Silent Heterochromatin. Cell 112: 725–736. doi:10.1016/S0092-8674(03)00123-5

Menko F. H., E. R. Maher, L. S. Schmidt, L. A. Middelton, K. Aittomäki, *et al.*, 2014 Hereditary leiomyomatosis and renal cell cancer (HLRCC): renal cancer risk, surveillance and treatment. Fam. Cancer 13: 637–44. doi:10.1007/s10689-014-9735-2

Mersman D. P., H.-N. Du, I. M. Fingerman, P. F. South, and S. D. Briggs, 2009 Polyubiquitination of the demethylase Jhd2 controls histone methylation and gene expression. Genes Dev. 23: 951–962. doi:10.1101/gad.1769209

Miller A., B. Yang, T. Foster, and A. L. Kirchmaier, 2008 Proliferating cell nuclear antigen and ASF1 modulate silent chromatin in Saccharomyces cerevisiae via lysine 56 on histone H3. Genetics 179: 793–809. doi:10.1534/genetics.107.084525

Mimitou E. P., and L. S. Symington, 2008 Sae2, Exo1 and Sgs1 collaborate in DNA double-strand break processing. Nature 455: 770–4. doi:10.1038/nature07312

Mimitou E. P., and L. S. Symington, 2010 Ku prevents Exo1 and Sgs1-dependent resection of DNA ends in the absence of a functional MRX complex or Sae2. EMBO J. 29: 3358–69. doi:10.1038/emboj.2010.193

Mizuguchi G., X. Shen, J. Landry, W.-H. Wu, S. Sen, *et al.*, 2004 ATP-driven exchange of histone H2AZ variant catalyzed by SWR1 chromatin remodeling complex. Science 303: 343–8. doi:10.1126/science.1090701

Morillo-Huesca M., M. Clemente-Ruiz, E. Andújar, F. Prado, and K. Antonellis, 2010 The SWR1 Histone Replacement Complex Causes Genetic Instability and Genome-Wide Transcription Misregulation in the Absence of H2A.Z, (M. Lichten, Ed.). PLoS One 5: e12143. doi:10.1371/journal.pone.0012143

Morrison A. J., J. Highland, N. J. Krogan, A. Arbel-Eden, J. F. Greenblatt, *et al.*, 2004 INO80 and γ-H2AX Interaction Links ATP-Dependent Chromatin Remodeling to DNA Damage Repair. Cell 119: 767–775. doi:10.1016/J.CELL.2004.11.037

Morrison A. J., J.-A. Kim, M. D. Person, J. Highland, J. Xiao, *et al.*, 2007 Mec1/Tel1 Phosphorylation of the INO80 Chromatin Remodeling Complex Influences DNA Damage Checkpoint Responses. Cell 130: 499–511. doi:10.1016/J.CELL.2007.06.010

Nakada D., K. Matsumoto, and K. Sugimoto, 2003 ATM-related Tel1 associates with double-strand breaks through an Xrs2-dependent mechanism. Genes Dev. 17: 1957–62. doi:10.1101/gad.1099003

Nakamura T. M., L.-L. Du, C. Redon, and P. Russell, 2004 Histone H2A phosphorylation controls Crb2 recruitment at DNA breaks, maintains checkpoint arrest, and influences DNA repair in fission yeast. Mol. Cell. Biol. 24: 6215–30. doi:10.1128/MCB.24.14.6215-6230.2004

Navadgi-Patil V. M., and P. M. Burgers, 2009 The unstructured C-terminal tail of the 9-1-1 clamp subunit Ddc1 activates Mec1/ATR via two distinct mechanisms. Mol. Cell 36: 743–53. doi:10.1016/j.molcel.2009.10.014

New J. H., T. Sugiyama, E. Zaitseva, and S. C. Kowalczykowski, 1998 Rad52 protein stimulates DNA strand exchange by Rad51 and replicationprotein A. Nature 391: 407–410. doi:10.1038/34950

Ng H. H., F. Robert, R. A. Young, and K. Struhl, 2003 Targeted recruitment of Set1 histone methylase by elongating Pol II provides a localized mark and memory of recent transcriptional activity. Mol. Cell 11: 709–19. doi:10.1016/S1097-2765(03)00092-3

Nguyen M. O., M. Jalan, C. A. Morrow, F. Osman, and M. C. Whitby, 2015 Recombination occurs within minutes of replication blockage by RTS1 producing restarted forks that are prone to collapse. Elife 4: e04539. doi:10.7554/eLife.04539

Nicolette M. L., K. Lee, Z. Guo, M. Rani, J. M. Chow, *et al.*, 2010 Mre11–Rad50–Xrs2 and Sae2 promote 5′ strand resection of DNA double-strand breaks. Nat. Struct. Mol. Biol. 17: 1478–1485. doi:10.1038/nsmb.1957

Nita M., and A. Grzybowski, 2016 The Role of the Reactive Oxygen Species and Oxidative Stress in the Pathomechanism of the Age-Related Ocular Diseases and Other Pathologies of the Anterior and Posterior Eye Segments in Adults. Oxid. Med. Cell. Longev. 2016: 3164734. doi:10.1155/2016/3164734

Niu H., W.-H. Chung, Z. Zhu, Y. Kwon, W. Zhao, *et al.*, 2010 Mechanism of the ATP-dependent DNA end-resection machinery from Saccharomyces cerevisiae. Nature 467: 108–11. doi:10.1038/nature09318

O'Connor M. J., 2015 Targeting the DNA Damage Response in Cancer. Mol. Cell 60: 547–560. doi:10.1016/j.molcel.2015.10.040

Osborn A. J., and S. J. Elledge, 2003 Mrc1 is a replication fork component whose phosphorylation in response to DNA replication stress activates Rad53. Genes Dev. 17: 1755–67. doi:10.1101/gad.1098303

Paciotti V., G. Lucchini, P. Plevani, M. P. Longhese, A. DeMaggio, *et al.*, 1998 Mec1p is essential for phosphorylation of the yeast DNA damage checkpoint protein Ddc1p, which physically interacts with Mec3p. EMBO J. 17: 4199–209. doi:10.1093/emboj/17.14.4199

Paciotti V., M. Clerici, G. Lucchini, and M. P. Longhese, 2000 The checkpoint protein Ddc2, functionally related to S. pombe Rad26, interacts with Mec1 and is regulated by Mec1-dependent phosphorylation in budding yeast. Genes Dev. 14: 2046–59.

Pai C.-C., R. S. Deegan, L. Subramanian, C. Gal, S. Sarkar, *et al.*, 2014 A histone H3K36 chromatin switch coordinates DNA double-strand break repair pathway choice. Nat. Commun. 5. doi:10.1038/ncomms5091

Pan X., P. Ye, D. S. Yuan, X. Wang, J. S. Bader, *et al.*, 2006 A DNA Integrity Network in the Yeast Saccharomyces cerevisiae. Cell 124: 1069–1081. doi:10.1016/J.CELL.2005.12.036

Papamichos-Chronakis M., J. E. Krebs, and C. L. Peterson, 2006 Interplay between Ino80 and Swr1 chromatin remodeling enzymes regulates cell cycle checkpoint adaptationin response to DNA damage. Genes Dev. 20: 2437–2449. doi:10.1101/gad.1440206

Papamichos-Chronakis M., and C. L. Peterson, 2008 The Ino80 chromatin-remodeling enzyme regulates replisome function and stability. Nat. Struct. Mol. Biol. 15: 338–345. doi:10.1038/nsmb.1413

Papamichos-Chronakis M., S. Watanabe, O. J. Rando, and C. L. Peterson, 2011 Global regulation of H2A.Z localization by the INO80 chromatin-remodeling enzyme is essential for genome integrity. Cell 144: 200–13. doi:10.1016/j.cell.2010.12.021

Papamichos-Chronakis M., and C. L. Peterson, 2013 Chromatin and the genome integrity network. Nat. Rev. Genet. 14: 62–75. doi:10.1038/nrg3345

Pâques F., and J. E. Haber, 1999 Multiple pathways of recombination induced by double-strand breaks in Saccharomyces cerevisiae. Microbiol. Mol. Biol. Rev. 63: 349–404.

Pardo B., L. Crabbé, and P. Pasero, 2016 Signaling Pathways of Replication Stress in Yeast. FEMS Yeast Res. 17: fow101. doi:10.1093/femsyr/fow101

Paull T. T., E. P. Rogakou, V. Yamazaki, C. U. Kirchgessner, M. Gellert, *et al.*, 2000 A critical role for histone H2AX in recruitment of repair factors to nuclear foci after DNA damage. Curr. Biol. 10: 886–895. doi:10.1016/S0960-9822(00)00610-2

Pedersen M. T., and K. Helin, 2010 Histone demethylases in development and disease. Trends Cell Biol. 20: 662–671. doi:10.1016/J.TCB.2010.08.011

Pellicioli A., S. E. Lee, C. Lucca, M. Foiani, and J. E. Haber, 2001 Regulation of Saccharomyces Rad53 Checkpoint Kinase during Adaptation from DNA Damage–Induced G2/M Arrest. Mol. Cell 7: 293–300. doi:10.1016/S1097-2765(01)00177-0

Petukhova G., S. Stratton, and P. Sung, 1998 Catalysis of homologous DNA pairing by yeast Rad51 and Rad54 proteins. Nature 393: 91–94. doi:10.1038/30037

Pfister S. X., S. Ahrabi, L.-P. Zalmas, S. Sarkar, F. Aymard, *et al.*, 2014 SETD2-dependent histone H3K36 trimethylation is required for homologous recombination repair and genome stability. Cell Rep. 7: 2006–18. doi:10.1016/j.celrep.2014.05.026

Pogribny I. P., S. A. Ross, C. Wise, M. Pogribna, E. A. Jones, *et al.*, 2006a Irreversible global DNA hypomethylation as a key step in hepatocarcinogenesis induced by dietary methyl deficiency. Mutat. Res. Mol. Mech. Mutagen. 593: 80–87. doi:10.1016/J.MRFMMM.2005.06.028

Pogribny I. P., S. A. Ross, V. P. Tryndyak, M. Pogribna, L. A. Poirier, *et al.*, 2006b Histone H3 lysine 9 and H4 lysine 20 trimethylation and the expression of Suv4-20h2 and Suv-39h1 histone methyltransferases in hepatocarcinogenesis induced by methyl deficiency in rats. Carcinogenesis 27: 1180–1186. doi:10.1093/carcin/bgi364

Poli J., C.-B. Gerhold, A. Tosi, N. Hustedt, A. Seeber, *et al.*, 2016 Mec1, INO80, and the PAF1 complex cooperate to limit transcription replication conflicts through RNAPII removal during replication stress. Genes Dev. 30: 337–54. doi:10.1101/gad.273813.115

Pollard P. J., J. J. Brière, N. A. Alam, J. Barwell, E. Barclay, *et al.*, 2005 Accumulation of Krebs cycle intermediates and over-expression of HIF1α in tumours which result from germline FH and SDH mutations. Hum. Mol. Genet. 14: 2231–2239. doi:10.1093/hmg/ddi227

Price B. D., and A. D. D'Andrea, 2013 Chromatin remodeling at DNA double-strand breaks. Cell 152: 1344–54. doi:10.1016/j.cell.2013.02.011

Prochazkova J., and J. I. Loizou, 2016 Programmed DNA breaks in lymphoid cells: repair mechanisms and consequences in human disease. Immunology 147: 11–20. doi:10.1111/imm.12547

Puddu F., T. Oelschlaegel, I. Guerini, N. J. Geisler, H. Niu, *et al.*, 2015 Synthetic viability genomic screening defines Sae2 function in DNA repair. EMBO J. 34: 1509–22. doi:10.15252/embj.201590973

Quinet A., D. Lemaçon, and A. Vindigni, 2017 Replication Fork Reversal: Players and Guardians. Mol. Cell 68: 830–833. doi:10.1016/j.molcel.2017.11.022

Raisner R. M., P. D. Hartley, M. D. Meneghini, M. Z. Bao, C. L. Liu, *et al.*, 2005 Histone Variant H2A.Z Marks the 5′ Ends of Both Active and Inactive Genes in Euchromatin. Cell 123: 233–248. doi:10.1016/J.CELL.2005.10.002

Ramakrishnan S., S. Pokhrel, S. Palani, C. Pflueger, T. J. Parnell, *et al.*, 2016 Counteracting H3K4 methylation modulators Set1 and Jhd2 co-regulate chromatin dynamics and gene transcription. Nat. Commun. 7: 11949. doi:10.1038/ncomms11949

Rangasamy D., L. Berven, P. Ridgway, and D. J. Tremethick, 2003 Pericentric heterochromatin becomes enriched with H2A.Z during early mammalian development. EMBO J. 22: 1599–607. doi:10.1093/emboj/cdg160

Rangasamy D., I. Greaves, and D. J. Tremethick, 2004 RNA interference demonstrates a novel role for H2A.Z in chromosome segregation. Nat. Struct. Mol. Biol. 11: 650–655. doi:10.1038/nsmb786

Ray Chaudhuri A., E. Callen, X. Ding, E. Gogola, A. A. Duarte, *et al.*, 2016 Replication fork stability confers chemoresistance in BRCA-deficient cells. Nature 535: 382–387. doi:10.1038/nature18325

Rizzardi L. F., E. S. Dorn, B. D. Strahl, and J. G. Cook, 2012 DNA replication origin function is promoted by H3K4 di-methylation in Saccharomyces cerevisiae. Genetics 192: 371–84. doi:10.1534/genetics.112.142349

Rodriguez-Rocha H., A. Garcia-Garcia, M. I. Panayiotidis, and R. Franco, 2011 DNA damage and autophagy. Mutat. Res. 711: 158–66. doi:10.1016/j.mrfmmm.2011.03.007

Rogakou E. P., D. R. Pilch, A. H. Orr, V. S. Ivanova, and W. M. Bonner, 1998 DNA double-stranded breaks induce histone H2AX phosphorylation on serine 139. J. Biol. Chem. 273: 5858–68. doi:10.1074/JBC.273.10.5858

Rogakou E. P., C. Boon, C. Redon, and W. M. Bonner, 1999 Megabase chromatin domains involved in DNA double-strand breaks in vivo. J. Cell Biol. 146: 905–16. doi:10.1083/JCB.146.5.905

Rondinelli B., E. Gogola, H. Yücel, A. A. Duarte, M. van de Ven, *et al.*, 2017 EZH2 promotes degradation of stalled replication forks by recruiting MUS81 through histone H3 trimethylation. Nat. Cell Biol. 19: 1371–1378. doi:10.1038/ncb3626

Ropars V., P. Drevet, P. Legrand, S. Baconnais, J. Amram, *et al.*, 2011 Structural characterization of filaments formed by human Xrcc4-Cernunnos/XLF complex involved in nonhomologous DNA end-joining. Proc. Natl. Acad. Sci. U. S. A. 108: 12663–8. doi:10.1073/pnas.1100758108

Rossi S. E., A. Ajazi, W. Carotenuto, M. Foiani, and M. Giannattasio, 2015 Rad53-Mediated Regulation of Rrm3 and Pif1 DNA Helicases Contributes to Prevention of Aberrant Fork Transitions under Replication Stress. Cell Rep. 13: 80–92. doi:10.1016/j.celrep.2015.08.073

Rossodivita A. A., A. L. Boudoures, J. P. Mecoli, E. M. Steenkiste, A. L. Karl, *et al.*, 2014 Histone H3 K79 methylation states play distinct roles in UV-induced sister chromatid exchange and cell cycle checkpoint arrest in Saccharomyces cerevisiae. Nucleic Acids Res. 42: 6286–99. doi:10.1093/nar/gku242

Rouse J., and S. P. Jackson, 2000 LCD1: an essential gene involved in checkpoint control and regulation of the MEC1 signalling pathway in Saccharomyces cerevisiae. EMBO J. 19: 5801–12. doi:10.1093/emboj/19.21.5801

Rouse J., and S. P. Jackson, 2002 Lcd1p Recruits Mec1p to DNA Lesions In Vitro and In Vivo. Mol. Cell 9: 857–869. doi:10.1016/S1097-2765(02)00507-5

Ruff P., R. A. Donnianni, E. Glancy, J. Oh, and L. S. Symington, 2016 RPA Stabilization of Single-Stranded DNA Is Critical for Break-Induced Replication. Cell Rep. 17: 3359–3368. doi:10.1016/j.celrep.2016.12.003

Rulten S. L., and K. W. Caldecott, 2013 DNA strand break repair and neurodegeneration. DNA Repair (Amst). 12: 558–567. doi:10.1016/J.DNAREP.2013.04.008

San Filippo J., P. Sung, and H. Klein, 2008 Mechanism of Eukaryotic Homologous Recombination. Annu. Rev. Biochem. 77: 229–257. doi:10.1146/annurev.biochem.77.061306.125255

Sanchez Y., B. A. Desany, W. J. Jones, Q. Liu, B. Wang, *et al.*, 1996 Regulation of RAD53 by the ATM-like kinases MEC1 and TEL1 in yeast cell cycle checkpoint pathways. Science 271: 357–60. doi:10.1126/SCIENCE.271.5247.357

Sandell L. L., and V. A. Zakian, 1993 Loss of a yeast telomere: arrest, recovery, and chromosome loss. Cell 75: 729–39.

Santisteban M. S., T. Kalashnikova, and M. M. Smith, 2000 Histone H2A.Z regulates transcription and is partially redundant with nucleosome remodeling complexes. Cell 103: 411–22. doi:10.1016/S0092-8674(00)00133-1

Santocanale C., and J. F. X. Diffley, 1998 A Mec1- and Rad53-dependent checkpoint controls late-firing origins of DNA replication. Nature 395: 615–618. doi:10.1038/27001

Santos-Rosa H., R. Schneider, A. J. Bannister, J. Sherriff, B. E. Bernstein, *et al.*, 2002 Active genes are tri-methylated at K4 of histone H3. Nature 419: 407–411. doi:10.1038/nature01080

Sass E., E. Blachinsky, S. Karniely, and O. Pines, 2001 Mitochondrial and Cytosolic Isoforms of Yeast Fumarase Are Derivatives of a Single Translation Product and Have Identical Amino Termini. J. Biol. Chem. 276: 46111–46117. doi:10.1074/jbc.M106061200

Schlacher K., N. Christ, N. Siaud, A. Egashira, H. Wu, *et al.*, 2011 Double-Strand Break Repair-Independent Role for BRCA2 in Blocking Stalled Replication Fork Degradation by MRE11. Cell 145: 529–542. doi:10.1016/j.cell.2011.03.041

Schlacher K., H. Wu, and M. Jasin, 2012 A Distinct Replication Fork Protection Pathway Connects Fanconi Anemia Tumor Suppressors to RAD51-BRCA1/2. Cancer Cell 22: 106–116. doi:10.1016/J.CCR.2012.05.015

Schwartz M. F., J. K. Duong, Z. Sun, J. S. Morrow, D. Pradhan, *et al.*, 2002 Rad9 phosphorylation sites couple Rad53 to the Saccharomyces cerevisiae DNA damage checkpoint. Mol. Cell 9: 1055–65. doi:10.1016/S1097-2765(02)00532-4

Seeber A., A. M. Hegnauer, N. Hustedt, I. Deshpande, J. Poli, *et al.*, 2016 RPA Mediates Recruitment of MRX to Forks and Double-Strand Breaks to Hold Sister Chromatids Together. Mol. Cell 64: 951–966. doi:10.1016/J.MOLCEL.2016.10.032

Seiler D. M., J. Rouquette, V. J. Schmid, H. Strickfaden, C. Ottmann, *et al.*, 2011 Double-strand break-induced transcriptional silencing is associated with loss of tri-methylation at H3K4. Chromosom. Res. 19: 883–899. doi:10.1007/s10577-011-9244-1

Sein H., S. Värv, and A. Kristjuhan, 2015 Distribution and Maintenance of Histone H3 Lysine 36 Trimethylation in Transcribed Locus, (R. Feil, Ed.). PLoS One 10: e0120200. doi:10.1371/journal.pone.0120200

Seto E., and M. Yoshida, 2014 Erasers of histone acetylation: the histone deacetylase enzymes. Cold Spring Harb. Perspect. Biol. 6: a018713. doi:10.1101/cshperspect.a018713

Seward D. J., G. Cubberley, S. Kim, M. Schonewald, L. Zhang, *et al.*, 2007 Demethylation of trimethylated histone H3 Lys4 in vivo by JARID1 JmjC proteins. Nat. Struct. Mol. Biol. 14: 240–242. doi:10.1038/nsmb1200

Shen X., R. Ranallo, E. Choi, and C. Wu, 2003 Involvement of Actin-Related Proteins in ATP-Dependent Chromatin Remodeling. Mol. Cell 12: 147–155. doi:10.1016/S1097-2765(03)00264-8

Shi L., L. Sun, Q. Li, J. Liang, W. Yu, *et al.*, 2011 Histone demethylase JMJD2B coordinates H3K4/H3K9 methylation and promotes hormonally responsive breast carcinogenesis. Proc. Natl. Acad. Sci. U. S. A. 108: 7541–6. doi:10.1073/pnas.1017374108

Shim E. Y., W.-H. Chung, M. L. Nicolette, Y. Zhang, M. Davis, *et al.*, 2010 Saccharomyces cerevisiae Mre11/Rad50/Xrs2 and Ku proteins regulate association of Exo1 and Dna2 with DNA breaks. EMBO J. 29: 3370–80. doi:10.1038/emboj.2010.219

Shimada K., P. Pasero, and S. M. Gasser, 2002 ORC and the intra-S-phase checkpoint: a threshold regulates Rad53p activation in S phase. Genes Dev. 16: 3236–52. doi:10.1101/gad.239802

Shimomura T., S. Ando, K. Matsumoto, and K. Sugimoto, 1998 Functional and physical interaction between Rad24 and Rfc5 in the yeast checkpoint pathways. Mol. Cell. Biol. 18: 5485–91. doi:10.1128/MCB.18.9.5485

Shinohara A., H. Ogawa, and T. Ogawa, 1992 Rad51 protein involved in repair and recombination in S. cerevisiae is a RecA-like protein. Cell 69: 457–70. doi:10.1016/0092-8674(92)90447-K

Shinohara A., and T. Ogawa, 1998 Stimulation by Rad52 of yeast Rad51- mediated recombination. Nature 391: 404–407. doi:10.1038/34943

Shinohara A., M. Shinohara, T. Ohta, S. Matsuda, and T. Ogawa, 1998 Rad52 forms ring structures and co-operates with RPA in single-strand DNA annealing. Genes to Cells 3: 145–156. doi:10.1046/j.1365-2443.1998.00176.x

Shroff R., A. Arbel-Eden, D. Pilch, G. Ira, W. M. Bonner, *et al.*, 2004 Distribution and Dynamics of Chromatin Modification Induced by a Defined DNA Double-Strand Break. Curr. Biol. 14: 1703–1711. doi:10.1016/J.CUB.2004.09.047

Siino J. S., I. B. Nazarov, M. P. Svetlova, L. V Solovjeva, R. H. Adamson, *et al.*, 2002 Photobleaching of GFP-labeled H2AX in chromatin: H2AX has low diffusional mobility in the nucleus. Biochem. Biophys. Res. Commun. 297: 1318–1323. doi:10.1016/S0006-291X(02)02383-5

Sikorski R. S., and P. Hieter, 1989 A system of shuttle vectors and yeast host strains designed for efficient manipulation of DNA in Saccharomyces cerevisiae. Genetics 122: 19–27.

Singer E., Y. B. Silas, S. Ben-Yehuda, and O. Pines, 2017 Bacterial fumarase and L-malic acid are evolutionary ancient components of the DNA damage response. Elife 6: e30927. doi:10.7554/eLife.30927

Sirbu B. M., F. B. Couch, J. T. Feigerle, S. Bhaskara, S. W. Hiebert, *et al.*, 2011 Analysis of protein dynamics at active, stalled, and collapsed replication forks. Genes Dev. 25: 1320–7. doi:10.1101/gad.2053211

Smith E. H., R. Janknecht, and L. J. Maher, 2007 Succinate inhibition of α-ketoglutarate-dependent enzymes in a yeast model of paraganglioma. Hum. Mol. Genet. 16: 3136–3148. doi:10.1093/hmg/ddm275

Smolka M. B., S. Chen, P. S. Maddox, J. M. Enserink, C. P. Albuquerque, *et al.*, 2006 An FHA domain-mediated protein interaction network of Rad53 reveals its role in polarized cell growth. J. Cell Biol. 175: 743–53. doi:10.1083/jcb.200605081

Sogo J. M., M. Lopes, and M. Foiani, 2002 Fork reversal and ssDNA accumulation at stalled replication forks owing to checkpoint defects. Science 297: 599–602. doi:10.1126/science.1074023

Solinger J. A., K. Kiianitsa, and W.-D. Heyer, 2002 Rad54, a Swi2/Snf2-like recombinational repair protein, disassembles Rad51:dsDNA filaments. Mol. Cell 10: 1175–88. doi:10.1016/S1097-2765(02)00743-8

Srivatsan A., B.-Z. Li, B. Szakal, D. Branzei, C. D. Putnam, *et al.*, 2018 The Swr1 chromatin-remodeling complex prevents genome instability induced by replication fork progression defects. Nat. Commun. 9: 3680. doi:10.1038/s41467-018-06131-2

Stein I., Y. Peleg, S. Even-Ram, and O. Pines, 1994 The Single Translation Product of the FUM1 Gene (Fumarase) Is Processed in Mitochondria before Being Distributed between the Cytosol and Mitochondria in Saccharomyces cerevisiae. Mol. Cell. Biol. 14: 4770–4778.

Strumberg D., A. A. Pilon, M. Smith, R. Hickey, L. Malkas, *et al.*, 2000 Conversion of Topoisomerase I Cleavage Complexes on the Leading Strand of Ribosomal DNA into 5′-Phosphorylated DNA Double-Strand Breaks by Replication Runoff. Mol. Cell. Biol. 20: 3977–3987. doi:10.1128/MCB.20.11.3977-3987.2000

Stulemeijer I. J. E., D. De Vos, K. van Harten, O. K. Joshi, O. Blomberg, *et al.*, 2015 Dot1 histone methyltransferases share a distributive mechanism but have highly diverged catalytic properties. Sci. Rep. 5: 9824. doi:10.1038/srep09824

Subba Rao K., 2007 Mechanisms of Disease: DNA repair defects and neurological disease. Nat. Clin. Pract. Neurol. 3: 162–172. doi:10.1038/ncpneuro0448

Sugiyama T., E. M. Zaitseva, and S. C. Kowalczykowski, 1997 A single-stranded DNA-binding protein is needed for efficient presynaptic complex formation by the Saccharomyces cerevisiae Rad51 protein. J. Biol. Chem. 272: 7940–5. doi:10.1074/JBC.272.12.7940

Sugiyama T., J. H. New, and S. C. Kowalczykowski, 1998 DNA annealing by RAD52 protein is stimulated by specific interaction with the complex of replication protein A and single-stranded DNA. Proc. Natl. Acad. Sci. U. S. A. 95: 6049–54. doi:10.1073/PNAS.95.11.6049

Sugiyama T., and S. C. Kowalczykowski, 2002 Rad52 protein associates with replication protein A (RPA)-single-stranded DNA to accelerate Rad51-mediated displacement of RPA and presynaptic complex formation. J. Biol. Chem. 277: 31663–72. doi:10.1074/jbc.M203494200

Sugiyama T., N. Kantake, Y. Wu, and S. C. Kowalczykowski, 2006 Rad52-mediated DNA annealing after Rad51-mediated DNA strand exchange promotes second ssDNA capture. EMBO J. 25: 5539–48. doi:10.1038/sj.emboj.7601412

Sulkowski P. L., C. D. Corso, N. D. Robinson, S. E. Scanlon, K. R. Purshouse, *et al.*, 2017 2-Hydroxyglutarate produced by neomorphic IDH mutations suppresses homologous recombination and induces PARP inhibitor sensitivity. Sci. Transl. Med. 9: eaal2463. doi:10.1126/scitranslmed.aal2463

Sulkowski P. L., R. K. Sundaram, S. Oeck, C. D. Corso, Y. Liu, *et al.*, 2018 Krebs-cycle-deficient hereditary cancer syndromes are defined by defects in homologous-recombination DNA repair. Nat. Genet. 50: 1086–1092. doi:10.1038/s41588-018-0170-4

Sun Z., D. S. Fay, F. Marini, M. Foiani, and D. F. Stern, 1996 Spk1/Rad53 is regulated by Mec1-dependent protein phosphorylation in DNA replication and damage checkpoint pathways. Genes Dev. 10: 395–406. doi:10.1101/GAD.10.4.395

Sun Z., J. Hsiao, D. S. Fay, and D. F. Stern, 1998 Rad53 FHA domain associated with phosphorylated Rad9 in the DNA damage checkpoint. Science 281: 272–4.

Sun Z.-W., and C. D. Allis, 2002 Ubiquitination of histone H2B regulates H3 methylation and gene silencing in yeast. Nature 418: 104–108. doi:10.1038/nature00883

Sung P., 1997 Function of yeast Rad52 protein as a mediator between replication protein A and the Rad51 recombinase. J. Biol. Chem. 272: 28194–7. doi:10.1074/JBC.272.45.28194

Svetlova M., L. Solovjeva, K. Nishi, I. Nazarov, J. Siino, *et al.*, 2007 Elimination of radiation-induced γ-H2AX foci in mammalian nucleus can occur by histone exchange. Biochem. Biophys. Res. Commun. 358: 650–654. doi:10.1016/J.BBRC.2007.04.188

Swan M. K., R. E. Johnson, L. Prakash, S. Prakash, and A. K. Aggarwal, 2009 Structural basis of high-fidelity DNA synthesis by yeast DNA polymerase delta. Nat. Struct. Mol. Biol. 16: 979–86. doi:10.1038/nsmb.1663

Sweeney F. D., F. Yang, A. Chi, J. Shabanowitz, D. F. Hunt, *et al.*, 2005 Saccharomyces cerevisiae Rad9 Acts as a Mec1 Adaptor to Allow Rad53 Activation. Curr. Biol. 15: 1364–1375. doi:10.1016/J.CUB.2005.06.063

Symington L. S., 2002 Role of RAD52 epistasis group genes in homologous recombination and double-strand break repair. Microbiol. Mol. Biol. Rev. 66: 630–70. doi:10.1128/MMBR.66.4.630-670.2002

Takahashi Y. H., J. S. Lee, S. K. Swanson, A. Saraf, L. Florens, *et al.*, 2009 Regulation of H3K4 trimethylation via Cps40 (Spp1) of COMPASS is monoubiquitination independent: implication for a Phe/Tyr switch by the catalytic domain of Set1. Mol. Cell. Biol. 29: 3478–86. doi:10.1128/MCB.00013-09

Tanaka K., and P. Russell, 2001 Mrc1 channels the DNA replication arrest signal to checkpoint kinase Cds1. Nat. Cell Biol. 3: 966–972. doi:10.1038/ncb1101-966

Tanaka K., and P. Russell, 2004 Cds1 phosphorylation by Rad3-Rad26 kinase is mediated by forkhead-associated domain interaction with Mrc1. J. Biol. Chem. 279: 32079–86. doi:10.1074/jbc.M404834200

Teixeira-Silva A., A. Ait Saada, J. Hardy, I. Iraqui, M. C. Nocente, *et al.*, 2017 The end-joining factor Ku acts in the end-resection of double strand break-free arrested replication forks. Nat. Commun. 8: 1982. doi:10.1038/s41467-017-02144-5

Tercero J. A., M. P. Longhese, and J. F. X. Diffley, 2003 A central role for DNA replication forks in checkpoint activation and response. Mol. Cell 11: 1323–36.

Ternette N., M. Yang, M. Laroyia, M. Kitagawa, L. O'Flaherty, *et al.*, 2013 Inhibition of mitochondrial aconitase by succination in fumarate hydratase deficiency. Cell Rep. 3: 689–700. doi:10.1016/j.celrep.2013.02.013

Thangavel S., M. Berti, M. Levikova, C. Pinto, S. Gomathinayagam, *et al.*, 2015 DNA2 drives processing and restart of reversed replication forks in human cells. J. Cell Biol. 208: 545–62. doi:10.1083/jcb.201406100

Tittel-Elmer M., C. Alabert, P. Pasero, and J. A. Cobb, 2009 The MRX complex stabilizes the replisome independently of the S phase checkpoint during replication stress. EMBO J. 28: 1142–56. doi:10.1038/emboj.2009.60

Toledo L. I., M. Altmeyer, M.-B. Rask, C. Lukas, D. H. Larsen, *et al.*, 2013 ATR prohibits replication catastrophe by preventing global exhaustion of RPA. Cell 155: 1088–103. doi:10.1016/j.cell.2013.10.043

Tolley E., and I. Craig, 1975 Presence of two forms of fumarase (fumarate hydratase E.C. 4.2.1.2) in mammalian cells: immunological characterization and genetic analysis in somatic cell hybrids. Confirmation of the assignment of a gene necessary for the enzyme expression to human chromosome 1. Biochem. Genet. 13: 867–83.

Tomlinson I. P. M., N. A. Alam, A. J. Rowan, E. Barclay, E. E. M. Jaeger, *et al.*, 2002 Germline mutations in FH predispose to dominantly inherited uterine fibroids, skin leiomyomata and papillary renal cell cancer. Nat. Genet. 30: 406–410. doi:10.1038/ng849

Toone W. M., B. L. Aerne, B. A. Morgan, and and L. H. Johnston, 1997 GETTING STARTED:Regulating the Initiation of DNA Replication in Yeast. Annu. Rev. Microbiol. 51: 125–149. doi:10.1146/annurev.micro.51.1.125

Tsang E., I. Miyabe, I. Iraqui, J. Zheng, S. A. E. Lambert, *et al.*, 2014 The extent of error-prone replication restart by homologous recombination is controlled by Exo1 and checkpoint proteins. J. Cell Sci. 127: 2983–94. doi:10.1242/jcs.152678

Tseng H.-M., and A. E. Tomkinson, 2004 Processing and joining of DNA ends coordinated by interactions among Dnl4/Lif1, Pol4, and FEN-1. J. Biol. Chem. 279: 47580–8. doi:10.1074/jbc.M404492200

Tsukada Y., J. Fang, H. Erdjument-Bromage, M. E. Warren, C. H. Borchers, *et al.*, 2006 Histone demethylation by a family of JmjC domain-containing proteins. Nature 439: 811–816. doi:10.1038/nature04433

Tu S., E. M. M. Bulloch, L. Yang, C. Ren, W.-C. Huang, *et al.*, 2007 Identification of histone demethylases in Saccharomyces cerevisiae. J. Biol. Chem. 282: 14262–71. doi:10.1074/jbc.M609900200

Van C., J. S. Williams, T. A. Kunkel, and C. L. Peterson, 2015 Deposition of histone H2A.Z by the SWR-C remodeling enzyme prevents genome instability. DNA Repair (Amst). 25: 9–14. doi:10.1016/J.DNAREP.2014.10.010

Vaze M. B., A. Pellicioli, S. E. Lee, G. Ira, G. Liberi, *et al.*, 2002 Recovery from checkpoint-mediated arrest after repair of a double-strand break requires Srs2 helicase. Mol. Cell 10: 373–85. doi:10.1016/S1097-2765(02)00593-2

Veaute X., J. Jeusset, C. Soustelle, S. C. Kowalczykowski, E. Le Cam, *et al.*, 2003 The Srs2 helicase prevents recombination by disrupting Rad51 nucleoprotein filaments. Nature 423: 309–312. doi:10.1038/nature01585

Venkatasubrahmanyam S., W. W. Hwang, M. D. Meneghini, A. H. Y. Tong, and H. D. Madhani, 2007 Genome-wide, as opposed to local, antisilencing is mediated redundantly by the euchromatic factors Set1 and H2A.Z. Proc. Natl. Acad. Sci. U. S. A. 104: 16609–14. doi:10.1073/pnas.0700914104

Verma P., and R. A. Greenberg, 2016 Noncanonical views of homology-directed DNA repair. Genes Dev. 30: 1138–54. doi:10.1101/gad.280545.116

Versini G., I. Comet, M. Wu, L. Hoopes, E. Schwob, *et al.*, 2003 The yeast Sgs1 helicase is differentially required for genomic and ribosomal DNA replication. EMBO J. 22: 1939–49. doi:10.1093/emboj/cdg180

Vialard J. E., C. S. Gilbert, C. M. Green, and N. F. Lowndes, 1998 The budding yeast Rad9 checkpoint protein is subjected to Mec1/Tel1-dependent hyperphosphorylation and interacts with Rad53 after DNA damage. EMBO J. 17: 5679–5688. doi:10.1093/emboj/17.19.5679

Wach A., A. Brachat, R. Pohlmann, and P. Philippsen, 1994 New Heterologous Modules for Classical or PCR-based Gene Disruptions in Saccharomyces cerevisiae. Yeast 10: 1793–1808.

Ward P. S., J. Patel, D. R. Wise, O. Abdel-Wahab, B. D. Bennett, *et al.*, 2010 The Common Feature of Leukemia-Associated IDH1 and IDH2 Mutations Is a Neomorphic Enzyme Activity Converting α-Ketoglutarate to 2-Hydroxyglutarate. Cancer Cell 17: 225–234. doi:10.1016/J.CCR.2010.01.020

Waters R., P. van Eijk, and S. Reed, 2015 Histone modification and chromatin remodeling during NER. DNA Repair (Amst). 36: 105–13. doi:10.1016/j.dnarep.2015.09.013

Weinert T. A., and L. H. Hartwell, 1988 The RAD9 gene controls the cell cycle response to DNA damage in Saccharomyces cerevisiae. Science 241: 317–22.

West S. C., 2003 Molecular views of recombination proteins and their control. Nat. Rev. Mol. Cell Biol. 4: 435–445. doi:10.1038/nrm1127

Wilson T. E., U. Grawunder, and M. R. Lieber, 1997 Yeast DNA ligase IV mediates non-homologous DNA end joining. Nature 388: 495–498. doi:10.1038/41365

Winzeler E. A., D. D. Shoemaker, A. Astromoff, H. Liang, K. Anderson, *et al.*, 1999 Functional characterization of the S. cerevisiae genome by gene deletion and parallel analysis. Science 285: 901–6. doi:10.1126/SCIENCE.285.5429.901

Wolner B., and C. L. Peterson, 2005 ATP-dependent and ATP-independent roles for the Rad54 chromatin remodeling enzyme during recombinational repair of a DNA double strand break. J. Biol. Chem. 280: 10855–60. doi:10.1074/jbc.M414388200

Wood A., J. Schneider, J. Dover, M. Johnston, and A. Shilatifard, 2003 The Paf1 Complex Is Essential for Histone Monoubiquitination by the Rad6-Bre1 Complex, Which Signals for Histone Methylation by COMPASS and Dot1p. J. Biol. Chem. 278: 34739–34742. doi:10.1074/jbc.C300269200

Woods S. A., S. D. Schwartzbach, and J. R. Guest, 1988 Two biochemically distinct classes of fumarase in Escherichia coli. Biochim. Biophys. Acta 954: 14–26.

Wu M., and A. Tzagoloff, 1987 Mitochondrial and cytoplasmic fumarases in Saccharomyces cerevisiae are encoded by a single nuclear gene FUM1. J. Biol. Chem. 262: 12275–82.

Wu X., T. E. Wilson, and M. R. Lieber, 1999 A role for FEN-1 in nonhomologous DNA end joining: the order of strand annealing and nucleolytic processing events. Proc. Natl. Acad. Sci. U. S. A. 96: 1303–8. doi:10.1073/PNAS.96.4.1303

Wu L., S. L. Davies, N. C. Levitt, and I. D. Hickson, 2001 Potential role for the BLM helicase in recombinational repair via a conserved interaction with RAD51. J. Biol. Chem. 276: 19375–81. doi:10.1074/jbc.M009471200

Wu D., L. M. Topper, and T. E. Wilson, 2008 Recruitment and dissociation of nonhomologous end joining proteins at a DNA double-strand break in Saccharomyces cerevisiae. Genetics 178: 1237–49. doi:10.1534/genetics.107.083535

Wysocki R., A. Javaheri, S. Allard, F. Sha, J. Côté, *et al.*, 2005 Role of Dot1-dependent histone H3 methylation in G1 and S phase DNA damage checkpoint functions of Rad9. Mol. Cell. Biol. 25: 8430–43. doi:10.1128/MCB.25.19.8430-8443.2005

Xiao M., H. Yang, W. Xu, S. Ma, H. Lin, *et al.*, 2012 Inhibition of α-KG-dependent histone and DNA demethylases by fumarate and succinate that are accumulated in mutations of FH and SDH tumor suppressors. Genes Dev. 26: 1326–38. doi:10.1101/gad.191056.112

Xu Y., M. Davenport, and T. J. Kelly, 2006 Two-stage mechanism for activation of the DNA replication checkpoint kinase Cds1 in fission yeast. Genes Dev. 20: 990–1003. doi:10.1101/gad.1406706

Xu W., H. Yang, Y. Liu, Y. Yang, P. Wang, *et al.*, 2011 Oncometabolite 2-hydroxyglutarate is a competitive inhibitor of α-ketoglutarate-dependent dioxygenases. Cancer Cell 19: 17–30. doi:10.1016/j.ccr.2010.12.014

Xu Y., M. K. Ayrapetov, C. Xu, O. Gursoy-Yuzugullu, Y. Hu, *et al.*, 2012 Histone H2A.Z controls a critical chromatin remodeling step required for DNA double-strand break repair. Mol. Cell 48: 723–33. doi:10.1016/j.molcel.2012.09.026

Yang B., and A. L. Kirchmaier, 2006 Bypassing the catalytic activity of SIR2 for SIR protein spreading in Saccharomyces cerevisiae. Mol. Biol. Cell 17: 5287–97. doi:10.1091/mbc.E06-08-0669

Yang B., 2008 Insights into the impact of histone acetylation and methylation on Sir protein recruitment, spreading and silencing in Saccharomyces cerevisiae. Purdue University, Indiana.

Yang B., J. Britton, and A. L. Kirchmaier, 2008 Insights into the Impact of Histone Acetylation and Methylation on Sir Protein Recruitment, Spreading, and Silencing in Saccharomyces cerevisiae. J. Mol. Biol. 381: 826–844. doi:10.1016/J.JMB.2008.06.059

Yang J., A. M. Jubb, L. Pike, F. M. Buffa, H. Turley, *et al.*, 2010 The histone demethylase JMJD2B is regulated by estrogen receptor alpha and hypoxia, and is a key mediator of estrogen induced growth. Cancer Res. 70: 6456–66. doi:10.1158/0008-5472.CAN-10-0413

Yang M., T. Soga, and P. J. Pollard, 2013 Oncometabolites: linking altered metabolism with cancer. 3652 J. Clin. Investig. 123: 4–10. doi:10.1172/JCI67228

Yeung M., and D. Durocher, 2011 Srs2 enables checkpoint recovery by promoting disassembly of DNA damage foci from chromatin. DNA Repair (Amst). 10: 1213–1222. doi:10.1016/J.DNAREP.2011.09.005

Yogev O., O. Yogev, E. Singer, E. Shaulian, M. Goldberg, *et al.*, 2010 Fumarase: A Mitochondrial Metabolic Enzyme and a Cytosolic/Nuclear Component of the DNA Damage Response, (S. Elledge, Ed.). PLoS Biol. 8: e1000328. doi:10.1371/journal.pbio.1000328

Yogev O., A. Naamati, and O. Pines, 2011 Fumarase: a paradigm of dual targeting and dual localized functions. FEBS J. 278: 4230–4242. doi:10.1111/j.1742-4658.2011.08359.x

Yuan J., R. Adamski, and J. Chen, 2010 Focus on histone variant H2AX: to be or not to be. FEBS Lett. 584: 3717–24. doi:10.1016/j.febslet.2010.05.021

Zegerman P., and J. F. X. Diffley, 2010 Checkpoint-dependent inhibition of DNA replication initiation by Sld3 and Dbf4 phosphorylation. Nature 467: 474–478. doi:10.1038/nature09373

Zellweger R., D. Dalcher, K. Mutreja, M. Berti, J. A. Schmid, *et al.*, 2015 Rad51-mediated replication fork reversal is a global response to genotoxic treatments in human cells. J. Cell Biol. 208: 563–79. doi:10.1083/jcb.201406099

Zeman M. K., and K. A. Cimprich, 2014 Causes and consequences of replication stress. Nat. Cell Biol. 16: 2–9. doi:10.1038/ncb2897

Zhang Y., M. L. Hefferin, L. Chen, E. Y. Shim, H.-M. Tseng, *et al.*, 2007 Role of Dnl4–Lif1 in nonhomologous end-joining repair complex assembly and suppression of homologous recombination. Nat. Struct. Mol. Biol. 14: 639–646. doi:10.1038/nsmb1261

Zhang Y., E. Y. Shim, M. Davis, and S. E. Lee, 2009 Regulation of repair choice: Cdk1 suppresses recruitment of end joining factors at DNA breaks. DNA Repair (Amst). 8: 1235–41. doi:10.1016/j.dnarep.2009.07.007

Zhang N., 2015 Epigenetic modulation of DNA methylation by nutrition and its mechanisms in animals. Anim. Nutr. 1: 144–151. doi:10.1016/J.ANINU.2015.09.002

Zhao X., E. G. Muller, and R. Rothstein, 1998 A suppressor of two essential checkpoint genes identifies a novel protein that negatively affects dNTP pools. Mol. Cell 2: 329–40. doi:10.1016/S1097-2765(00)80277-4

Zhao X., A. Chabes, V. Domkin, L. Thelander, and R. Rothstein, 2001 The ribonucleotide reductase inhibitor Sml1 is a new target of the Mec1/Rad53 kinase cascade during growth and in response to DNA damage. EMBO J. 20: 3544–3553. doi:10.1093/emboj/20.13.3544

Zhao X., and R. Rothstein, 2002 The Dun1 checkpoint kinase phosphorylates and regulates the ribonucleotide reductase inhibitor Sml1. Proc. Natl. Acad. Sci. U. S. A. 99: 3746–51. doi:10.1073/pnas.062502299

Zhu Z., W.-H. Chung, E. Y. Shim, S. E. Lee, and G. Ira, 2008 Sgs1 helicase and two nucleases Dna2 and Exo1 resect DNA double-strand break ends. Cell 134: 981–94. doi:10.1016/j.cell.2008.08.037

Zou L., and S. J. Elledge, 2003 Sensing DNA damage through ATRIP recognition of RPA-ssDNA complexes. Science 300: 1542–8. doi:10.1126/science.1083430

Zou L., D. Liu, and S. J. Elledge, 2003 Replication protein A-mediated recruitment and activation of Rad17 complexes. Proc. Natl. Acad. Sci. U. S. A. 100: 13827–32. doi:10.1073/pnas.2336100100